DISRUPTION OF SOLUBLE EPOXIDE HYDROLASE DIMERIZATION AS A NOVEL THERAPEUTIC TARGET FOR STROKE

By

Jonathan W. Nelson

A THESIS/DISSERTATION

Presented to the Department of Molecular and Medical Genetics
and the Oregon Health & Science University
School of Medicine
in partial fulfillment of
the requirements for the degree of

Doctor of Philosophy

April 2013

School of Medicine

Oregon Health & Science University

CERTIFICATE OF APPROVAL

This is to certify that the PhD dissertation of

Jonathan W. Nelson

has been approved

Nabil J. Alkayed, Mentor

Philip Copenhaver, Chair

Anthony P. Barnes, Member

Xiangshu Xiao, Member

Ines Koerner, Member

TABLE OF CONTENTS

List of Figures

List of Tables

List of Abbreviations

4-PCO: 4-phenylchalcone oxide

AA: Arachidonic Acid

ANOVA: Analysis of variance

AUC: Analytical ultracentrifugation

AUDA: 12-(3-Adamantan-1-yl-ureido)-dodecanoic acid

BiFC: Bimolecular fluorescent complementation

BRET: Bioluminescent resonance energy transfer

BSA: Bovine Serum Albumin

CFP: Cyan Fluorescent Protein

chEH: Cholesterol Epoxide Hydrolase

CHO: Chinese Hamster Ovarian

cLuc-C-terminal of luciferase

COX: Cyclooxygenase

CYP450: Cytochrome P450

DHET: Dihydroxyeicosatrienoic acid

EDHF: Endothelial derived hyperpolarizing factor

EETs: Epoxyeicosatrienoic Acids

EGF: Epidermal Growth Factor

EH: Epoxide hydrolase

EM: Empty

EP7: Epoxyfluor7

HETE: Hydroxyeicosatetraenoic acid

FRET: Förster resonance energy transfer

GFAP: Glial fibrillary acidic protein

GFP: Green fluorescent protein

HEK: Human Embryonic Kidney Cells

HH: Hepoxilin hydrolase

IACUC: Institutional Animal Care and Use Committee

IL-β: interleukin beta

IL-6:interleukin 6

INF-γ: interferon gamma

LC-MS/MS: Liquid-chromatography tandem mass spectroscopy

LOX: Lipoxygenase

LP: Lipid phosphatase

LSM: Laser Scanning Microscopy

LTA_4H :Leukotriene A_4 hydrolase

MAP2: Microtubule-associated protein 2

MCAO: Middle cerebral artery occlusion

mEH: Microsomal Epoxide Hydrolase

nLuc-N terminal of luciferase

NT: Not Transfected

PBD: Peroxisome Biogenesis Disorders

PCC: Pearson's correlation coefficient

Pex5: Peroxin 5

PFA: Paraformaldehyde

$PLA_{2:}$ phospholipase A2

PLI: Peroxisome Localization Index

p-NPP: p-Nitrophenyl Phosphate

PPAR: Peroxisome proliferator-activated receptor

PTS: Peroxisome Targeting Signal

ROS: Reactive Oxygen Species

SEC: Size exclusion chromatography

sEH: Soluble epoxide hydrolase

sEHKO: Soluble epoxide hydrolase knockout

SFL-PFAC: Split-firefly luciferase protein fragment-assisted complementation

SHR: Spontaneously hypertensive rats

SHRSP: Stroke-prone spontaneously hypertensive rats

SNK: Student-Newman-Keuls

SNP: Single Nucleotide Polymorphism

STAIR: Stroke therapy academic industry roundtable

TAT-Trans-activator of transcription

t-AUCB: trans-4- [4-(3-adamantan-1-yl-ureido)-cyclohexyloxy]-benzoic acid

TNF-α: tumor necrosis factor alpha

tPA: Tissue Plasminogen Activator

TRPV4: transient receptor potential cation channels, subfamily V, member 4

RFP: Red Fluorescent Protein

WYK: Wistar Kyoto rat

WT: Wild type

YFP: Yellow Fluorescent Protein

Acknowledgements

It has been said that it takes a village to raise a child, and in my case, the same can be said for raising a PhD student. I am so grateful for all of the people who have supported me on this journey toward graduating with a PhD. This childhood dream of mine would not be possible without the help of all the following people.

The first person I need to acknowledge is my PhD mentor, Nabil Alkayed. It would be impossible to describe how grateful I am that you never let me settle for anything less than my very best. You constantly challenged me to grow, and always believed in me, even in my moments of doubt. I could not imagine a better mentor for my PhD.

The next group of people I want to thank are the members of my Thesis Advisory Committee. Phillip Copenhaver, you were an amazing chair to my committee and I am grateful for all of your help navigating tough obstacles throughout my PhD while also never hesitating to remind me to relax and enjoy the process. Paul Barnes, thank you for always being available for intellectual, technical, and emotional support. Stefanie Kaech-Petrie, you were an incredible mentor and guide into the exciting world of microscopy. And finally, Xiangshu Xiao, without your introduction to split-firefly luciferase I don't think this thesis would have been possible.

Next, to the entire faculty and staff in the Department of Anesthesiology and Perioperative Medicine who helped my scientific development in countless seminars and journal clubs, thank you. In particular, I want to acknowledge Ines Koerner for not only providing the foundation of my project by describing the effect of human

polymorphisms of sEH on neuronal ischemic injury, but also asking me to be a collaborator in her project which resulted in a chapter of this thesis.

I would like to acknowledge all of my fellow researchers in the lab including, Jennifer Young, Kasia Davis, Dominic Siler, Jeff Iliff, Sari Jouihan, and Katie Schenning. In particular, I want to especially acknowledge Jennifer Young for supporting me through all of the challenges of working in a lab and the countless times she provided me with intellectual, technical, and emotional support.

I am thankful for all of volunteers that worked with me: Rishi Subrahmanyan, Anjali Das, Sol Summers, David Horn, and Rohan Borkar. Even if your work did not end up as a part of this thesis, you each contributed to my growth as a scientist. I know that each of you have the potential to develop into amazing scientists.

Additionally, I express my gratitude to all of the professors at OHSU who gave their time through lectures and advice; especially Ujwal Shinde for teaching me how to use PyMol, and Stephen Lloyd for advice about developing a high throughput sEH dimerization screen.

Last but certainly not least, my family.

My wife Kaity, you have been a bedrock through my PhD journey. You were always there for me, amidst my successes and failures, through early mornings and late nights in the lab, and in times of joy and moments of panic. I am grateful for every time you reminded me that balance was important in life, and for never giving up on helping me

find that balance, even when it seemed impossible at times. I could not have earned this PhD without you.

Finally, I am so grateful for the rest of my family, all of whom have supported me in countless ways in my journey as a student. Thank you!

Dissertation Abstract

Soluble epoxide hydrolase (sEH) is a promising therapeutic target for multiple cardiovascular diseases, including stroke. Available inhibitors of sEH target the enzyme's hydrolase catalytic site, which metabolizes lipid molecules shown to be protective against ischemic brain damage called epoxyeicosatrienoic acids. Recently, a human missense polymorphism (R287Q), in the gene that encodes for sEH, designated *ephx2*, was shown to afford a reduction in risk from stroke, despite the fact that the residue is not localized near the hydrolase catalytic site. This suggests the existence of an alternative strategy to reduce sEH enzymatic activity. Based on the localization of the R287 residue on the homodimerization interface of sEH, and previous work showing sEH protein harboring the R287Q polymorphism forms a greater amount of monomers than the wildtype enzyme, I hypothesized that the R287Q polymorphism was conferring protection from ischemia by disrupting dimerization. Specifically, I hypothesized that dimerization was a key regulator for two important aspects of sEH function, hydrolase activity and subcellular localization. To test these hypotheses, I developed a series of mutations predicted to either stabilize or destabilize sEH dimerization by manipulating an inter-monomeric salt-bridge localized at the sEH dimerization interface. I used a split-firefly luciferase complementation system to evaluate the dimerization status of each mutation before quantifying their hydrolase activity. I found that monomeric sEH has decreased activity compared to dimeric sEH, leading to the conclusion that dimerization regulates sEH hydrolase enzymatic activity. Next, I used the previously characterized

dimerization constructs, fused to green fluorescent protein (GFP), to test the effect of dimerization on the subcellular localization of sEH. I found that disrupting sEH dimerization increases peroxisomal localization in primary cortical mouse neurons. Finally, I tested the hypothesis that peroxisomal localization of sEH is protective against ischemic injury. I injected TAT-fused sEH proteins with either an intact or defective peroxisome targeting sequence (PTS) into sEH knockout mice before subjecting them to experimental stroke. I found that mice treated with sEH, which was capable of translocating to peroxisomes, had less brain damage compared to mice treated with sEH protein that is restricted to the cytosol. Taken together, this data suggests that disrupting dimerization may be a novel therapeutic approach for targeting sEH.

Chapter 1

Targeting Soluble Epoxide Hydrolase Dimerization As a Stroke Therapy[a]

Abstract

Stroke is a leading cause of death and serious disability worldwide. While most strokes are preventable with lifestyle changes, therapeutic options once stroke occurs are limited. Therefore, new, safe and effective therapeutic agents are needed. A potential new promising target for stroke therapy is soluble epoxide hydrolase (sEH). Both pharmacological inhibition and genetic knockout of sEH have been shown to be protective in experimental models of cerebral ischemia. Additionally, human single nucleotide polymorphisms (SNPs) in the gene that encodes for sEH, designated *ephx2*, have been correlated with stroke incidence and outcome. This chapter introduces sEH in the context of the five other mammalian epoxide hydrolases before delving specifically into sEH biology. Research into sEH's protein structure, role in metabolizing epoxyeicosatrienoic acids (EETs), regional localization in brain, as well as subcellular localization are discussed in relation to brain function and disease. After evaluating the prospect of using current sEH inhibitors in clinical trials for the treatment of stroke based on the Stroke Therapy Academic and Industry Roundtable (STAIR) criteria, this

[a] Sections of this chapter were originally published in Translational Stroke Research: From Target Selection to Clinical Trials. 2012. Pages 277-294. "Soluble Epoxide Hydrolase as a Stroke Target" by Jonathan W. Nelson, Nabil J. Alkayed ©. They are reprinted here with kind permission of Springer Science+Business Media.

chapter proposes the idea of a novel strategy for inhibiting sEH through the disruption of dimerization.

Stroke and Society

Approximately 800,000 Americans will have a stroke this year. This means that every 40 seconds, on average, someone in the United States has a stroke. Of those individuals, 137,000 will lose their life, making stroke the 4th leading cause of death in the United States. Furthermore, stroke survivors often suffer from crippling disabilities, resulting in indirect costs exceeding 70 billion dollars a year (1).

It is clear that stroke is a devastating disease that occurs far too frequently in our society. The most common form of stroke, ischemia, develops after years of plaque buildup along vessel walls (2). Eventually, a plaque ruptures, releasing a clot that travels through the circulatory system, ultimately finding a blood vessel that is too small for the clot to pass through in the brain. Trapped, the clot restricts blood flow, starving cells in the affected area of oxygen and essential nutrients needed for survival. This sets up a cascade of cellular events culminating in the death of a large number of neurons in tissue lacking perfusion. This area is commonly referred to as the infarct core (3).

One of the first cellular responses to a reduction in oxygen and glucose is the switch to anaerobic glycolysis triggering an increase in free radical formation. Free radical production is further stimulated when cells become reperfused with oxygen. Free radicals are damaging to most cellular processes; however, they are particulary harmful to mitochondria, often leading to mitochondrial failure (3). With the loss of functional

mitochondria, there is not enough energy in the cell to maintain the membrane potential and neurons begin to depolarize. The breakdown of the membrane potential has a number of consequences, ultimately resulting in dead neurons (4). First, it causes an influx of sodium, chloride, and calcium resulting in cytotoxic edema which kills neurons through the process of necrosis. Second, there is an excessive extracellular release of toxic glutamate causing local excitotoxicity further enhancing cell death. Thirdly, there is activation of pro-death pathways culminating in cell death through an apoptotic pathway (3). Adding insult to injury, dead cells in the brain recruit an inflammatory response that exacerbates damage to the infarcted area (5).

Prevention and Treatment of Stroke

The good news is that most strokes are preventable. A large international study examining the factors associated with stroke found that as few as five factors could account for over 80% of strokes. Specifically, hypertension, smoking status, waist-to-hip ratio, diet risk score, and physical activity all contributed to an individual's risk of having stroke (6). These are all manageable risk factors that can be controlled to actively minimize the risk of having a stroke.

The bad news is that once you have a stroke, the therapeutic options are incredibly limited. Despite decades and hundreds of millions of dollars spent doing research, there remains only one FDA approved drug for the treatment of stroke, tissue plasminogen activator or tPA (7). tPA (also known as alteplase) is a thrombolytic agent that works by activiating a proteolytic cascade that dissolves the occluding clot thus limiting the

duration of ischemia (8). While restoration of oxygen and glucose to the brain is a critical step in treating a stroke, tPA does not address the cascade of intra-cellular signals within neurons activated by ischemia that eventually cause their death. Furthermore, tPA is not without its downside. It significantly increases the risk of hemorrhage transformation (9). Because of this, tPA can only be given at a hospital and is only beneficial if given within 4.5 hours from the onset of the stroke (10).

Clearly, new therapeutic strategies beyond tPA are urgently needed. Unfortunately, therapeutic strategies for treating stroke that have looked promising in the lab have fallen short of clinical realization (11). Rational therapies targeting intra-cellular signals known to induce cell death including glutamate excitotoxicity, calcium induced depolarization, and free radical accumulation have shown promise at the bench, yet have been abandoned or failed to pass phase III clinical trials because they have failed to show a positive therapeutic effect (11). However, previous failures have not stopped the search for an effective neuroprotective strategy for treating stroke as there are many ongoing clinical trials examining new treatments for stroke (12).

The focus of my research was a protein called soluble epoxide hydrolase (sEH) which had previously been identified as a novel therapeutic target for stroke (13). The next sections provide a background to give context to sEH before discussing previous therapeutic strategies targeting sEH. Finally, I propose a novel therapeutic strategy for inhibiting sEH based on the protective effect afforded by a human polymorphism of sEH (14,15).

Soluble Epoxide Hydrolase and Stroke

Epoxide Hydrolases

Epoxide hydrolases (EH, EC 3.3.2.3) are a large family of enzymes that catalyze the conversion of an epoxide group to a corresponding vicinal diol. Found ubiquitously in nature, they play a key role in the degradation of both environmental and metabolic epoxides into water-soluble products to facilitate their clearance. Through gene duplication and divergent evolution, EHs became specialized to perform vital functions beyond metabolic conversion of xenobiotics (16). Concomitant with EH evolution, epoxide containing molecules have transitioned beyond metabolic byproducts into important mediators of signal transduction (17). Thus, EH's play a large variety of roles ranging from cytoprotection to cell signaling, making them attractive therapeutic targets (18).

In mammals, five distinct EH enzymes have been identified[b]: microsomal epoxide hydrolase (mEH), cholesterol epoxide hydrolase (ChEH), hepoxilin hydrolase (HH), leukotriene A_4 hydrolase (LTA_4H) and soluble epoxide hydrolase (sEH) (18). The first EH purified from mammals was mEH; a 50kD protein containing a hydrophobic amino terminus which, as its name implies, acts as a membrane anchor to microsomes (19,20). The major function of mEH in the cell is the detoxification of metabolically derived arene epoxides (21). In contrast to mEH, relatively little is known about ChEH. While its activity and endogenous substrate are known, the gene encoding ChEH has yet to be identified

[b] Since the publication of this manuscript an additional epoxide hydrolase was identified: EH3 (151)

(22). HH also has yet to have its coding gene identified. A defining feature of HH is its high substrate specificity for hepoxilins which play key roles in inflammation, smooth muscle tone, and carbohydrate metabolism (18). Interestingly, a recent article suggests that HH and sEH are actually the same enzyme (23). In contrast to the other EHs, LTA_4H is a bifunctional zinc metaloprotease with both EH and aminopeptidase activities (24). Interestingly, the two catalytic domains share a common carboxyl recognition site and therefore a substrate for one catalytic domain inhibits the catalytic activity of the other domain (25).

Knowledge of other EHs is important in not only providing a perspective on the final EH, sEH, it also may be useful in solving mysteries that remain unanswered about the enzyme. This is particularly important because sEH, the focus of this chapter, is a potential therapeutic target for the treatment of stroke.

Soluble Epoxide Hydrolase Protein

Soluble epoxide hydrolase (sEH) is a 62.5kD homodimeric protein encoded by the gene *ephx2* (26). Similar to LTA_4H, sEH is a bifunctional enzyme with both EH and lipid phosphatase (LP) activity (27). Both the amino-terminal LP domain and carboxyl-terminal EH domain contain a canonical α/β-hydrolase fold; however, based on sequence analysis the domains evolved from different ancestral genes. The EH domain most likely evolved from haloalkane dehalogenase while the LP domain evolved from haloacid dehalogenase (28). The fused sEH gene has been identified in the purple sea urchin (*Strongylocentrotus purpuratus*) but not in the nematode *Caenorhabditis elegans,*

hinting at the timeline of the sEH gene fusion event (29). Interestingly, more recent sEH orthologs in frog and chicken contain a LP domain lacking phosphatase activity, suggesting both that 1) sEH has only recently become a functional LP and 2) the evolutionary driving force for the gene fusion event was not enzymatic but possibly structural (30).

The structure of both murine (31) and human (32) sEH proteins have been solved through protein crystalization. Unlike LTA_4H, the two catalytic domains do not share any residues. They are separated by a proline-rich linker suggesting that the activity of the two domains are independent of the other (32). However, the domain-swapped quaternary architecture of sEH has fueled speculation that there may be communication between the two domains (27) (Figure 1). In support of this theory, the EH enzymatic activity of the sEH enzyme in which the LP has been deleted is reduced compared to the complete sEH protein (33). Additionally, mutations in LP domain of sEH affect EH enzymatic activity (34) and conversely, mutations in the EH affect LP activity (35). However, in support of the other hypothesis in which there is no communication between EH and LP domains, Cronin et al. demonstrated that the enzymatic activity of each domain is unaffected by the presence of a substrate for the opposite domain. Furthermore, they showed that the LP activity of sEH is unchanged in the presence of EH inhibitors (36). More work needs to be done in order to understand the interaction

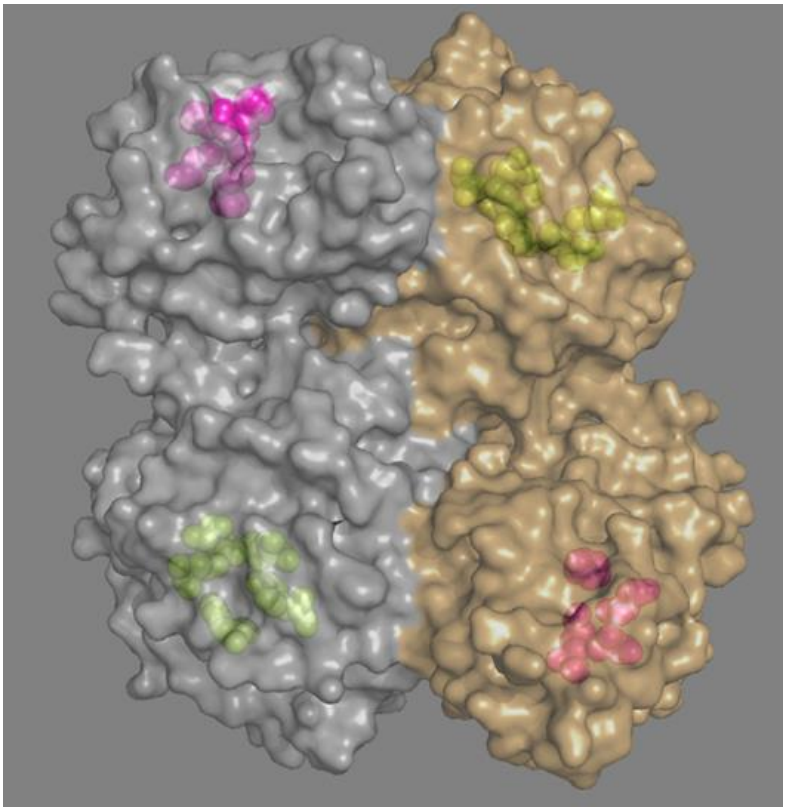

Figure 1 Crystal structure of sEH.

sEH forms a domain-swapped dimer between two monomers (Tan and Gray). The epoxide hydrolase domain (Yellow) binds to the lipid phosphatase domain (purple) of the opposite monomer.

between these two catalytic domains. A major remaining hurdle is the identification of an endogenous substrate for the sEH LP domain[c].

While the catalytic mechanism of the LP domain has been described, the endogenous substrate for this domain remains elusive (37). It was demonstrated that sEH is capable of dephosphorylating an intermediate in cholesterol metabolism, isoprenoid phosphate (35). Further work has shown that both sEH domains may play a direct role in the regulation of cholesterol metabolism (38). Despite this, there is no consensus as to what the endogenous substrate of the LP domain is. Given that the majority of known phosphatases are involved in cell signaling, it is likely that the LP domain of sEH plays an important role in the regulation of a physiological function (39). Therefore until this endogenous substrate has been identified there is a fundamental gap in the sEH field for multiple reasons. Without an identified substrate for the LP domain it is impossible to 1) correctly interpret sEH knockout phenotypes, 2) determine the interaction between the LP domain and EH domain or 3) understand how inhibitors of EH activity affect levels of the LP substrate.

sEH is distributed between the cytosol and peroxisomes. This localization pattern is primarily thought to be the result of a partially active peroxisome targeting signal 1 (PTS1) on the carboxyl terminus of sEH. Instead of the canonical Ser-Lys-Leu, human sEH contains Ser-Lys-Met (40). The substitution of a methionine for a leucine for the final residue in human PTS1 reduces the affinity of sEH to the peroxisome transport protein

[c] Since the publication of this manuscript, two groups identified a potential endogenous substrates for the LP domain of soluble epoxide hydrolase, lysophophatidic acids (LPA) (147,152)

Pex5, resulting in poor import and thus cytosolic localization. Interestingly, the mouse and rat PTS1 signal, Ser-Lys-Ile, is even less active than the human PTS1 (41). There may be other factors; however, that influence the subcellular localization of sEH (40,41).

The purpose for sEHs localization pattern in peroxisomes is another unresolved issue in the sEH field. The following evidence supports a functional role for sEH in peroxisomes. Plant orthologues of sEH are similarly distributed to both the cytosol and glyoxysomes (specialized plant peroxisomes) (18). Additionally, treating mice with clofibrate (a peroxisome proliferation inducing agent) increased sEH activity, supporting a functional link between the number of peroxisomes and sEH (42). However, a substrate for either the EH or LP domain of the sEH contained within peroxisomes remains unknown.

While there is agreement that sEH is distributed between both the cytosol and to peroxisomes, exactly which cells express sEH is currently under dispute. sEH is undeniably expressed in the liver, kidney, and heart among other human tissues tested for immunoreactivity (40,43). sEH is also expressed in the brain, which is of particular interest to stroke researchers. Its expression in human brain has been validated by Western blotting, immunohistochemistry, and an enzymatic activity assay (44). Expression of sEH in mouse brain has also been validated by liquid chromatography tandem mass spectroscopy (LC-MS/MS) (45), Western blotting (46), and immunohistochemistry. Interestingly, expression of sEH in the brain has been shown to be sexually dimorphic with higher sEH protein expression in male mice (47). This finding is supported by further data indicating that estrogen is a negative regulator of sEH

expression in the brain (48). This would suggest that sEH may play a larger role in the pathology of male mice than female mice. Indeed, targeted disruption of sEH resulted in improvements in the hypertension of male but not female knockout animals (49).

Multiple studies have attempted to identify which cells in the brain express sEH; however, some of the data is conflicting in this regard. To date, there has only been one study using human tissue to localize sEH. This study localized sEH to multiple cell types in the brain including neurons, glia, and endothelia (44). Most studies agree that sEH is expressed in the vasculature (15,50,51). However, expression of sEH in neurons is under dispute. While an additional study clearly demonstrates expression in neurons (13), others directly contradict this finding and report that sEH is primarily expressed in glia with only sparse neuronal expression in the medulla (50) or amygdala (52). Data about the cell-specific expression of sEH from cell culture models suggests that both rat primary cultured astrocytes (53) and neurons are immunoreactive for sEH antibodies (15).

Regardless of which cells in the brain express sEH, its abundance strongly suggests it plays a critical role in central nervous system physiology. Based on our current understanding, the most likely role is the regulation of the eicosanoid signaling molecule epoxyeicosatrienoic acids (EETs); the endogenous substrate for its EH domain.

sEH and Epoxyeicosatrienoic Acids

Epoxyeicosatrienoic acids are synthesized from arachidonic acid (AA) by cytochrome P450 epoxygenases (CYP450). The CYP450 pathway has been described as the third arm

of AA metabolism; the first two pathways being lipoxygenase (LOX) and cyclooxygenase (COX) pathways which produce leukotrienes and prostaglandins respectively. AA metabolites are known therapeutic targets to commonly proscribed drugs, including aspirin and singular (Figure 2) (54).

Epoxygenation of AA, particularly by CYP450 2C or 2J isoforms, can occur on any one of the four double bonds present, resulting in four regio-isomers, 5,6-, 8,9-, 11,12- or 14,15-EET (55). In addition to regio-isomer specificity, EETs can also either be *R,S* or *S,R* enantiomers resulting in eight chemically distinct EETs (56). Both the regio-isomer and stereo-isomer profile of EETs varies between CYP450 synthesizing enzyme isoform(57). This is particularly important because the physiological function varies between each EET isoform. Although often lumped together, it is important to note that different EETs have different functions (58).

EETs, acting through multiple mechanisms, have beneficial effects on the outcome of ischemic brain injury. The effects of EETs have been attributed to its contribution to the endothelial derived hyperpolarizing factor (EDHF) response (59). By contributing to the EDHF response, EETs maintain vascular tone thus improving hemodynamics during ischemic events. It is becoming increasingly clear that the EDHF response plays a key role in parenchymal arterioles, rather than in larger cerebral arteries (60).

Recent studies however have shown that the influence of EETs extends beyond acting as an EDHF (61). In particular, EETs have been shown to play a role in neuroprotection, promotion of angiogenesis, as well as suppression of platelet aggregation, oxidative

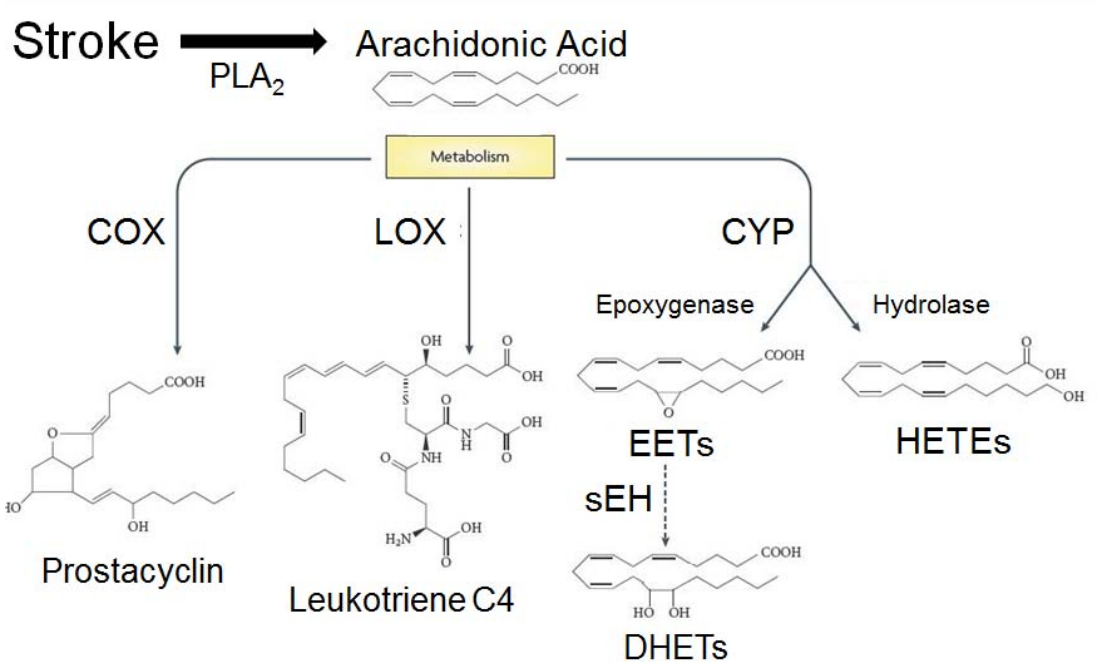

Figure 2 Epoxyeicosatrienoic acid pathway.

One of the cellular responses to stroke is the activation of phospholipase A_2 (PLA_2) which liberates arachidonic acid from the plasma membrane. Epoxyeicosatrienoic Acids (EETs) are synthesized from arachidonic acid by cytochrome (CYP) P450 epoxygenases. EETs are metabolized to their inactive diol form dihydroxyeicosatrienoic acid (DHET) by soluble epoxide hydrolase (sEH). Other metabolites formed from Arachidonic Acid include prostacyclin by cyclooxygenases (COX), Leukotriene's by Lipoxygenases (LOX) and Hydroxyeicosatetraenoic acid by cytochrome P450 hydrolases. Modified from (54).

stress, and post-ischemic inflammation (62). This broad profile of effects has been comprehensively reviewed (62).

Despite the identification of a broad spectrum of effects, the exact mechanism of action of EETs remains unknown. The most plausible explanation is that EETs mediate their actions through binding to an EETs specific receptor (56). In line with this thinking, EETs have been shown to interact with large-conductance calcium activated potassium channels (BK_{Ca}) (63), transient receptor potential cation channels, subfamily V, member 4 (TRPV4) (64), thrombaxane receptors (65), and prostagalandin EP_2 receptors (66).

In addition to interactions with membrane bound receptors, EETs or EET metabolites are peroxisome proliferator-activated receptor (PPAR) ligands. Through binding of the fatty acid binding domain of PPARα (67,68) or PPARγ (69), EETs turn on the transcriptional activity of PPARs. The anti-inflammatory effects of EETs in particular, may be explained through activation of PPARγ (70). Furthermore, the colocalization of EETs synthesizing enzymes and PPARs strengthens the hypothesis of an interaction between the two (71).

While there are many beneficial actions of EETs, they are attenuated by the enzyme sEH which mitigates their biological activity by conversion of an epoxide to a vicinal diol creating dihydroxyeicosatrienoic acids (DHETs) (72). While EETs are regulated through multiple mechanisms including degradation through β-oxidation and incorporation into membrane lipids, metabolism through the sEH pathway has been shown to have the greatest effect on EETs bioavailability (73). Particularly pertinent to the this chapter,

14,15 EET is the preferred substrate metabolized by sEH and therefore most likely to be affected by sEH inhibition or gene deletion (72).

Given that sEH is the most potent regulator of EETs' diverse biological actions, it is no surprise that mutations in the gene encoding for sEH, *ephx2*, have been linked to multiple pathological conditions including ischemia.

sEH Single Nucleotide Polymorphisms (SNPs)

The ephx2 gene is comprised of 19 exons spanning 45kb on the short arm of chromosome 8 (74). The large number of exons as well as the large distance between them makes it exceptionally cost-inefficient to sequence the entire *ephx2* gene. Consequently, the majority of genetic association studies have sought associations with previously identified polymorphisms from past studies or community resources such as HapMap (www.hapmap.org) rather than seeking to identify novel mutations (75).

Of the mutations and polymorphisms identified in the *ephx2* gene, arguably the most interesting are the missense mutations that change the amino acid sequence of sEH. Multiple missense mutations have been identified that are located within both the LP and EH domains (Figure 3). Of these, six have been extensively examined for their effect on sEH properties such as EH activity (34), LP activity (76), and subcellular localization (41). As noted earlier, some of the most interesting findings have been that mutations in one domain of sEH affect the enzymatic activity of the other. However, because the EH activity of sEH is most understood the effect of each polymorphism is often interpreted solely in light of its effect on EETs metabolism.

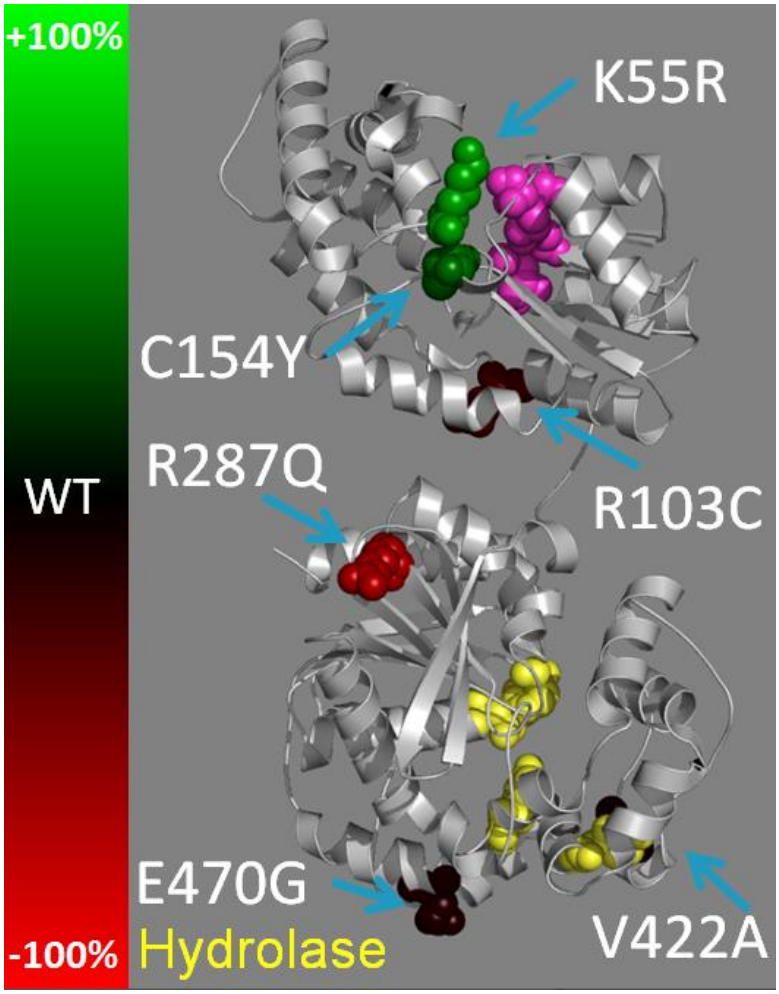

Figure 3. Effect of human polymorphisms of sEH on hydrolase activity.

Common human polymorphisms are colored on the crystal structure of sEH (PBD ID: 1S8O). They are colored on a heat map according to their effect on hydrolase enzymatic activity (77) with polymorphisms that increase hydrolase activity colored green while polymorphisms that decrease activity colored in red. The hydrolase catalytic site is colored in yellow, while the phosphatase catalytic site is colored purple.

Ephx2 polymorphisms have been linked to familial hypercholesterolemia (78), subclinical atherosclerosis (79), coronary heart disease (80), subclinical cardiovascular disease (81), and vasodilatory response (82). Of these, perhaps the most interesting was the association of the K55R mutation with increased risk of cardiovascular heart disease (CHD) within the study population (80). The K55R mutation is known to increase EH activity which therefore would lead to a decrease in cardioprotective EETs levels. It therefore follows that the K55R mutation would be associated with an increased risk of CHD.

More than any other disease, *ephx2* polymorphisms have been studied for their link to ischemic protection or risk (Table 1). One of the first studies to associate *ephx2* polymorphisms with cerebral ischemia found that haplotypes within *ephx2* can either increase or decrease an individual's risk of stroke (83). This is a very interesting finding because it demonstrates that the same protein, sEH, can either be advantageous of disadvantageous depending on its polymorphism status. This is consistent with previous work demonstrating that *ephx2* polymorphisms can either increase or decrease EH activity.

More specific than a haplotype, the same mutation that increased CHD risk, K55R, was shown to increase the stroke risk for Swedish males (84). Conversely, another study directly linked the R287Q polymorphism of sEH to protection from ischemic stroke (14). Previous work demonstrated that the R287Q polymorphism affects sEH by decreasing its EH activity. Therefore this polymorphism should result in increased levels of EETs, in

Ethnicity	Population Number	Main Finding	Reference
ARIC	315 cases, 1,021 controls	Haplotypes can increase or decrease incidence of stroke	(83)
Chinese	200 cases, 350 controls	The R287Q polymorphism was protective from stroke	(14)
Europeans	601 cases, 736 controls	One intronic polymorphism was associated with stroke	(75)
Danish	1430 cases, 37159 controls	No association with *ephx2* polymorphisms and stroke	(85)
Swedish	197 cases, 5560 controls	The K55R polymorphism increased the risk of stroke	(84)

Table 1. Genetic association studies linking *ephx2* variants with stroke.

particular during ischemia, resulting in protection. Further linking the R287Q polymorphism specifically to neuroprotection, it was shown that introducing sEH harboring the R287Q polymorphism to primary cultured rat neurons results in decreased cell death when the neurons were subjected to an *in vitro* model of stroke, oxygen-glucose deprivation (15).

Because of the insight gained from biochemical studies characterizing the effect of sEH polymorphisms on enzymatic activity, investigators have made specific hypotheses about which polymorphisms would be associated with protection. For instance, one study only genotyped polymorphisms of sEH shown to reduce enzymatic activity and looked for protection from both cerebral and myocardial ischemia (85). Unfortunately, this study was unable to find any statistically significant associations. It is important to note that the protective association between the R287Q polymorphism and ischemia has not always been replicated (75). However, this is probably due to the fact that stroke is a complex disorder with multiple factors playing crucial roles is patient outcomes.

In addition to sEH polymorphisms being associated with human cardiovascular disease, mutations in the *ephx2* gene in animal models of cardiovascular disease have been identified that affect activity and expression level. Genetic differences between spontaneously hypertensive rats (SHR) and Wistar-Kyoto rats (WKY) from Charles River were shown to be responsible for increased levels sEH expression in SHR rats. However the inverse expression pattern was found true for SHR and WKY rats from the

Heidelberg SP substrain suggesting an association of these polymorphisms with sEH expression but not hypertension (86). Another study found a variant of *ephx2* that increased transcription, protein expression, and activity was associated with spontaneously hypertensive heart failure rats (SHHF) (87). Further linking sEH to stroke, SNPs contained within the promoter of *ephx2* are also thought to be responsible for differences in the levels of sEH expression and activity determined in SHR/A3 (stroke prone) and SHR/N (stroke resistant) rats (88).

Clearly, these studies identifying a link between *ephx2* polymorphism status and ischemic risk support a role for sEH in ischemic outcome. Investigations into how genetic knockout of sEH affects ischemic outcomes have further supported a link between *ephx2* and ischemia.

sEH Knockout (sEHKO) Mice

Soluble epoxide hydrolase knockout (sEHKO) mice were first generated in 2000 for the purpose of studying the effect of sEH on hypertension (49). Since then, sEHKO mice have been an invaluable tool for studying the effect of sEH on cardiac arrest (89), inflammation (90), cholesterol regulation (38), atherosclerosis (91), vascular remodeling (92), hyperlipidemia (93), hyperglycemia (94), as well as myocardial and cerebral ischemia.

In addition to maintaining blood flow during ischemia, sEH gene deletion also attenuates the inflammatory response to ischemia (48). While expression of inflammatory cytokines tumor necrosis factor alpha (TNF-alpha), interleukin 6 (IL-6),

interferon gamma (INF-gamma), interleukin beta (IL-beta) were upregulated in the ipsilateral hemisphere (stroke side) compared to the contralateral hemisphere, this induction was significantly reduced in sEHKO mice compared to wild-type mice.

While sEHKO mice were shown to be protected from experimental ischemia, they had reduced survival after cardiac arrest and cardiopulmonary resuscitation (89). This finding was unexpected, but may be explained by EETs' potent effect as a vasodilator. Because sEHKO mice have increased levels of EETs, and thus dilated vessels, sEHKO mice were unable to restore sufficient blood upon resuscitation. It is unlikely that sEHKO mice have a cardiac dysfunction given that they had indistinguishable cardiac mass and myocardial function compared to wild type mice. Additionally, EETs have been shown to be pulmonary vasoconstrictors which may also have contributed to the reduced survival of sEHKO mice after cardiac arrest and cardiopulmonary resuscitation.

Interpreting the phenotypes of knockout animals is difficult, and sEHKO mice in particular have multiple confounders. As noted earlier, while sEHKO mouse phenotypes are often interpreted in light of their effect on EETs, sEHKO mice also lack the LP domain. Another confounder of sEHKO mice involves physiologic compensation. Because sEHKO mice lack sEH throughout development, this allows time for alternative mechanisms to develop to make up for the lack of sEH activity. This was observed in one study which showed that sEHKO mice compensate for increased levels of vasodilating EETs with increased levels of vasoconstricting 20-HETE (95).

Knockout confounders notwithstanding, sEHKO mice support a protective role for inhibiting the activity of sEH during ischemia. However, in order to translate this basic science finding into the clinic, specific pharmacological agents needed to be developed that inhibit sEH.

Development of sEH Inhibitors

Because the main function of sEH is thought to be the regulation of EETs through its EH domain, potent and selective inhibitors for this domain have been developed for research and clinical use. Even though these inhibitors have been shown not to influence sEH's other enzymatic activity, LP, they are still termed sEH inhibitors. On a side note, there are a few sEH lipid phosphates inhibitors available, although they have not been as extensively developed or studied as EH inhibitors (33).

Based on the crystal structure of sEH and the catalytic mechanism epoxide hydrolysis, it was noted that amides or urea groups fit exceptionally well into the EH catalytic pocket. Specifically, that the carbonyl oxygen of either an amide or urea would interact with Tyrosine 381 and Tryrosine 465 while the N-H group would act as a hydrogen donor to Aspartate 333, the nucleophile that attacks epoxide bonds (96). In addition to ureas and amides, chalcone oxides, carbamates, acyl hydrazones, trans-3-phenylglycidols, and aminoheterocycles have been developed as sEH inhibitors. These inhibitors are however not commonly used (96). Currently, the best sEH inhibitors are 1,3-disubstituted ureas, amides, and carbamates with IC_{50} values in the low nanomolar range (97). The most currently used inhibitors are selective, however it was observed

that the sEH inhibitor AUDA activates peroxisome proliferator-activated receptor alpha (PPAR alpha) (98).

Supporting previous work demonstrating that elevated EETs levels are beneficial against a number pathological conditions, sEH inhibitors have multiple effects. They are anti-inflammatory, anti-algesic, anti-atherosclerotic, anti-hypertensive, as well as renal, neuronal and myocardial protective (97). This wide profile of effects has made the development of sEH inhibitors an attractive target for both basic research and pharmacological companies. Indeed, University of California, Arete, Boehringer Ingelheim, Merck, and GlaxoSmithKline have all filed patents regarding the development and application of sEH inhibitors (96).

sEH Inhibitors and Ischemia

The multiple effects of increasing EETs with sEH inhibitors makes testing their effect on ischemic brain damage a natural fit. Specifically, decreasing inflammation, apoptosis, and thrombosis, all should have a beneficial effect on improving stroke outcomes (62). In fact, multiple sEH inhibitors have been used in several animal models which have all shown protection from cerebral ischemia (Table 2).

Alkayed and colleagues identified sEH inhibition as a viable therapeutic strategy for the treatment of stroke (13). They found that giving mice the sEH inhibitor AUDA-BE, either 30 minutes before a 2-hour middle cerebral artery occlusion (MCAO) or at the time of reperfusion, significantly decreased infarct volume compared to vehicle treated mice. Unexpectedly, and in contrast to findings with sEHKO mice, they did not observe any

Ischemia sEH Inhibitor Studies					
Inhibitor	**Model**	**Dose**	**Administration**	**Duration**	**Reference**
AUDA	Rats	25mg/L	Drinking Water	6 weeks	(99)
AUDA-BE	Mice	10mg/kg	Intraperitoneal	0, 30 min	(13)
4-PCO	Primary Neurons	1 µM	Culture Media	60 min	(15)
AUDA	Rats	2mg/day	Drinking Water	6 weeks	(61)
t-AUCB	Rats	2mg/day	Drinking Water	1 week	(61)

Table 2. sEH inhibitor studies demonstrating ischemic protection.

difference in blood flow as measured by iodoantipyrine autoradiography; however, they were able to link the protection to EETs. When they treated mice both with AUDA-BE and MS-PPOH, an inhibitor of EETs synthesis, the ischemic protection of the sEH inhibitor was lost.

Another research group showed that chronic treatment with a slightly different sEH inhibitor, AUDA, improved stroke outcome in stroke-prone spontaneously hypertensive rats (SHRSP) (99). AUDA was given to SHRSP for six weeks before receiving a MCAO. Similar to the results found by Alkayed and colleagues, AUDA treated SHRSP mice had a smaller infarct volume. This effect was found to be independent of changes in blood pressure or vascular structure even though they observed an increase in the passive compliance of cerebral vessels with AUDA treatment.

In another study, the sEH inhibitor t-AUCB was shown to protect SHRSP rats from ischemic brain damage (61). In this study, SHRSP rats were treated for one week with t-AUCB before being subjected to MCAO. t-AUCB is a chemically significantly different inhibitor from AUDA or AUDA-BE in that it does not have the long fatty acid chain thought responsible for AUDA's PPAR-alpha activation. Therefore the ischemic protection observed in t-AUCB treated mice suggests that AUDA's effect was largely mediated by its effect on EETs stabilization and not on PPAR-alpha activation.

Additionally, this study observed transcriptional changes apoptotic genes in brains from AUDA treated rats. Interestingly, they found a reduction in pro-apoptotic transcription factors in both SHRSP and WYK rats compared to vehicle treated rats. This change in

pro-apoptotic transcription factors supports a role for neural in addition to vascular protection by treatment with sEH inhibitors. Further supporting a role for sEH inhibitors as neuroprotective agents, a study using the sEH inhibitor 4-PCO found that primary cultured rat neurons over-expressing sEH where protected from oxygen-glucose deprivation-induced cell death (15).

These studies all agree that the use of sEH inhibitor is protective against stroke. In fact, they suggest that sEH inhibitors may be protective against the effects of cerebral ischemia by multiple mechanisms making them even a more attractive therapeutic option than previous stroke therapeutics that target a single mechanism. Therefore, the question should be asked: are we ready for sEH inhibitor clinical trials for stroke?

Are We Ready For a sEH Inhibitor Clinical Trial for Stroke?

Within this chapter, multiple lines of evidence have been presented that suggest sEH is a novel and exciting target for the treatment of stroke. From human and rodent genetic polymorphisms that are linked to stroke risk, to the protective effects against ischemia of both sEH gene deletion and pharmacological inhibition on ischemia, study after study supports the protective effect of increasing EETs levels through the inhibition of sEH. Furthermore, the availability of an sEH inhibitor which has successfully completed phase I clinical trials makes moving forward with sEH clinical trials for the treatment of stroke even more tempting. But, are we ready?

The STAIR preclinical criteria were generated to aid in making this exact judgment (100). The STAIR, or Stroke Therapy Academic and Industry Roundtable, was formed in

response to the repeated failure of clinical trials for the treatment of stroke. In particular, strategies that block calcium channels, scavenge free radicals (e.g. NXY-059), and glutamate receptor antagonists were moved through clinical trials without success despite laboratory evidence to the contrary.

To better judge whether a neuroprotective strategy has sufficient supporting evidence to warrant a clinical trial, the STAIR panel produced a set of preclinical research criteria. These criteria were designed to enhance the likelihood of a favorable clinical trial outcome if utilized by investigators.

The STAIR preclinical criteria have been summarized into ten key points (101). As can been seen in Table 3, sEH inhibitors meet six of the ten criteria. These include evidence of ischemic protection from more than one laboratory. Animal testing of sEH inhibitors has also shown them to be protective in more than one species including a human disease model. Furthermore, sEH inhibitors can be delivered in a feasible manner, such as 1 hour after the time of occlusion. However, there are STAIR preclinical criteria that sEH inhibitors have not yet met. These include testing in both male and female mice, as well as testing at two different doses of inhibitor. Furthermore, behavioral measurements have not been made on animals treated with sEH inhibitors, in particular long term behavioral studies are lacking. Therefore, based on the STAIR preclinical recommendations, more work is needed before sEH inhibitors are considered for clinical trials.

Item	Criteria	Description	sEH status	Reference
1	Lab validation	Focal model tested in two or more laboratories	+	(13,99)
2	Animal species	Focal model tested in two or more species	+	(13,99)
3	Animal Health	Focal model tested in old or diseased animals	+	(99)
4	Sex of animals	Focal model tested in male and female animals	-	
5	Reperfusion	Tested in temporary and permanent models of focal ischemia	+	(13,99)
6	Time window	Drug administered 1 hour after occlusion in focal model	+	(13)
7	Dose Response	Drug administered using at least two doses in focal model	-	
8	Delivery	Tested using a feasible mode of delivery	+	(50,61)
9	Endpoint	Both behavioral and histological outcomes measured	-	
10	Long-term	Outcome measured 4 weeks after occlusion in focal models	-	

Table 3. sEH and the initial STAIR criteria.

Adapted from (101).

Unfortunately, publication of the STAIR preclinical criteria in 1999 did not improve the effectiveness of subsequent clinical trials for stroke. Therefore, in 2009 the STAIR preclinical criteria were expanded. In addition to emphasizing the importance of the initial criteria, further recommendations were made. These include suggestions that laboratory stroke studies should be designed to ensure they are sufficiently powered to support their conclusion. They also recommend that it is essential that stroke studies be randomized and blinded. Furthermore, they emphasize the importance of preclinical experiments on aged and diseased animals, especially animals with comorbid conditions such as hypertension, diabetes, and hypercholesterolemia. Finally, they recommend collecting a biomarker in the animal studies that can also be obtained from patients during the clinical trial to indicate the therapeutic treatment is working in humans as it did in preclinical animal studies.

Currently, sEH inhibitors have not been reported to have met any of these amended STAIR criteria. Therefore they should act as a guide for current investigators to focus their sEH ischemia studies in addition to the missing components of the initial STAIR criteria. A retrospective analysis of stroke clinical trials up to 2006 showed that the effectiveness of treatment strategies in clinical trials was not different than those reported in preclinical experiments, emphasizing the importance of thorough preclinical studies (101). Therefore a more complete preclinical evaluation of sEH inhibitors is essential for making the decision to move them forward through clinical trials.

Soluble Epoxide Hydrolase Dimerization As a Novel Therapeutic Target

While inhibiting sEH, by targeting the hydrolase catalytic site, has yielded promising results as a stroke therapeutic, it has yet to be translated into the clinic, leaving the door open to the development of novel strategies for inhibiting sEH. Furthermore, the protective effect afforded by the R287Q human polymorphism, which is not localized near the hydrolase catalytic site of sEH, suggests that targeting the hydrolase catalytic site may not be the only effective strategy for targeting sEH for therapeutic effect.

Studying the mechanism behind the protective effect afforded by the R287Q human polymorphism is the focus of my thesis. I wanted to elucidate the mechanism by which sEH protein harboring the R287Q human polymorphism was shown not only to be associated with a decreased incidence of stroke (14), but also protects neurons from ischemic injury (15).

Multiple lines of evidence suggest that sEH forms a domain-swapped dimer, such as a dimeric crystal structure (31), and size-exclusion chromatography showing sEH eluting through a column at a molecular weight corresponding to 130 kD, the expected weight for a dimer (76). However, the R287Q human polymorphism causes a shift in the dimerization state of sEH resulting in roughly equal amounts of sEH monomer and sEH dimer (76). This suggests that the R287 residue plays an important role in stabilization of sEH dimerization.

This dimer-stabilizing role is supported by the localization of the R287 residue within the sEH dimer structure (Figure 4A, blue arrow) (34). It is localized in the center of the sEH

dimerization interface in close proximity to the E254 residue of the opposite binding monomer (102) (Figure 4B). This is significant, because when a positive charged residue is in close proximity to a negatively charged residue, it is able to form a strong bond called a salt-bridge (103). In the case of sEH, the E254 and R287 residues are forming a dimer-stabilizing salt-bridge.

I hypothesized that the disruption in sEH dimerization by the R287Q polymorphism was responsible for two effects. First, decreasing sEH hydrolase activity (34) and second, shifting sEH to localize to peroxisomes (41). Furthermore, I hypothesized that both of these actions were mechanisms of protection.

However, before I outline the goals of my thesis, I will briefly discuss the role that dimerization has been shown to play in other proteins

Dimerization and Protein Function

Biological systems rarely act in isolation, and one way that networks of protein act together is through assembly into dimers or higher order oligomers (104). When a protein interacts with itself, which is the case for sEH, it is termed homodimerization. One study estimates that roughly 45% of human proteins dimerize (105). However, it should be noted that this may be an over-estimate because one of the techniques used to determine dimerization, protein crystallography, has led to a large number of false-positive dimers (104).

Dimerization can be a means by which proteins regulate their function in response to environmental conditions. When in an oxygen rich environment, hemoglobin forms

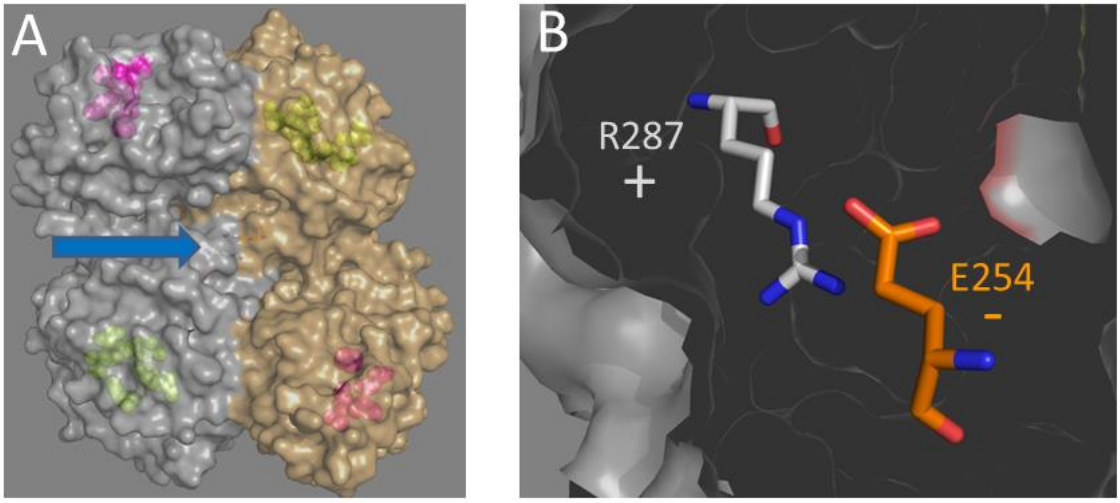

Figure 4. Location of E254R-R287E salt bridge.

A) The R287 residue is localized to the center of the sEH protein on the dimerization interface (blue arrow). B) The positively charged R287 residue is localizes close to the negatively charged E254 residue of the opposing binding partner forming a dimer-stabilizing salt-bridge.

dimers which have a higher affinity for oxygen than tetramers. Dimerization can also cause enzyme activation such as in the case of caspase-9 which binds to Apaf-1 causing an apoptotic cascade (106). Conversely, dimerization has also been shown to negatively regulate enzymes such as in the case of the protein tyrosine phosphatase-α (RPTPalpha) (107). In this case, the dimerization interface for the enzyme is its catalytic site, which in a dimer form is occupied by the binding protein.

The large number of dimerizing enzymes has generated multiple hypotheses on the evolutionary origins behind dimerization (108). One hypothesis is that 3D domain swapping is the a driving mechanism behind dimerization (109). This hypothesis is a particularly interesting given the fact that sEH is a domain-swapped dimer. In this hypothesis, domain swapping provides a preformed associating interface, negating the need for chance association or multiple mutations necessary to promote dimerization as speculated by other hypotheses (110).

A wealth of tools have been developed to study protein interactions such as dimerization (111). These include, but are not limited to, bimolecular fluorescent protein complementation (BifC), Förster resonance energy transfer (FRET), bioluminescent energy transfer (BRET), immunoprecipitation, crystallography, crosslinking, size exclusion chromatography (SEC), and analytical ultracentrifugation (AUC). Each tool or technique has its strengths and weaknesses. For example, BiFC is an excellent tool used to visual dimerization within living cells; however, the interaction between the associating fragments may act as an artificial stabilizing force leading to

false-positive associations (112). On the other hand, tools like crystallography, SEC, and AUC, which often do not require any modification to proteins, require a large mass of highly concentrated and purified protein that can be prohibitive to many experimental systems (113).

In addition to regulating enzymatic activity, dimerization often plays a key role in the dynamic localization of proteins. The importance of correctly targeted localization of proteins within the cells is discussed next.

Localization and Protein Function

Eukaryotic cells are divided into spatially discrete subdomains called organelles. The evolution of these organelles is a controversial field. While it is generally agreed upon that some organelles, such as mitochondria, arose through endosymbiosis, the mechanism by which other organelles, such as peroxisomes, arose remains unclear (114). Regardless of the evolutionary origins of different organelles, their existence allows for the metabolic compartmentalization of essential pathways within the cell.

However, for these discrete organelles to carry out their metabolic functions, proteins need to correctly localize to them. Indeed, a large number of diseases are the result of a protein not localizing to the correct subcellular compartment (115). These diseases can be the result of transcription factors unable to localize to the nucleus, miss-targeting of mitochondrial enzymes, or even mutations resulting in proteins being trapped in the endoplasmic reticulum (115).

One of the clearest examples of the importance of proper protein localization in health are peroxisome biogenesis disorders (PBD). PBD are a large spectrum of disorders that result from defective peroxisomes. While PBD can be caused by mutations that affect proteins essential for peroxisome membrane integrity, they also can be caused simply by mutations in the gene that encodes for the peroxisome transport protein gene peroxin 5 (Pex5) (116). This example is particularly illustrative because it links the localization, but not the expression of a protein, to a disease state. Simply the misslocalization of proteins out of peroxisomes results in abnormal metabolism resulting in some PBD (117).

Similar to studying dimerization, a wealth of tools have been developed to study protein localization. One common tool is the use of antibodies that can be used to visualize proteins through immunocytochemistry or immunohistochemistry. One of the benefits of using antibodies is that it allows for the visualization of endogenously expressed proteins in either cells or tissue. However, one of the major concerns when using antibodies to study protein localization is their specificity to binding to the protein target.

Another tool for studying protein localization is the fusion of a fluorescent protein, such as green fluorescent protein (GFP), to a protein of interest. This has the advantage of being able to image in living cells (118). Additionally, fusing proteins with GFP negates the need for the development of antibodies that specifically bind to the protein of interest. However, one of the weaknesses of GFP fusion is that it affects the system that

is being studied. Specifically, that GFP fusion and overexpression may result in aberrant localization of a protein.

Peroxisomes and sEH

Peroxisomes are small single membrane compartments that are found in all eukaryotic cells (119). They are between .5 and 1.5 μm in diameter and have an oval like shape. In mammals, peroxisomes play an important role multiple metabolic pathways, including those for very-long-chain fatty acids, reactive oxygen species, and epoxides (120). As discussed previously, the importance of these pathways is highlighted by peroxisome biogenesis disorders resulting from defective peroxisomes (117).

Peroxisome function is dependent on the import of proteins into the peroxisomes. To achieve this, peroxisomes have developed two distinct protein import pathways. One pathway is dependent on the peroxisome transport protein peroxin 5 (Pex5) while the other is dependent on the peroxisome transport protein peroxin 7 (Pex7). Which pathway proteins use to translocate to peroxisomes is dependent on their peroxisome targeting signal (PTS) (121). Pex5 transport dependent proteins contain the C-terminal PTS1 tripeptide sequence (S/C/A)(K/R/H)(L/M), while Pex7 transport dependent proteins contain the N-terminal PTS2 peptide sequence (R/K)(L/V/I)X5(H/Q)(L/A) (41). These sequences act as a ligand for the association between targeted proteins and their associated transport protein.

The enzyme that is the focus of this thesis, sEH, is capable of translocating to peroxisomes (40). This ability to translate was shown to be the result of a weak PTS1 on

its C-terminus. sEH also has a non-functional PTS2 consensus sequence (41). sEH is the only human protein to end in the Serine-Lysine-Methonine (-SKM) tripeptide sequence, which has less affinity for the peroxisome transport protein peroxin 5 (Pex5) than the canonical PTS tripeptide Serine-Lysine-Leucine (-SKL) (122). Indeed, the dual localization of sEH between the cytosol and peroxisomes can be shifted exclusively to the peroxisomes by changing the sEH C-terminal PTS to -SKL (41). However, the lower affinity of –SKM may not provide a complete answer to sEH's dual localization, as recent evidence suggests the protein quaternary structure of sEH may also be a contributing factor to the distribution of sEH within the cell (41).

Specifically, sEH protein harboring the R287Q polymorphism was shown to have enhanced peroxisome localization in Chinese Hamster Ovarian (CHO) cells (41) despite having the same –SKM PTS as wildtype sEH. This same polymorphism was previously shown to partially disrupt sEH dimerization suggesting a correlation between the dimerization of sEH and its subcellular localization (76). For my thesis, I wanted to further investigate the relationship between dimerization and the subcelluar localization of sEH.

Overview of Thesis

I set out to test the hypothesis that dimerization is required for the proper sEH functioning. More specifically, that the ischemic protection afforded by the R287Q human polymorphism of sEH is directly related to its effect on dimerization.

I hypothesized that disrupting sEH dimerization would have two effects (Figure 5). First, that disrupting dimerization would decrease sEH hydrolase activity and second, shift sEH localization to peroxisomes (41). Furthermore, I hypothesized that both of these actions were mechanisms of ischemic protection.

In chapter 2, I test the hypothesis that dimerization is required for the hydrolase activity of sEH. I use site-directed mutagenesis to create mutations that alter the dimerization state of sEH and quantify the change in dimerization and hydrolase enzymatic activity.

In chapter 3, I test the hypothesis that dimerization regulates the subcellular localization of sEH. I fuse the same mutations used in chapter 1 to green fluorescent protein (GFP) and quantify the colocalization of GFP-sEH signal with peroxisomes in primary cultured cortical mouse neurons. In chapter 4, I test the hypothesis that peroxisome translocation of sEH plays a protective role in ischemia by reintroducing sEH protein with or without a peroxisome targeting signal to sEH knockout mice before subjecting them to a model of stroke.

I conclude, in chapter 5, with a summary my findings and discuss ongoing work exploring the possibility of pharmacologically inhibiting sEH dimerization. Finally, I discuss questions that remain unanswered and propose experiments that may provide some answers.

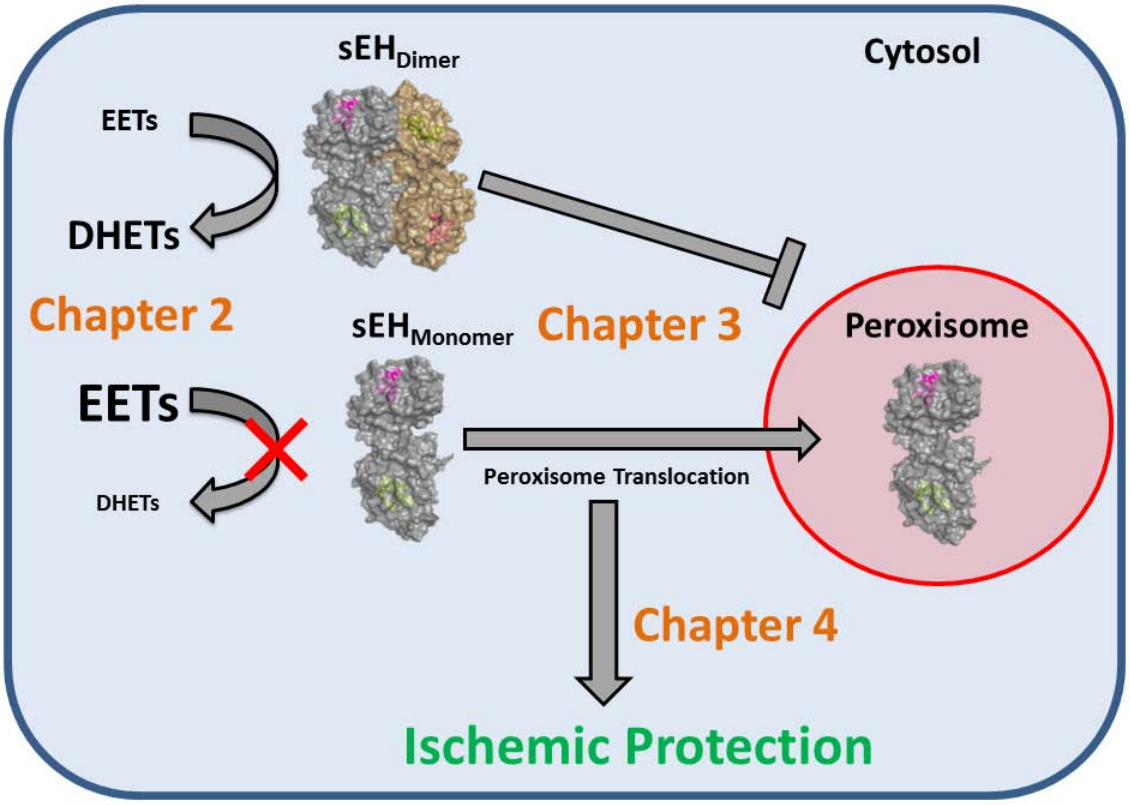

Figure 5. Diagram of thesis chapters.

As a dimer sEH is active with epoxide hydrolase and is restricted from peroxisomes. In chapter 2, I test the hypothesis that disrupting sEH dimerization decreases hydrolase activity which would result in increased levels of EETs. Next, in chapter 3, I test the hypothesis that disrupting dimerization enhances translocation of sEH into peroxisomes. Finally, in chapter 4, I test the hypothesis that peroxisome translocation of sEH is protective against ischemic injury.

Chapter 2

Dimerization and Soluble Epoxide Hydrolase Activity[d]

Jonathan W. Nelson, Rishi M. Subrahmanyan, Sol A. Summers, Xiangshu Xiao and Nabil J. Alkayed

Abstract

Soluble epoxide hydrolase (sEH) plays a key role in the metabolic conversion of the protective eicosanoid 14,15-epoxyeicosatrienoic acid (14,15-EET) to 14,15-dihydroxyeicosatrienoic acid (14,15-DHET). Accordingly, inhibition of sEH hydrolase activity has been shown to be beneficial in multiple models of cardiovascular diseases; thus identifying sEH as a valuable therapeutic target. Recently, a common human polymorphism (R287Q) was identified that reduces sEH hydrolase activity and is localized to the dimerization interface of the protein suggesting a relationship between sEH dimerization and activity. To directly test the hypothesis that dimerization is essential for the proper function of sEH, we generated mutations within the sEH protein that would either disrupt or stabilize dimerization. We quantified the dimerization state of each mutant using a split-firefly luciferase protein fragment-assisted complementation system (SFL-PFAC). The hydrolase activity of each mutant was determined using a commercially available fluorescent assay. We found that mutations that disrupted dimerization also eliminated hydrolase enzymatic activity. In contrast, a mutation that stabilized dimerization restored hydrolase activity. Finally, we

[d] This research was originally published in the Journal of Biological Chemistry. Jonathan W. Nelson, Rishi M. Subrahmanyan, Sol A. Summers, Xiangshu Xiao and Nabil J. Alkayed. Dimerization and Soluble Epoxide Hydrolase Activity. Journal of Biological Chemistry. 2013; 288 (11): 7697-703 © the American Society for Biochemistry and Molecular Biology.

investigated the kinetics of sEH dimerization, and found that the R287Q human polymorphism was metastable and capable of swapping dimer partners quicker than the WT enzyme. These results indicate that dimerization is required for sEH hydrolase activity. Disrupting sEH dimerization may, therefore, serve as a novel therapeutic strategy for reducing sEH hydrolase activity.

Introduction

Soluble epoxide hydrolase (sEH) forms a domain-swapped dimer where the hydrolase domain of one monomer binds to the phosphatase domain of the opposite monomer (27,36). While sEH exhibits two enzymatic activities, it is the hydrolase activity, which converts the protective eicosanoid 14,15-epoxyeicosatrienoic acid (14,15-EET) to its vicinal diol 14,15-dihydroxyeicosatrienoic acid (14,15-DHET) that is most understood (62). Inhibition of sEH hydrolase activity either by pharmacological tools or gene deletion has been shown to be protective in multiple models of cardiovascular diseases; thus identifying sEH as a valuable therapeutic target (13,46). Additionally, multiple missense human polymorphisms have been identified throughout the structure of the protein that alter the hydrolase enzymatic activity of sEH (34). Specifically, an R287Q human polymorphism has been shown *in vitro* to decrease the hydrolase activity (34). Surprisingly, the R287 residue is not located near the hydrolase catalytic site, suggesting that its effect on the enzyme cannot be explained by a simple perturbation of the active site fold or by interference with substrate binding. Based on the crystal structure of sEH (31), the R287 residue is localized near the center of the enzyme on the dimerization interface (34). This would suggest that the effect of this polymorphism may be

functionally linked to its effect on dimerization. Further supporting a critical role for this residue in the stabilization of sEH dimerization is its close proximity (within 4 Å) to the E254 residue on the opposing monomer, where it may be forming an inter-monomeric salt-bridge (34,76). Indeed, it has been shown previously that sEH protein harboring the R287Q polymorphism forms increased amount of monomer compared to the wild type protein (76). We set out to directly test the hypothesis that sEH dimerization is required for hydrolase activity using mutational analysis. We mutated the residues in the putative E254-R287 dimer-stabilizing salt-bridge to either disrupt or stabilize sEH dimerization. We established a split-firefly luciferase protein fragment-assisted complementation (SFL-PFAC) system to validate sEH dimerization and measured sEH hydrolase activity with a fluorescent substrate of sEH (123–125). Understanding the mechanism by which the R287Q polymorphism (Hapmap frequency between .08 and .24) affects sEH enzyme is highly clinically relevant, and may shed light on the pleotropic clinical manifestations of this polymorphism (14,81,82,126). Additionally, this research supports the development of novel therapeutic strategies for inhibiting sEH hydrolase activity.

Experimental Procedures

Mutagenesis of sEH Salt-Bridge Residues

Mutagenesis of sEH was generated using the Quikchange Site Directed Mutagenesis Kit (Stratagene) according to the manufacturer's instructions. Mutagenesis primers to create R287E and E254R mutations were designed with QuikChange Primer Design Program (http://www.stratagene.com/qcprimerdesign). Briefly, 100 ng of sEH wild type

template and 100 ng of each mutagenic primer were used in the reaction with a total reaction volume of 25 µl. After 30 cycles of PCR amplification of DNA template, 1 µl of DpnI restriction enzyme was added to 10 µl of each amplification reaction and incubated at 37 °C for 3 h. 1.5 µl of the DpnI-treated DNA from each mutagenesis reaction was used to transform XL10-Gold ultracompetent cells. The DNA was purified using Qiagen purification kit according to the manufacturer's instructions. All mutations were confirmed by DNA sequencing.

Creation of sEH-Luciferase construct

C- and N-terminal split-firefly fragments were described previously (125). Human soluble epoxide hydrolase was amplified with PCR using primers that added a 3' NheI site and a 5' SacI site and ligated into the split-firefly luciferase vectors. All constructs were verified by restriction enzyme digestion and DNA sequencing.

Transfection of HEK cells

Human embryonic kidney (HEK) cells were either singly or cotransfected according to the manufactures recommendations with different expression plasmids premixed with Lipofectamine^{TM} 2000 (Invitrogen) and cultured overnight in Opti-MEM medium.

Luciferase Activity Assay

Transfected HEK cells were lysed with Passive Lysis Buffer (Promega) supplemented with protease inhibitor cocktail (Roche). The luminometer assays for firefly luciferase activity were performed using Promega Dual-Luciferase reporter assay system according to

instructions. The luciferase activity was measured using Lumat LB 9507 luminometer (Berthold Technologies).

Hydrolase Activity Assay

Soluble epoxide hydrolase activity was determined using Epoxy Fluor 7 (EP7) (Cayman Chemical Company). Cells were lysed in Passive Lysis Buffer (Promega) supplemented with protease inhibitor cocktail (Roche) on ice before immediate quantification of hydrolase activity. Hydrolase activity was assessed as previously described (123). Briefly, reactions were carried out in 200 μL of 25 mM BisTris-HCl containing 1 mg/mL bovine serum albumin (BSA) and the substrate EP7. The resulting solution was incubated at 37°C in a black 96-well flat bottom plate (Corning). Fluorescence of hydrolyzed EP7 was determined using an excitation wavelength of 330 nm (bandwidth=20 nm) and an emission wavelength of 465 nm (bandwidth=20 nm) on a plate reader (VICTOR, Wallac/Perkin Elmer).

Determination of K_m and V_{max}

K_m and V_{max} of sEH constructs were determined using the following concentrations of EP7: 0.5, 1, 2.5, 5, 7.5, 10, 20, and 40 μM. 10 μL of crude cell lysates from each transfection was used in each reaction, and the amount of DMSO was kept constant at 1.6%. Data was collected from three independently transfected cultures in duplicate. Substrate concentration was plotted against initial velocities for each construct to derive K_m and V_{max} using Prism 5 (Graphpad).

Protein Rendering

Pymol was used for protein modeling (Delano scientific). The crystal structure for mouse sEH (PDB ID: 1CR6) (31) was used for modeling the sEH salt-bridge because it was crystallized as a dimer. In the human enzyme, the R287 and E254 residues are homologous to the mouse R285 and E252 residues.

Immunoblotting

Transfected HEK cell lysates were separated by SDS-PAGE (90 min, 200 V) and transferred to Amersham Hybond-LFP membranes (GE Healthcare) at 35 V for 2 h. After blocking with 3% ECL Advanced Blocking Agent (GE healthcare) in PBS containing 0.1% Tween. sEH-Luciferase constructs were detected with anti-Flag HRP-conjugated antibody (Sigma, 1:1000). Antibody was incubated on membrane for 2 hours at room temperature before being washed out 3 times in PBS-T. Chemiluminescence was then detected using Super Signal West Dura Extended Duration Substrate (Thermo Scientific) with a FluorChem FC2 (Alpha Innotech). Densitometry was quantifying with AlphaView software (Alpha Innotech).

Statistics

For multiple group comparisons, one-way analysis of variance (ANOVA) was performed, followed by Student-Newman-Keuls (SNK) post-hoc analysis. For dimerization time-course studies, repeated measures, two-way ANOVA was performed with one factor being time and the other being mutation status, followed by SNK post-hoc analysis.

Results

Generation of sEH dimerization mutants

Based on the dimeric structure of sEH, the R287 residue is located in the center of the protein (Figure 6A) and on the dimerization interface (Figure 6B). Furthermore, the R287 residue is localized in close proximity to the E254 residue of the opposing monomer, which would form a putative dimer-stabilizing salt-bridge (Figure 6C). Two salt-bridge pairs, R287-E254 and E254-R287, are presumed to form. These residues are 3.6 Å and 3.8 Å apart from each other, which are within the typical distance range for a stabilizing salt-bridge (103). To generate mutants of sEH which would either disrupt or stabilize dimerization, we performed mutational analysis on this putative E254-R287 salt-bridge (Figure 6D). First, we mutated the R287 residue to a glutamate residue (R287E), thereby placing two negatively charged residues opposite to each other. Based on the previous observation that the human polymorphism (R287Q) only partially disrupted sEH dimerization (34), we hypothesized that our more severe mutation would completely abolish dimerization. Additionally, we generated another mutant of sEH, which we hypothesized would also abolish dimerization by changing E254 to an arginine (E254R), thus placing two positively charged amino acids opposing each other. Finally, we combined both the R287E and E254R mutations, which may rescue sEH dimerization by re-forming the dimer-stabilizing salt-bridges, but in the reverse orientation of WT.

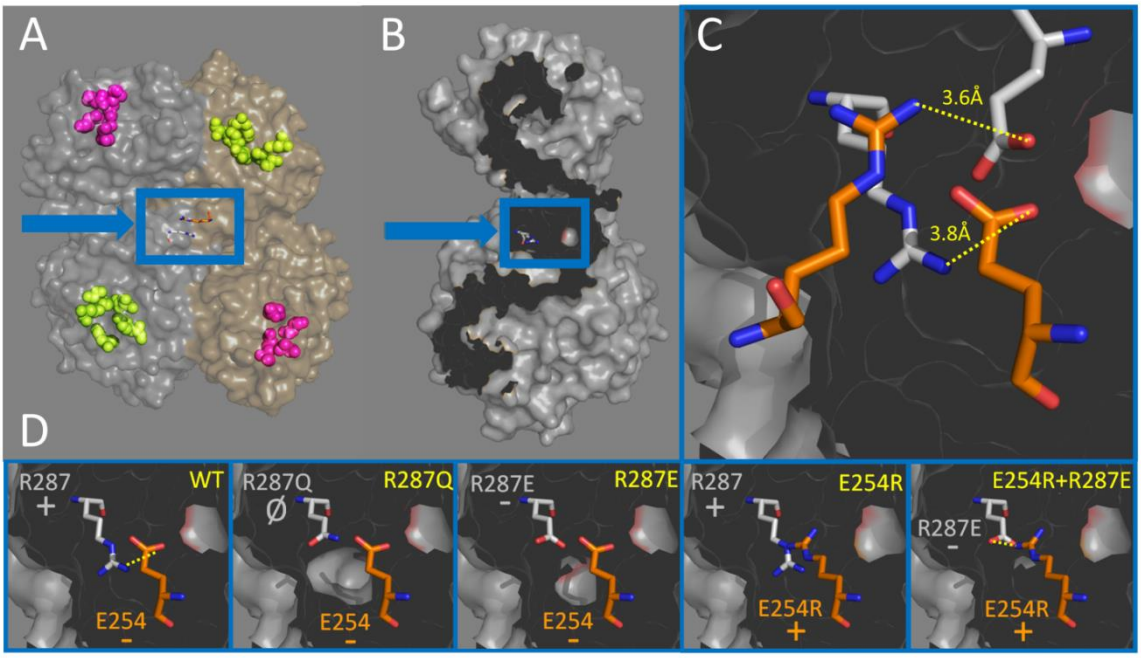

Figure 6. sEH dimerization architecture and dimerization mutations.

A, one monomeric subunit of sEH (tan) binds to another monomeric subunit (grey) of sEH. The R287 residue (blue arrow and box) located away from the hydrolase active site (yellow) and phosphatase active site (purple). B) the R287 residue (blue arrow and box) is localized on the dimerization interface of sEH (dark grey). C, Two salt-bridge pairs are formed between the E254 and R287 residues in the dimer structure which are 3.6Å and 3.8Å apart. Residues from one sEH monomeric subunit are grey, while residues from the opposite monomeric subunit are orange. D, diagram of how one salt-bridge pair changes with the WT, R287Q, R287E, E254R, and E254R+R287E constructs. The construct name is in yellow, while the residue name and charge of the amino acid are either grey or orange, depending on which monomeric subunit they are from.

Split Luciferase System as a Reporter Assay for sEH Dimerization

To simultaneously measure sEH dimerization and hydrolase activity, we employed a split-firefly luciferase protein fragment-assisted complementation strategy (SFL-PFAC) (124,125). Firefly luciferase can be split into a C-terminal and N-terminal fragment which are catalytically inactive separately. However, luciferase activity can be restored if two binding proteins can bring the luciferase fragments together. We used this system to monitor sEH homodimerization by attaching the split-firefly luciferase fragments to the C-terminus of sEH separated by a short glycine-serine rich linker (Fig 7A, B, C). Despite domain-swapped dimer orientation, the C-terminals of sEH are in close proximity to each other which facilitate efficient complementation of luciferase fragments (Fig 7B). Next, we cotransfected sEH-nLuc and sEH-cLuc into HEK cells. Consistent with our hypothesis, the individual N- and C- terminal luciferase fusions were devoid of any activity by themselves (Fig 7D). Coexpression of sEH-nLuc and sEH-cLuc in HEK cells resulted in robust increase of luciferase activity (sEH-WT) compared to expression of luciferase terminals unattached to sEH (Empty, EM), establishing SFL-PFAC as a reporter assay for measuring sEH dimerization (Fig 7E).

Dimerization Is Required For sEH Hydrolase Enzymatic Activity

In order to test our hypothesis that dimerization is required for hydrolase activity, we subcloned WT and mutant sEH cDNA (R287E, E254R, and R287E+E254R) in frame with the N- or C- terminals of firefly luciferase. We transfected HEK cells overnight using Lipofectamine^{TM} 2000 and then lysed the cells to perform a luciferase assay to quantify dimerization and a hydrolase assay to quantify enzymatic activity. We found that both

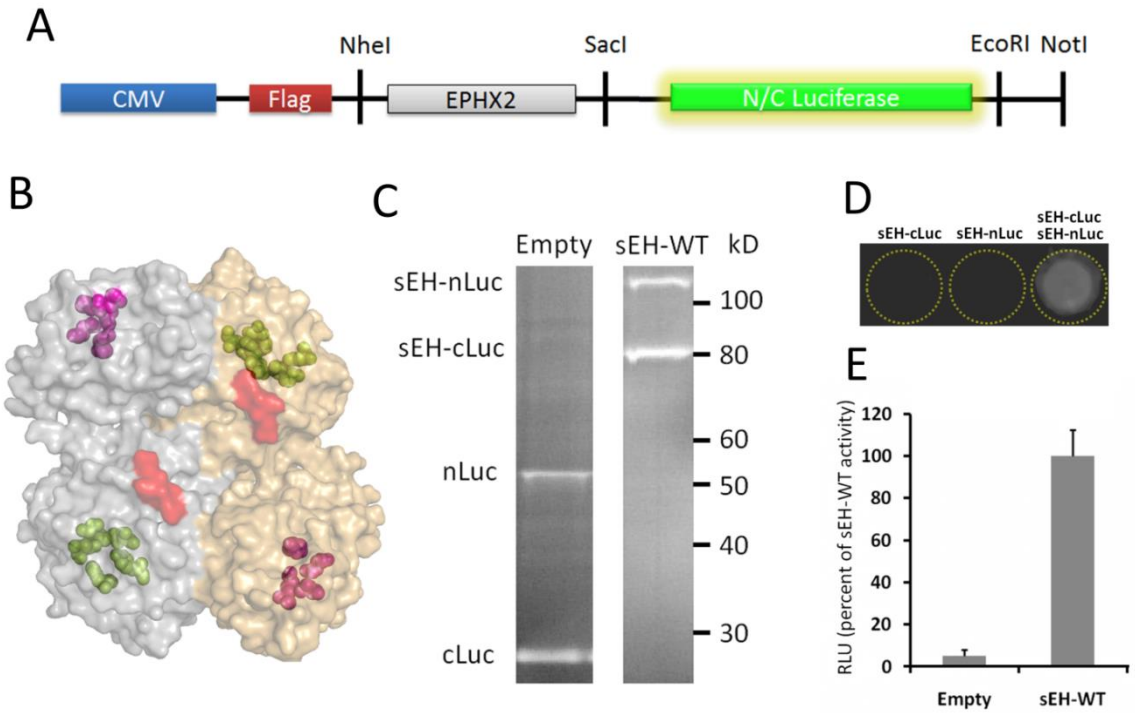

Figure 7. Split-firefly luciferase measures sEH dimerization.

A, schematic representation of the sEH-luciferase expressing plasmid. *Ephx2* is the gene name for sEH. B, Orientation and proximity of the C-terminal ends (red) of sEH dimer where luciferase fragments were attached. C, Western blot of HEK cell lysate cotransfected with either split firefly luciferase constructs unattached (empty) or attached to sEH (sEH-WT). D, CCD exposure of HEK cell lysates producing light when cotransfected with sEH-WT but not when singly transfected. E, Compared to lysates expressing the two terminals of luciferase alone, attaching sEH increase in luciferase activity. Bar graph data represents mean ± S.E.M. RLU indicates relative light units.

the R287E and E254R mutations abolished the dimer formation as evidenced by loss of luciferase activity (Figure 8A) ($p<0.05$ compared to WT). Importantly, these two mutations also inactivate hydrolase enzymatic activity (Fig 8B) ($p<0.05$ compared to WT). On the other hand, the double mutant E254R+R287E restores both dimerization and hydrolase activity ($p<0.05$ compared to E and R for both luciferase and hydrolase activity). Surprisingly, while the R287Q mutant did not have a significantly different luciferase activity than WT sEH, it did show a decrease in hydrolase activity ($p<0.05$ compared to WT) consistent with what has been previously reported (34). Additionally, we determined the K_m and relative V_{max} of each of the sEH constructs (Fig 8C). We found that the decrease in enzyme activity caused by disrupting dimerization was the result of decreasing the V_{max} of the enzyme rather than increasing the K_m (Table 4). Specifically, the dimerization-impaired mutants R287E and E254R had only 8.5% and 7.8% of the relative V_{max} of WT respectively, whereas the dimerization-stabilizing mutation R287E+R254R increased relative V_{max} to 36.9% of WT. To confirm that the differences between luciferase and hydrolase activities in these mutants were not due to differences in transfection efficiencies, we quantified expression of sEH constructs by Western blotting, which showed no significant differences in levels of expression (Fig 8D, 8E).

The kinetics of sEH dimerization

We performed kinetic analysis to examine the rate of sEH dimerization. To do this we transfected HEK cells with individual sEH constructs attached to either terminus of luciferase, extracted the protein and mixed the lysates together before measuring

Figure 8. Luciferase and hydrolase activity of sEH dimerization mutants.

A, luciferase activity from lysate of HEK cells transfected with sEH dimerization mutants relative to WT. N=7 independently transfected cultures. Bar graph data represents mean ± S.E.M. RLU indicates relative light units. * indicates p <.05 compared to WT, R287Q, and E254R+R287E by one-way ANOVA. B, hydrolase activity from lysate of HEK cells transfected with sEH dimerization mutants relative to WT. N=7 independently transfected cultures. Bar graph data represents mean ± S.E.M. RFU indicates relative fluorescent units.* indicates p <.05 compared to WT, R287E, E254R, and E254R+R287E by one-way ANOVA. ** indicates p <.05 compared to WT, R287Q, and E254R+R287E by one-way ANOVA. *** indicates p <.05 compared to WT, R287Q, E254R, and R287E by one-way ANOVA. C, Plot of the velocity of hydrolase activity at various substrate concentrations of EP7. Graph data represents mean ± S.E.M of a representative experiment. D, Immunoblot of sEH luciferase constructs transfected into HEK cells. Lane 1 – WT, Lane 2 – R287Q, Lane 3 – R287E, Lane 4 – E254R, Lane 5 – E254R+R287E, Lane 6 – Not Transfected. E, quantification of sEH-luciferase Western blots. N=4 independently transfected cultures. n.s. = not significant by one-way ANOVA.

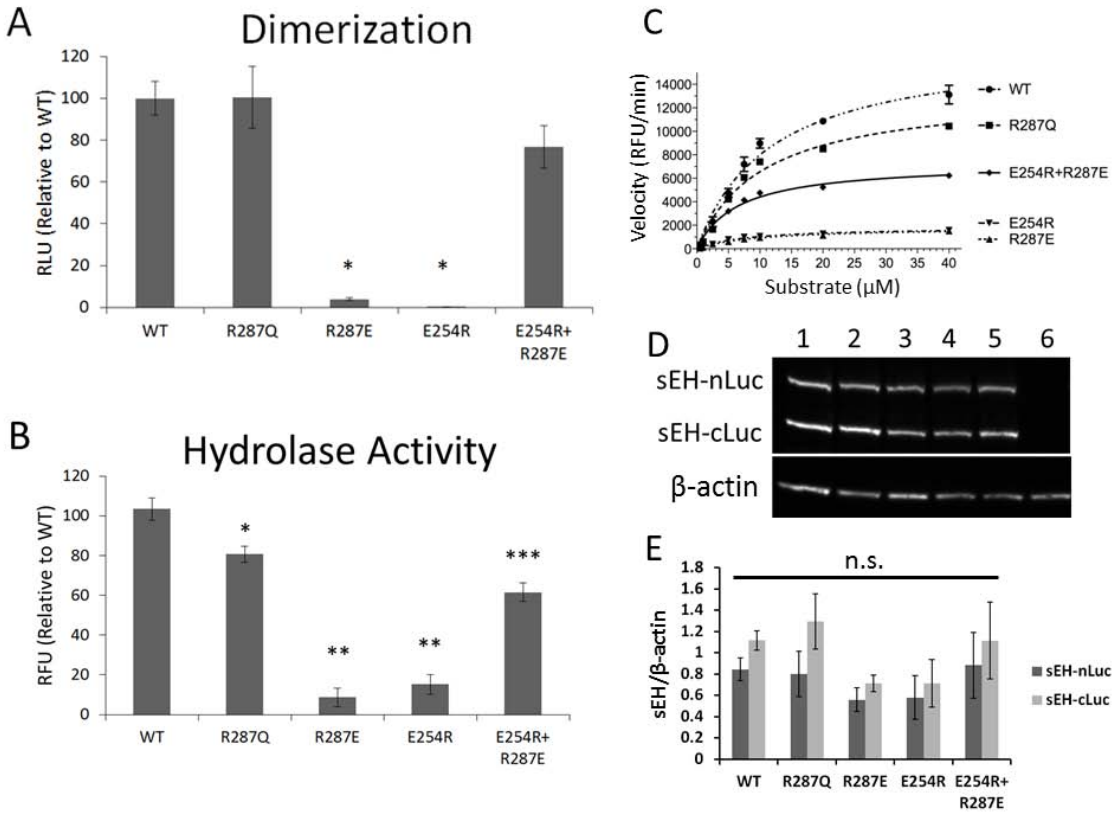
A
Dimerization
RLU (Relative to WT)
120
100
80
60
40
20
0
*
*
WT
R287Q
R287E
E254R
E254R+ R287E
B
Hydrolase Activity
RFU (Relative to WT)
120
100
80
60
40
20
0
*
**
**
***
WT
R287Q
R287E
E254R
E254R+ R287E
C
Velocity (RFU/min)
14000
12000
10000
8000
6000
4000
2000
0
0 5 10 15 20 25 30 35 40
Substrate (μM)
WT
R287Q
E254R+R287E
E254R
R287E
D
1 2 3 4 5 6
sEH-nLuc
sEH-cLuc
β-actin
E
n.s.
sEH/β-actin
1.8
1.6
1.4
1.2
1
0.8
0.6
0.4
0.2
0
WT
R287Q
R287E
E254R
E254R+ R287E
sEH-nLuc
sEH-cLuc

	K_m (μM)		Relative V_{max}	
	Mean	**SEM**	**Mean**	**SEM**
WT	15.08	2.70	100.0	13.1
R287Q	10.17	0.65	61.4	5.5
R287E	6.96	1.52	8.5	0.5
E254R	5.84	1.10	7.8	0.9
E254R+R287E	6.91	0.68	36.9	0.6

Table 4. Hydrolase activity kinetic constants.

Km (μM) and relative *Vmax* of hydrolase enzymatic activity with EP7 substrate. Values were determined from three independently transfected cultures with readings in duplicate.

luciferase activity every 30 minutes for 2 hours. Interestingly, we found that mixed lysates from the R287Q mutation of sEH had significantly enhanced luciferase activity compared to WT enzyme (greater than 4000% of WT at 2 hours) or the two ends of luciferase unattached to sEH (greater than 4000% of empty (EM) at 2 hours) (Figure 9A). Interestingly, the WT enzyme showed no increase in luciferase activity over the two hour period compared to the unattached luciferase terminals (104% of EM at 2 hours). We interpreted this to mean that the dimer formed between the WT monomers is so strong that it would not break apart to form new dimers to result in luciferase activity. On the other hand, the R287Q mutation causes a metastable dimer such that sEH protein harboring the R287Q mutation is able to break apart and form a new dimer with another partner. Mixing lysates from the other dimerization constructs showed that the R287E constructs had slightly higher luciferase activity than all constructs except for R287Q (400% of EM at 2 hours) (Figure 9B). In order to validate that the WT protein dimer is sufficiently strong that it is unable to break apart and form new dimer, we performed a competition study. We mixed lysates from R287Q in a similar manner as in Figure 4A, except that at 15 minutes, we added lysates from either untransfected HEK cells (NT) or cells transfected with WT or R287Q sEH protein, which were not attached to a terminal of luciferase. We hypothesized that adding R287Q unattached to luciferase would decrease luciferase activity by forming luciferase inactive sEH-Luc/sEH dimers; however, adding WT protein would not decrease dimerization because WT protein would not be able to break apart to form any sEH-Luc/sEH dimers. Consistent with our

Figure 9. Kinetics of dimer formation in soluble epoxide hydrolase.

A, luciferase activity from mixed lysate of HEK cells transfected with sEH dimerization constructs attached to a single terminal of luciferase or domains unattached to sEH (EM). N=3 independent mixes. Graph data represents Mean ± S.D. * indicates p <.05 compared to EM and WT by two-way repeated-measures ANOVA. B, **l**uciferase activity from mixed lysate of HEK cells transfected with sEH dimerization constructs attached to a single terminal of luciferase. N=3 independent mixes. Graph data represents Mean ± S.D. * indicates p <.05 compared to EM, WT, E254R, ** indicates p <.05 compared to EM, WT, E254R, and E254R+R287E by two-way repeated-measures ANOVA. C, R287Q mixed lysate treated at 15 minutes with lysates from HEK cells untransfected (NT) or transfected with non-luciferase tagged WT or R287Q at two different doses either a low dose (1x) or a high dose (2x). RLU indicates relative light units. N=3 independent mixes. Data was normalized value immediately before treatment at 15 minutes. Graph data represents Mean ± S.D. * indicates p<.05 for NT and WT compared to Q (2x), ** indicates p<.05 for NT and WT compared to Q (1x) and Q (2x) as well as Q (1x) compared to Q (2x) by two-way repeated-measures ANOVA.

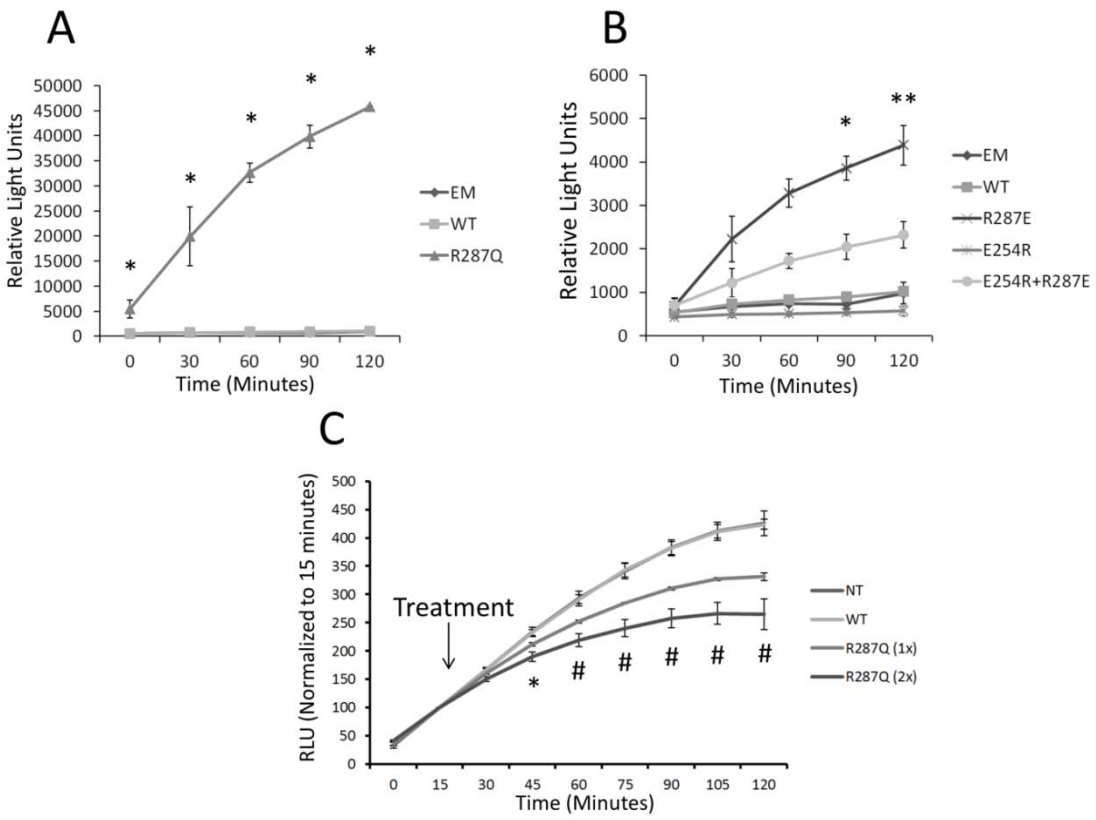
A
Relative Light Units
50000
45000
40000
35000
30000
25000
20000
15000
10000
5000
0
0
30
60
90
120
Time (Minutes)
EM
WT
R287Q
B
Relative Light Units
6000
5000
4000
3000
2000
1000
0
0
30
60
90
120
Time (Minutes)
EM
WT
R287E
E254R
E254R+R287E
C
RLU (Normalized to 15 minutes)
500
450
400
350
300
250
200
150
100
50
0
0
15
30
45
60
75
90
105
120
Time (Minutes)
Treatment
NT
WT
R287Q (1x)
R287Q (2x)

hypothesis, we found that only adding R287Q protein decreased luciferase signal compared to adding lysate from untransfected cells (Figure 9C). Furthermore, we found that the amount of R287Q protein we added (1x vs. 2x) directly correlated with the amount of luciferase inhibition. This finding further validates the specificity of the SFL-PFAC assay for measuring sEH dimerization.

Discussion

Soluble epoxide hydrolase in its native form is a domain-swapped homodimer. We investigated if dimerization is required for its hydrolase enzymatic activity. Specifically, we used mutation analysis of a putative inter-monomeric salt-bridge to manipulate the dimerization state of the enzyme. We found that the E254-R287 salt-bridge interaction is essential for dimerization as well as activity. By disrupting dimerization with either the R287E or E254R mutation, we abolished both dimerization and hydrolase activity. However, by combining the two mutations (E254R+R287E) together, we reversed the salt bridge and rescued both sEH dimerization and activity. We interpret these results to mean that sEH dimerization is required for hydrolase activity.

We were surprised to find that the R287Q human polymorphism did not show a decrease in luciferase activity, while still having lower hydrolase activity compared to the WT enzyme. Based on published reports, we expected to see a decrease in both activities (31,34,76). One likely explanation for this unexpected result is that the complimented split-luciferase fragments somehow artificially stabilize the metastable R287Q protein. Therefore, the luciferase-active and hydrolase-active heterodimer ($H^{+}L^{+}$,

Figure 10. Model of sEH luciferase dimerization.

Cells transfected with sEH form three populations of dimers: sEH-cLuc/sEH-nLuc which are hydrolase and luciferase active (H^+L^+), as well as sEH-cLuc/sEH-cLuc and sEH-nLuc/sEH-nLuc which are hydrolase active but luciferase inactive (H^+L^-). In the WT protein, these three populations are static because the E254-R287 salt bridge bond stabilizes the dimer. In contrast, the R287Q polymorphism disrupts dimerization such that the equilibrium shifts towards hydrolase and luciferase inactive monomers (H^-L^-). However, the complimented luciferase fragments stabilize the metastable R287Q dimer resulting in similar levels of luciferase activity compared to the WT enzyme. One sEH monomer is colored gray, while the other is tan. C-terminal luciferase is colored yellow,

while the N-terminal of luciferase is colored blue.

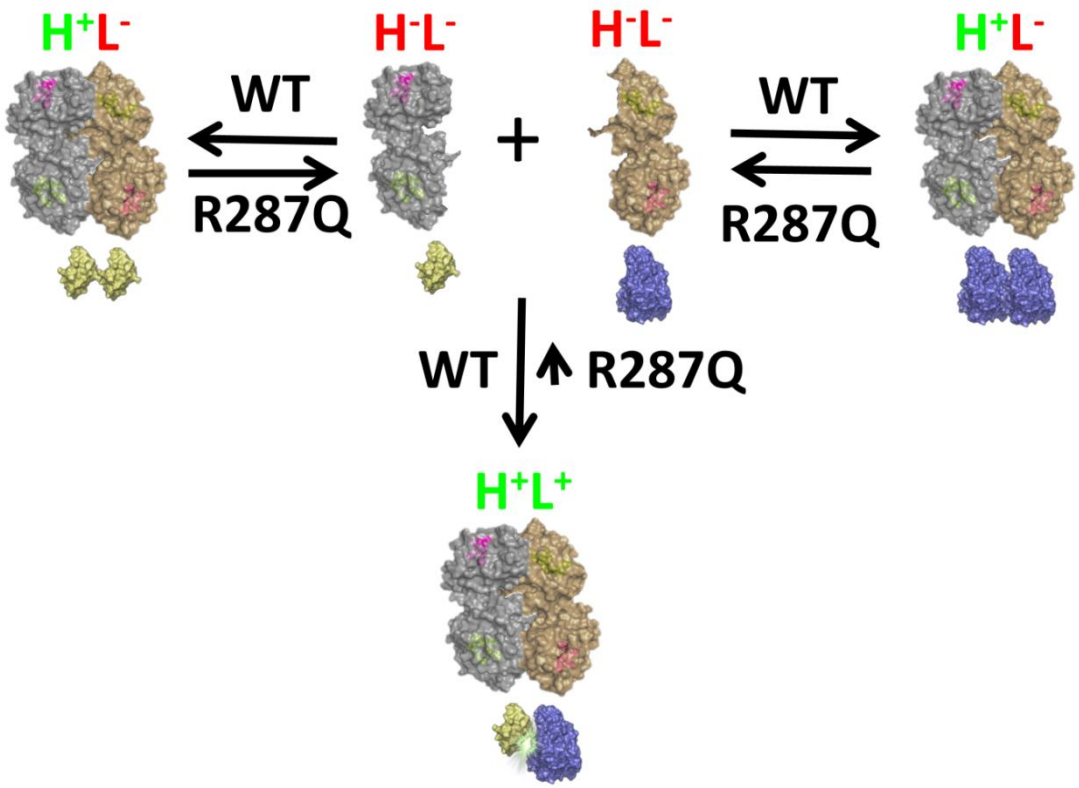
H+L-
H-L-
H-L-
H+L-
WT
R287Q
+
WT
R287Q
WT
R287Q
H+L+

Figure 10) is preferentially formed over the luciferase-inactive homodimers (H^+L^-, Figure 10) at equilibrium. Other bimolecular fluorescent complementation (BiFC) systems have previously been shown to artificially increase the stability of protein-protein interactions; however, those studies used protein fragments that form covalent chromophores when complimented such as in split-YFP (127). We intentionally chose a split-firefly luciferase system because the system is reversible and thus less likely to artificially stabilize the dimer (128). Nevertheless, the data in figure 8 suggests this possibility with the R287Q protein. To our knowledge this is the first instance of artificial stabilization of a protein using split-firefly luciferase system, and is probably due to the fact that the R287Q mutation causes a metastable protein. The R287Q protein is the only metastable construct (Fig 9A and B) and thus the luciferase activity is only increased with this protein. Additionally, based on the experiments in figure 9C, the stabilization caused by luciferase fragments is secondary to the actual sEH protein homodimerization because proteins without luciferase fragments are able to competitively bind the sEH luciferase construct thus suppressing luciferase activity. Together, this leads us to conclude that the luciferase activity is accurately reflecting the dimerization state for WT, R287E, E254R, and E254R+R287E proteins.

We also measured the kinetics of sEH homodimerization. Interestingly, we found that sEH harboring the R287Q human polymorphism rapidly forms new dimer pairs, while the WT enzyme remained static, indicating that the E254-R287 interaction is strong enough to hold the dimerization state. This result may explain why previous studies

have detected hydrolase enzymatic activity of the monomer fraction of sEH (76). While it would be possible to separate sEH monomers from dimers, once the monomers are separated, they would rapidly form enzymatically active dimers while the activity was being measured.

It has been speculated that the E254-R287 residues may form an intra-monomeric salt-bridge rather than an inter-monomeric salt-bridge (34). Analysis of the sEH crystal structure by ESBRI (129) yields inter-monomeric salt-bridges between the E254 and R287 residues. Indeed, our results argue that they form an inter-monomeric salt-bridge because of their critical role in stabilizing sEH dimerization. It might also be argued that the dimer-disrupting mutations may be affecting the stability of the protein; however, this is unlikely because introducing double mutations results in the rescue of both dimerization and hydrolase activity.

sEH is a bifunctional enzyme with hydrolase and phosphatase catalytic activity (27,36). While we addressed the hypothesis that sEH dimerization is required for hydrolase activity, one limitation of our study is that it does not examine the effect of dimerization on phosphatase activity. Such studies, however, are limited by the availability of sEH-specific phosphatase substrates. Nevertheless, the effect of dimerization on phosphatase enzymatic activity remains an interesting an important question, which should be addressed in future studies as new research tools become available and as new roles for the phosphatase domain in the biology of sEH emerge.

sEH plays a role in the development and outcome of multiple cardiovascular diseases through its role in the metabolism of EETs (54). Understanding sEH biology is, therefore, highly clinically relevant. The investigation of the dimerization kinetics of a common human polymorphism of sEH, R287Q, also has important clinical implications. Based on the finding that the R287Q human polymorphism is metastable, the clinical effects linked to this human polymorphism must be viewed in the light of its effect on sEH dimerization, in addition to its effect on hydrolase enzymatic activity (14,81,82,126). We speculate that disrupting dimerization may represent a novel means by which sEH activity can be regulated within the cells. However, further work is required to understand how dimerization may be an endogenous regulator of sEH function. Finally, the data presented in this manuscript suggests that disrupting sEH dimerization may serve as a novel therapeutic approach to inhibiting sEH enzymatic activity. The split-firefly luciferase system described within this manuscript may provide the framework for creating a high-throughput sEH dimerization drug screen.

In conclusion, we find that sEH hydrolase activity is dependent on sEH dimerization. We developed a novel technique for monitoring the effect that sEH mutations have on dimerization as well as establishing a model system for controlling the dimerization status of sEH that can be used in future experiments to monitor the effect of sEH dimerization on other aspects of sEH biology.

Chapter 3

Disrupting Dimerization Translocates Soluble Epoxide Hydrolase to Peroxisomes

Jonathan W. Nelson, Anjali J. Das, and Nabil J. Alkayed

Abstract

Soluble epoxide hydrolase (sEH) is a homodimeric enzyme that is localized to both the cytosol and peroxisomes. Recently, a human missense polymorphism in the gene that encodes for sEH (R287Q) was shown to affect the protein by enhancing peroxisomal localization. Combining a previous finding that this same polymorphism slightly disrupts dimerization suggests a link between sEH dimerization and peroxisome localization. In the current study, we systematically test the hypothesis dimerization is a key regulator of sEH subcellular localization. Specifically, we used sEH proteins that alter the dimerization state of sEH by mutating amino acids involved in a dimer-stabilizing salt-bridge. We fused these sEH proteins to green fluorescent protein and cotransfected them into primary cortical mouse neurons with a red fluorescent protein targeted to peroxisomes. We imaged the neurons with confocal microscopy and quantified the colocalization of sEH with peroxisomes using Pearson's correlation coefficient. Based on Pearson's correlation coefficient of cytosolic restricted and peroxisome enriched sEH, we developed a peroxisome localization index as a measure of the fraction of sEH that is localized to either cytosol of peroxisomes. We find that sEH constructs that form dimers preferentially localize to the cytosol. In contrast, sEH constructs that have disrupted dimerization preferentially localize to peroxisomes. We conclude that the dimerization

status of sEH plays a key role in peroxisome translocation. Based on the protective and dimer disrupting effect afforded by the R287Q polymorphism, enhancing peroxisome translocation may be a novel protective strategy for minimizing the harmful effects of sEH.

Introduction

Soluble epoxide hydrolase (sEH) is therapeutic target for multiple cardiovascular diseases, including stroke (54). Both gene deletion and pharmacological inhibition of sEH have been shown to be neuroprotective after ischemia (13,46). Further linking sEH to stroke risk are human polymorphisms have been associated with either an increased or decreased incidence of stroke. Specifically, a lysine to arginine substitution at protein position 55 (K55R) was shown to increase the risk of stroke (84), while a arginine to glutamine substitution at position 287 (R287Q) was shown to decrease the risk of stroke (14). Additionally, the R287Q polymorphism was shown to protect neurons from an *in vitro* model of ischemia (15). At the time, the effects of both these polymorphisms were contributed to their influence on sEH's ability to hydrolyze neuroprotective fatty acid epoxides called epoxyeicosatrienoic acids. Indeed, the K55R polymorphism has been shown to increase sEH hydrolase activity, while the R287Q has been shown to decrease its activity (34,80). However, recently it has been shown that the R287Q polymorphism affects sEH protein in ways other than enzymatic activity. Specifically, it shifts the subcellular distribution of sEH from of the cytosol and into another subcellular compartment (41).

Endogenous sEH distributes between the cytosol and peroxisomes (40). This localization pattern was shown to be the result of a weak peroxisome targeting signal (PTS) on its C-terminus (41). sEH is the only human protein to end in the Serine-Lysine-Methonine (-SKM) tripeptide sequence, which has less affinity for the peroxisome transport protein peroxin 5 (Pex5) than the canonical PTS tripeptide Serine-Lysine-Leucine (-SKL) (122). Indeed, the distribution of sEH between the cytosol and peroxisomes can be shifted exclusively to the peroxisomes by changing the sEH C-terminal PTS to -SKL (41). However, the lower affinity of –SKM may not provide a complete answer to sEH's distribution, as recent evidence suggests the protein quaternary structure of sEH may also be a contributing factor to the distribution of sEH within the cell (41).

Specifically, sEH protein harboring the R287Q polymorphism was shown to have enhanced peroxisome localization in Chinese Hamster Ovarian (CHO) cells (41) despite having the same –SKM PTS as wildtype sEH. This same polymorphism was previously shown to partially disrupt sEH dimerization suggesting a correlation between the dimerization of sEH and its subcellular localization (76).

We set out to directly test the hypothesis that dimerization regulates the subcellular distribution of sEH by using previously validated mutations in the sEH protein that alter its dimerization state by mutating amino acids involved in a dimer-stabilizing salt-bridge (102). We fused these sEH constructs to GFP before transfecting them into primary cortical neurons neurons, a cell type relevant to endogenous sEH localization and stroke (13,44). We then imaged the neurons with laser-scanning confocal microscopy and

quantified sEH's colocalization with peroxisomes using Pearson's correlation (130) . Additionally, based on this correlation analysis, we developed a peroxisome localization index (PLI) which measures the distribution of sEH between the cytosol and the peroxisomes.

Understanding the factors that influence the distribution sEH has important clinical relevance, as peroxisome localization of sEH may play a protective role in cells. Indeed, while one plausible explanation for the protective effect of the R287Q human polymorphism is its decreased hydrolase activity, another equally plausible explanation is that its enhanced peroxisome translocation, in part, confers ischemic protection. This research may lead to strategies that artificially manipulate the subcellular distribution of sEH for therapeutic purpose.

Experimental Procedures

GFP-sEH and RFP-SKL Plasmids

sEH cDNA containing sEH dimerization mutations were amplified with primers creating a 5'-EcoRI and 3'-NotI restriction site for subcloning in-frame into a vector expressing enhanced green fluorescent protein (GFP) driven by a elongation factor α (EF1α) promoter (102). PCR mediated mutagenesis was used to either delete the C-terminal peroxisome targeting signal (GFP-sEH-ΔPTS), or replace it with the canonical PTS1 motif Serine-Lysine-Leucine (GFP-sEH-SKL) (see primers in Table 5). To label neuronal peroxisomes, mCherry fused to the C-terminal canonical PTS1 motif SKL (RFP-SKL) was obtained as a gift from Dr. Tom Maynard.

Primer Name	Primer Sequence (5'->3')
EcoRI-sEH-5'	aaaaGAATTCacgctgcgcgcggccgt
sEH-NotI-3'	ttttGCGGCCGCctacatctttgagacca
sEH-SKL-BamHI-NotI-3'	ttttGCGGCCGCGGATCCttacagctttgacttcagcatctttgagaccaccggt
sEH-ΔPTS-SacI-NotI-3'	ttttGCGGCCGCGAGCTCttagaccaccggtgggttccggg

Table 5. GFP-sEH primers.

Primer name and sequence used for cloning sEH into GFP expression vector as well as primers used to mutate the C-terminal of sEH to either end is canonical peroxisome targeting signal (Serine-Lysine-Leucine (SKL)) or without a peroxisome targeting signal (ΔPTS). Basepairs in capital letters are restriction endonuclease sequences used for subcloning.

Primary Cortical Mouse Neuronal Culture

Primary cortical mouse neurons were prepared from either C57/BL6 (Charles River) mouse brains at E16 as previously described (131). Cortices were dissected in HEPES-buffered HBSS and dissociated by digestion with 0.1% papain (Worthington Biochem). Cells were seeded at 600,000 cells/well onto poly-D-lysine (100 μg/ml) coated 18mm round coverslips in 12 well plates, and were maintained in a humidified incubator in air with 5% CO_2. Neurons were cultured in Neurobasal medium without phenol red (Invitrogen), supplemented with 2% B27 (Invitrogen), 1% Glutamax (Invitrogen) and 1% penicillin/streptomycin (Invitrogen). Cultures consisted of >90% microtubule-associated protein 2 (MAP2)-positive and <10% glial fibrillary acidic protein (GFAP)-positive cells on day *in vitro* 10 (DIV 10).

Plasmid Purification and Transfection

GFP-sEH and RFP-SKL plasmids were purified with a Maxi Kit (Qiagen) according to manufacturer's protocol and diluted to a final concentration of 900ng/μL. Lipofectamine 2000 (Invitrogen) was mixed with 900ng of each plasmid in accordance with the manufactures instructions. All transfections were done in 1000μl of supplemented Neurobasal+ media per well for 1 hour before changing to fresh maintenance medium on DIV7. Cells were fixed 72h after transfection on DIV 10 in 4% PFA. Hoechst (Invitrogen) staining of the nuclei was performed at a final concentration of 3.2μM in PBS for 90 seconds before being washed out and mounted with Fluoromount G (Southern Biotech).

HEK Cells and Western Blot

Human Embyronic Kidney (HEK) cells were maintained and transfected as previously described (102). Recombinant sEH and GFP proteins were synthesized as previously described for antibody controls (15). Western blot was performed as previously described (102). Rabbit anti-sEH 1:400 (Cayman Chemical) and rabbit anti-GFP 1:1000 (Cell signaling) were used as primary antibodies. 1:2000 anti-Rabbit Cy3 (GE Healthcare) antibody was used as a secondary antibody. Immunoblots were detected on a Typhoon Imaging system (GE-Healthcare).

Image Acquisition

Images were acquired on an LSM 510 using a Plan Apochromat 63x/1.4NA oil objective lens. GFP was excited with a 488nm laser and detected at 500-530nm. RFP was excited at a 543nm laser and detected beyond 560nm. Laser intensities were optimized for each individual image to take advantage of the full dynamic range of signal without saturation. As expected with a transient transfection, each condition contained a mixed population of dim and bright cells. The depth of the each neuron was captured with 2048 x 2048 pixel (68 x 68 μm) resolution centered on the nucleus with 16-bit depth coverage. Images were acquired from between 2 and 5 independent neuronal cultures and from at least 3 independently transfected coverslips. The number of images analyzed for each group is presented in each figure.

Image Analysis

Images were analyzed for co-localization with IMARIS (Bitplane) using the colocalization module. For all GFP-sEH groups, a single representative optical section was used to measure Pearson's correlation coefficients. Raw images were thresholded equally in the GFP (6.65% signal) and RFP channel (6.80% signal), and then masked in the green channel at (5.69%) before calculating coefficients between the GFP (sEH) and RFP-SKL (demarcating peroxisomes) signals. All statistics were performed on Pearson's correlation coefficient values; however, we developed a peroxisome localization index (PLI) to better understand the distribution of GFP-sEH between the cytosol and peroxisomes. The PLI is a linear approximation of sEH distribution that sets the maximum possible of sEH peroxisome localization at the average value of GFP-sEH-SKL (GFP-sEH with a canonical peroxisome targeting signal) and the minimum possible peroxisome localization at the average value of GFP-sEH-ΔPTS (GFP-sEH without a C-terminal peroxisome targeting signal). The result of the PLI is a scale between 0 and 1 where a completely cytosolic GFP-sEH would equal 0, while a completely peroxisomal GFP-sEH would equal 1.

$$Peroxisome\ Localization\ Index = \frac{Ave.Pearson's\ Value\ \ - Ave.\ \ GFP\ sEH\ \Delta PTS\ value}{Ave.\ \ GFP\ sEH\ SKL\ value - Ave.\ \ GFP\ sEH\ \Delta PTS\ value}$$

Image Presentation

ZEN software (Zeiss) and Photoshop (Adobe) were used to create images presented in manuscript. Images presented are maximum intensity projections of a 2µm substack highlighting a dendritic process and part of the neuronal cell body from full view images used for analysis. While raw images were analyzed, for presentation purposes brightness and contrast have been adjusted in the figures.

sEH Modeling

To create the model of sEH peroxisome translocation, Pymol (Delano Scientific) was used to create illustration of sEH (PBD ID:1CR6), peroxisome transport protein Pex 5 (PBD ID:1FCH), and peroxisome transport signal (PBD ID:1FCH).

Statistics

Data is presented as mean ± s.e.m of Pearson's correlation coefficient values. To determine if there was a difference in co-localization between GFP-sEH wild-type and different mutant groups, one-way analysis of variance was performed (ANOVA), followed by Student-Newman-Keuls (SNK) post-hoc analysis. Data is presented in separate graphs; and the same GFP-sEH-WT data is presented in Figure 2 as Pearson's correlation coefficient, and in Figure's 3 and 4 as PLI in order to illustrate effects of sEH mutations on the localization of GFP-sEH compared to the wildtype protein.

Results

Modeling sEH subcellular localization through GFP fusion

In order to study the effects of dimerization on the localization of human soluble epoxide hydrolase (sEH), we employed a green fluorescent protein (GFP) fusion system. This model was previously utilized to study the effects of human polymorphisms on the subcellular distribution of sEH in Chinese hamster ovarian (CHO) cells (41). We fused GFP to the N-terminal of sEH in order to preserve the C-terminal peroxisome targeting signal (PTS) of sEH (Figure 11A).

Figure 11. Assessing sEH subcellular localization through GFP fusion**.**

A, Schematic of GFP-sEH vector. GFP was fused to the N-terminal of sEH in order to preserve the C-terminal peroxisome targeting signal (PTS) of sEH. Expression of GFP-sEH fusion protein is driven by elongation factor 1-alpha (EF1α) promoter. B, Western blot of HEK cell lysate transfected with GFP-sEH and recombinant proteins. GFP-sEH is the appropriate molecular weight for a predicted GFP-sEH fusion and is immunoreactive with both α-sEH as well as α-GFP antibodies, Lane 1: GFP-sEH, Late 2: untransfected HEK cell, Lane 3: recombinant sEH, Lane 4: recombinant GFP. C) Primary cortical neurons transfected with GFP or GFP-sEH fusion protein. Transfection with GFP results in a diffuse stain throughout the cytoplasm and nucleus (white arrow) of the transfected cell. Transfection with GFP-sEH fusion protein, on the other hand, results in both a diffuse and punctate (white arrowheads) pattern with no labeling of the nucleus (white arrow). Scalebar on full image is 10μm and scalebar on insets is 5μm.

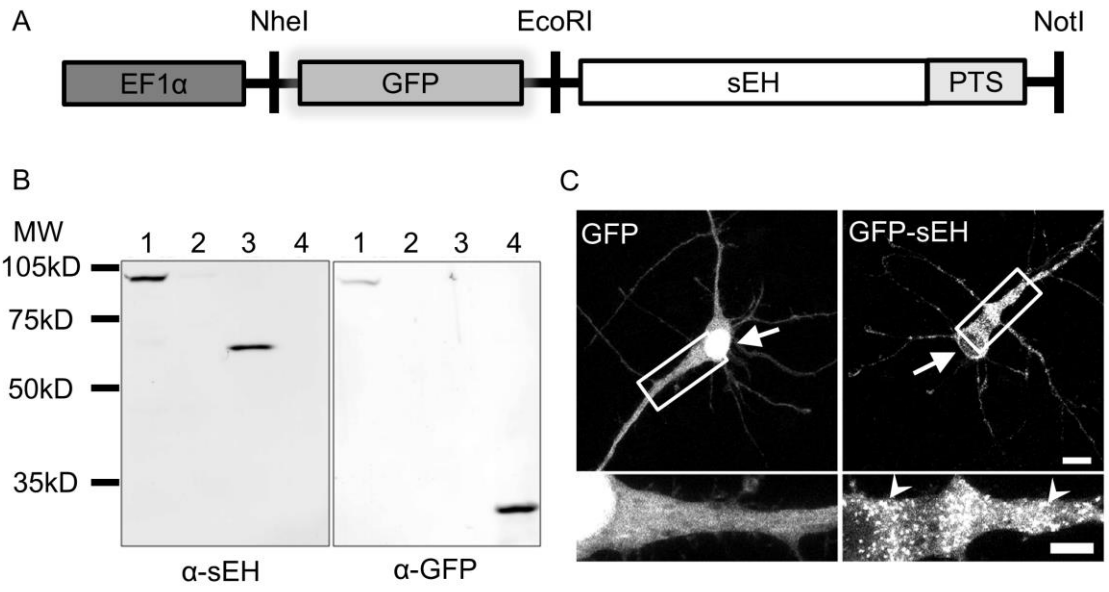
A
NheI
EcoRI
NotI
EF1α
GFP
sEH
PTS
B
MW
1 2 3 4 1 2 3 4
105kD
75kD
50kD
35kD
α-sEH
α-GFP
C
GFP
GFP-sEH

To confirm the fusion of GFP to sEH, we performed a Western blot on HEK cell lysates which were transfected with wildtype sEH (GFP-sEH-WT) in addition to recombinant sEH and GFP proteins. We find that HEK cells transfected with GFP-sEH are immunoreactive for both anti-sEH and anti-GFP antibodies, with a band of the expected size of 90kD for a GFP-sEH fusion protein (Figure 11B).

To visualize the localization pattern of sEH within primary cortical neurons, we transfected cultured neurons on DIV 7 with either GFP or GFP-sEH-WT and allowed the cells to express proteins and reach localization equilibrium for 72 hours before fixing the cells on DIV 10. In order to obtain high resolution images, neurons were imaged using high-resolution laser-scanning confocal microscopy. We found that cells expressing GFP have a diffuse fluorescent pattern in the cytoplasm and the nucleus of neurons, while cells transfected with GFP-sEH-WT showed a diffuse and punctate signal with nuclear exclusion (Figure 11C), consistent with what has previously been reported in other cell types (40,41).

Analysis of sEH subcellular localization

To confirm that the punctate appearance of GFP-sEH-WT is the result of sEH translocation into peroxisomes, we cotransfected GFP-sEH constructs with a red fluorescent protein (RFP) fused to the canonical peroxisome targeting signal serine-lysine-leucine (SKL). Fusion of fluorescent protein to –SKL has been extensively used to label peroxisomes in living cells (132–134). As expected, we find that GFP-sEH-WT

Figure 12. Quantification of sEH subcellular localization.

Primary neurons cotransfected with GFP-sEH fusion protein and peroxisome marker RFP-SKL. A, GFP, RFP, and merged image from a neuron transfected with GFP-sEH-WT. GFP-sEH-WT fusion results in a diffuse and punctate stain. GFP-sEH-WT punctate colocalize with RFP-SKL (white arrowheads) reflecting the dual distribution of GFP-sEH-WT between the cytosol and peroxisomes. B, GFP, RFP, and merged image from a neuron transfected with GFP-sEH-ΔPTS. Deletion of the peroxisomal targeting signal in sEH results in a diffuse localization pattern. C, GFP, RFP, and merged image from a neuron transfected with GFP-sEH-SKL. Fusion of a canonical peroxisomal targeting signal results in an enhanced punctate pattern that correlates with RFP-SKL (white arrowheads) indicative of predominantly peroxisome localization. D, Quantification of intensity correlation in the green and red channel in single optical sections of primary neurons transfected GFP-sEH fusion protein by Pearson's correlation. Transfection with GFP-sEH-WT results in a Pearson's colocalization value significantly higher than cells transfected with GFP-sEH-ΔPTS but significantly lower than neurons transfected with GFP-sEH-SKL. * indicates $P<.05$ by one-way ANOVA. # indicates $P<.05$ by one-way ANOVA. White number in bar graph represents number of images analyzed in each group. Scalebar is 5µm.

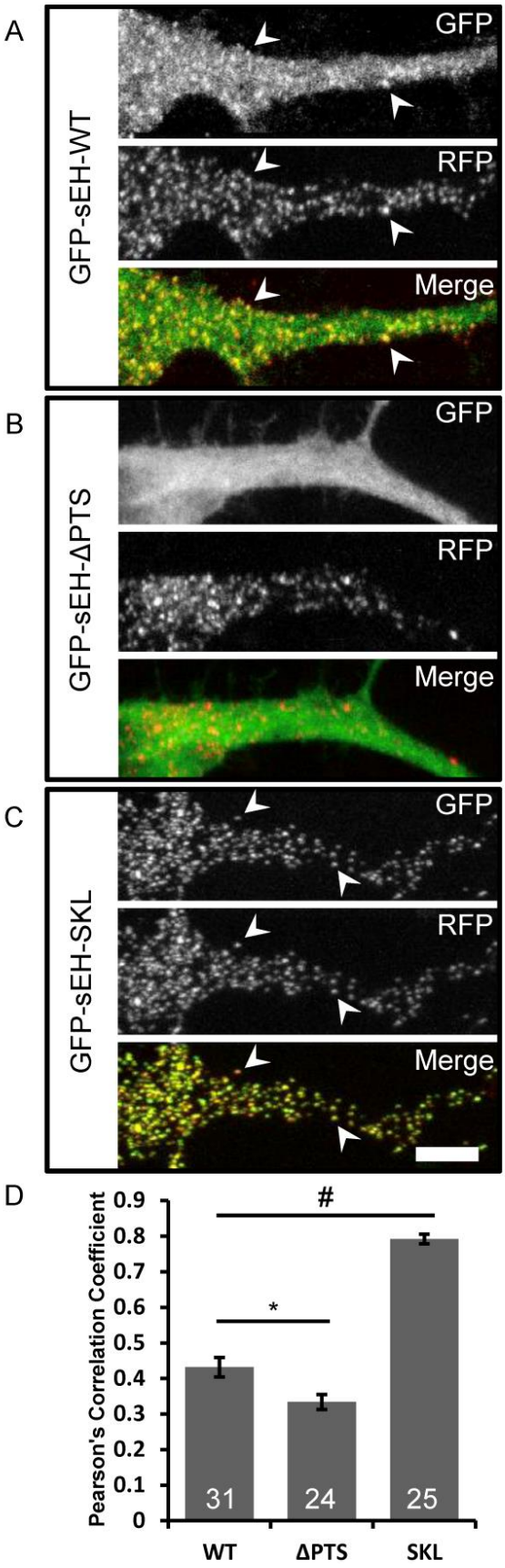
A
GFP-sEH-WT
GFP
RFP
Merge
B
GFP-sEH-ΔPTS
GFP
RFP
Merge
C
GFP-sEH-SKL
GFP
RFP
Merge
D
Pearson's Correlation Coefficient
0.9
0.8
0.7
0.6
0.5
0.4
0.3
0.2
0.1
0
#
*
31
24
25
WT
ΔPTS
SKL

punctate colocalizes with the RFP used to label peroxisomes (Figure 12A, white arrowheads).

Having confirmed that the distribution of wildtype sEH is between the cytosol and peroxisomes, we mutated the PTS of sEH in order to artificially restrict from or enrich for sEH in peroxisomes. To do this, we used PCR mutagenesis to either delete the PTS of sEH (GFP-sEH-ΔPTS) or enhance it by mutating the C-terminus of sEH to end in the canonical PTS –SKL (GFP-sEH-SKL).

As expected, we find that deletion of the C-terminal PTS (-SKM) of sEH (GFP-sEH-ΔPTS) results in a diffuse pattern similar to neurons transfected with GFP (Figure 12B). In contrast, sEH ending with the C-terminal PTS signal –SKL has an exclusively punctate appearance that colocalizes with peroxisomes (Figure 12C, white arrowheads) (41)

In order to quantify the distribution of sEH between the cytosol and peroxisomes, we measured Pearson's correlation coefficients (PCC) between the GFP-sEH and the peroxisome marker RFP-SKL. PCC is an established measure of colocalization between two signals ranging from -1 (perfect exclusion) to 1 (perfect colocalization) (130). Important for our study, PCC measures the correlation between two signals and not the absolute intensity of the signals. Therefore, PCC should not be sensitive to variability in expression due to transient transfection. We find that GFP-sEH-WT has a PCC of (.43±.03) with the peroxisome marker. As expected, deletion of the C-terminal PTS of sEH GFP-sEH-ΔPTS) significantly decreases the PCC (.33±.02, $p<.05$ compared to GFP-

sEH-WT), while mutating sEH to end in –SKL significantly increases the PCC (.79±.01, p<.05 compared to GFP-sEH-WT) (Figure 12D).

Disrupting sEH dimerization preferentially localizes sEH to peroxisomes

Having established a GFP-sEH transfection model and a method for quantifying sEH peroxisomal localization, we were ready to test the hypothesis that dimerization regulates the distribution of sEH between the cytosol and peroxisomes. Previously, a human polymorphism in sEH (R287Q) was shown to slightly disrupt the homodimerization of sEH (76). This same polymorphism was also shown to preferentially localize to the peroxisome compared to the wildtype protein. This lead the authors to hypothesize that dimerization was regulator of the subcellular distribution of sEH (41). Consistent with the previous work in CHO cells, we find that sEH harboring the R287Q polymorphism (GFP-sEH-R287Q) forms a punctate pattern that colocalizes with peroxisomes in neurons (Figure 13A).

To better test the hypothesis that dimerization regulates the distribution of sEH within the neurons, we used novel mutations shown to affect the dimerization of sEH. We previously characterized systematic mutations that control the dimerization state of sEH (102). By mutating amino acids that form an essential dimer-stabilizing salt-bridge (E254 and R287), we demonstrated that we could either completely disrupt or stabilize sEH dimerization. Specifically, we demonstrated that both E254R and R287E mutations severely disrupt sEH dimerization, while combining the two mutation (E254R+R287E) mutations stabilizes dimerization by inverting the dimer-stabilizing salt-bridge (102).

Figure 13. Dimerization mutants of sEH preferentially localize to peroxisomes.

Primary neurons cotransfected with GFP-sEH fusion protein and peroxisome marker RFP-SKL. A, GFP, RFP, and merged image from a neuron transfected with GFP-sEH-R287Q. GFP-sEH-R287Q fusion results in a punctate pattern that highly correlates with RFP-SKL (white arrowheads) indicative of predominantly peroxisome localization. B, GFP, RFP, and merged image from a neuron transfected with GFP-sEH-R287E. GFP-sEH-R287E fusion results in a punctate pattern that correlates with RFP-SKL (white arrowheads) indicative of predominantly peroxisome localization. C, GFP, RFP, and merged image from a neuron transfected with GFP-sEH-E254R. GFP-sEH-E254R fusion results in a punctate pattern that correlates with RFP-SKL (white arrowheads) indicative of predominantly peroxisome localization. D, Quantification of peroxisome localization index (PLI) of GFP-sEH fusion proteins reflecting the distribution between the cytosol and peroxisome. Compared to GFP-sEH-WT fusion, which results in .27 PLI (normalized WT data presented in Figure 2), GFP-sEH-R287Q, GFP-sEH-R287E, and GFP-sEH-E254R result in .68-.81 PLI. * indicates $p<.05$ compared with WT, n.s. indicates "not significant" by one-way ANOVA. White number in bar graph represents number of images analyzed in each group. Scalebar is 5µm.

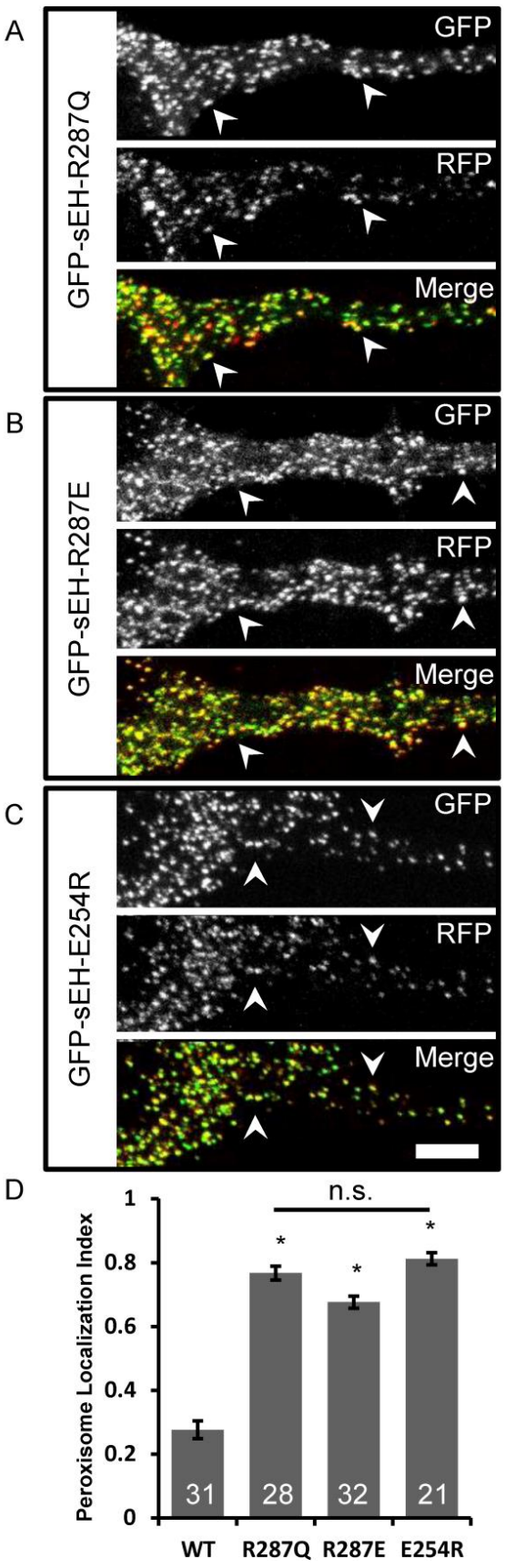
A
GFP-sEH-R287Q
GFP
RFP
Merge
B
GFP-sEH-R287E
GFP
RFP
Merge
C
GFP-sEH-E254R
GFP
RFP
Merge
D
n.s.
*
*
*
Peroxisome Localization Index
1
0.8
0.6
0.4
0.2
0
31
28
32
21
WT
R287Q
R287E
E254R

We used these three constructs of sEH to test the hypothesis that dimerization regulates the subcellular distribution of sEH. We find that transfection with either GFP-sEH-R287E (Figure 13B) or GFP-sEH-E254R (Figure 13C) result in a punctate signal that colocalizes with peroxisomes (Figure 13B and 13C, white arrowheads).

In order to quantify the distribution of sEH between the cytosol and the peroxisomes we developed the peroxisome localization index (PLI, see methods). The PLI describes the fraction of sEH mutant protein localized to either the cytosol by setting the value of a completely cytosolic sEH (GFP-sEH-ΔPTS) to 0 and a completely peroxisomal sEH (GFP-sEH-SKL) to 1. We find that all dimer disrupting mutations significantly increase peroxisome localization from .27±.03 (GFP-sEH-WT) to .77±.02, .68±.02, and .81±.02 (GFP-sEH-R287Q, GFP-sEH-R287E, and GFP-sEH-E254R respectively) (Figure 13D). While the peroxisome localization of the disrupted dimerization constructs were not different from each other, they all were significantly less than GFP-sEH-SKL ($p<.05$).

In contrast to disrupting dimerization, stabilizing sEH dimerization by combining the E254R and R287E mutations (GFP-sEH-E254R+R287E) results in a diffuse and punctate pattern in which the punctate signal colocalizes with peroxisomes (Figure 14A, white arrows). This diffuse pattern is similar to the pattern observed in GFP-sEH-WT. Quantification of neurons transfected with GFP-sEH-E254R+R287E reveals that it is statistically different from cytosolic sEH ($p<.05$ compared to GFP-sEH-ΔPTS) and dimer-disrupted sEH ($p<.05$ compared to GFP-sEH-R287Q, GFP-sEH-R287Q, and GFP-sEH-

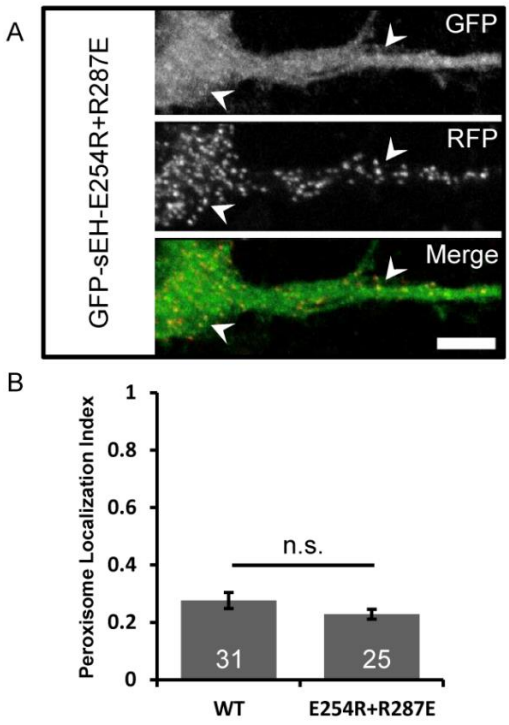

Figure 14. Stabilizing sEH dimerization restricts peroxisome localization.

Primary neurons cotransfected with GFP-sEH fusion protein and peroxisome marker RFP-SKL. A, GFP, RFP, and merged image from a neuron transfected with GFP-sEH-E254R+R287E. GFP-sEH-E254R+R287E fusion results in a diffuse and punctate stain. GFP-sEH-E254R+R287E punctate colocalize with RFP-SKL (white arrowheads) reflecting the dual distribution of GFP-sEH-E254R+R287E between the cytosol and peroxisomes similar to GFP-sEH-WT. B, Quantification of peroxisome localization index (PLI) of GFP-sEH fusion proteins reflecting the distribution between the cytosol and peroxisome. There is no significant difference in PLI comparing GFP-sEH-E254R+R287E and GFP-sEH-WT (same WT data presented in figure 3); n.s. indicates “not significant” by one-way ANOVA. White number in bar graph represents number of images analyzed in each group. Scalebar is 5µm.

R287Q), but statistically indistinguishable from GFP-sEH-WT (.23±.02 vs. .27±.03). (Figure 14B).

Discussion

sEH is an exciting therapeutic target stroke that is distributed between two different subcellular compartments. We systematically tested the hypothesis that dimerization regulates the subcellular distribution of sEH between the cytosol and peroxisomes within primary neurons. We used previously validated mutations of sEH that either disrupt or stabilize dimerization and fused them with GFP to examine their localization in primary cortical neurons (102). Additionally, we developed a peroxisome localization index (PLI) based on Pearson's correlation against a peroxisome marker to quantify the fraction of sEH localized to either the cytosol or peroxisomes.

We find that two different constructs of sEH previously shown to form dimers (GFP-sEH-WT and GFP-sEH-R287E+E254R) distribute in an equilibrium between the cytosol and peroxisomes, with the majority residing in the cytosol. In contrast, all three sEH constructs (GFP-sEH-R287Q, GFP-sEH-R287E, GFP-sEH-E254R) which disrupt dimerization, have predominantly peroxisome localization. We take this as strong evidence that dimerization plays a role in the regulation of sEH subcellular localization.

Interestingly, there was no increase in the peroxisome localization of GFP-sEH-R287E and GFP-sEH-E254R compared to GFP-sEH-R287Q, despite the fact that R287E and E254R mutations were shown to disrupt dimerization more significantly than the R287Q

polymorphism (102). This would suggest that only a slight disruption in sEH dimerization is necessary to shift the localization to favor peroxisomal targeting.

Our findings suggest a model of sEH translocation similar to what has previously been proposed for a human polymorphism of sEH (41). Our data is consistent with the idea that dimer formation of sEH competes with binding the peroxisome transport protein peroxin 5 (Pex5) resulting in a majority of sEH to be localized to the cytosol (Figure 15A). However, as a monomer, the binding conditions of –SKM and Pex5 become more favorable (Figure 15B) resulting in translocation into peroxisome (Figure 15C).

One potential limitation of this study is its reliance on an GFP expression system to study the localization of a protein. However, the localization pattern that we observe in our GFP-sEH expression system is consistent with biochemical studies which have detected epoxide hydrolase activity in both the cytosolic and peroxisome fraction of mouse liver cell (135). Furthermore, the expression pattern we observe for GFP-sEH-WT is consistent with immunohistochemistry of human tissue stained for sEH and peroxisome antibodies (40).

Localization of a protein is an important determinant of the function of a protein. Indeed, protein misslocalization is associated with multiple diseases (115). The commonly accepted function of sEH is its role in the metabolism and inactivation of the lipid signaling molecule epoxyeicosatrieinoic acids or EETs. Because EETs are released from the plasma membrane by phospholipase A_2 into the cytosol, this action of sEH is thought to be carried out in the cytosol.

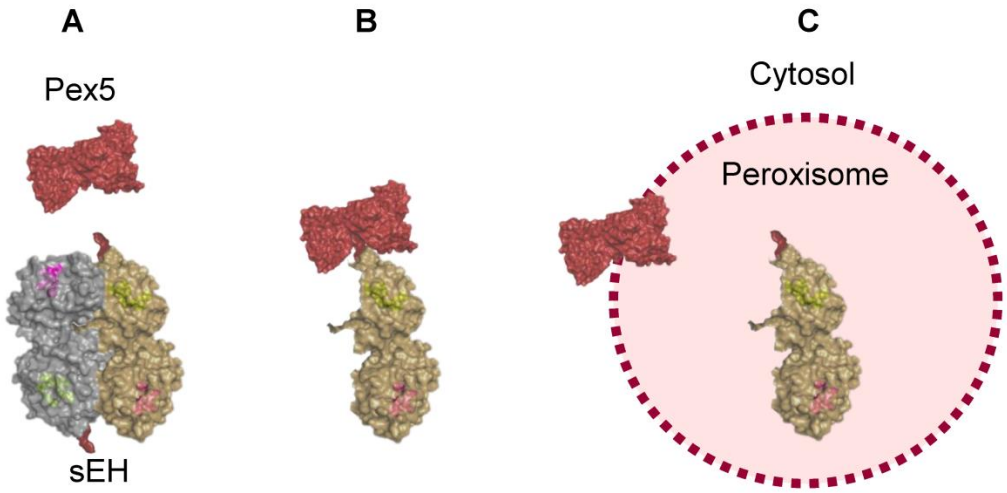

Figure 15. Model of sEH peroxisome translocation.

Artistic representation of sEH (grey and tan) and Pex5 (red) binding and translocation. A, as a dimer, Pex5 binding to the endogenous peroxisome targeting signal (PTS) of sEH is unfavorable resulting in mostly cytosolic localization. B, however, as a monomer binding to the endogenous PTS of sEH become more favorable. C, Disruption of sEH dimerization; therefore, preferentially translocates it into peroxisomes.

On the other hand, what role sEH plays in the peroxisomes is not so clear. Peroxisomes are largely responsible for the metabolism of reactive oxygen species (ROS) within the cell (120). Stressful conditions can lead to peroxisome dysfunction, such as ischemia/reperfusion injury, and the resulting defect in ROS metabolism may lead to increase in the formation of toxic fatty acid epoxides in peroxisomes. This has led to the speculation that the peroxisomal epoxide hydrolase activity detoxifies these products (136). This role for sEH is consistent with the protection from ischemia afforded by R287Q human polymorphism (14,15).

Indeed, the idea that peroxisome localization of sEH serves a protective function is an attractive one. Potentially, this action may be protective through two independent mechanisms; 1) sequestration of the enzyme away from EETs in the cytosol thereby elevating levels of these protective molecules and 2) detoxification of fatty acid epoxides in dysfunctional peroxisomes.

In conclusion, this study demonstrates that disrupting sEH dimerization results in enhanced translocation of the enzyme to peroxisomes. This places new emphasis on the role that sEH is playing in peroxisomes, especially for understanding the clinical phenotypes associated with the R287Q human polymorphism(14,81,82,126). This work is supportive of the idea that disrupting sEH dimerization is a novel therapeutic target for stroke. Work in the next chapter elucidates the protective role that sEH peroxisome localization plays in ischemic injury.

Chapter 4

Peroxisomal translocation of soluble epoxide hydrolase protects against ischemic stroke injury

Jonathan W. Nelson, Wenri Zhang, Nabil J. Alkayed, Ines P. Koerner

Abstract

Soluble epoxide hydrolase (sEH) is a risk factor for multiple cardiovascular diseases, including stroke. sEH is thought to exacerbate ischemic damage through the metabolism and inactivation of neuroprotective lipid molecules called epoxyeicosatrienoic acids within the cytosol. Under native conditions, however, sEH is not solely localized to the cytosol. Its C-terminal peroxisome targeting signal (PTS) facilitates the translocation of a fraction of sEH into peroxisomes. Recently, a missense human polymorphism of sEH (R287Q) which enriches the protein for peroxisome localization has been shown to confer ischemic protection. This suggests that while localized in the cytosol, sEH is harmful; however, when translocated to the peroxisomes, sEH is protective. To directly test the hypothesis that peroxisomal localization of sEH is protective against ischemia, we introduced variants of human sEH into sEH-null mice using TAT-protein transduction before subjecting the mice to experimental stroke through middle cerebral artery occlusion. We found that treatment with either wildtype sEH or sEH harboring the R287Q polymorphism, both of which translocate to peroxisomes, protect sEH knockout mice from ischemic damage. However, deletion of the C-terminal peroxisome targeting signal, restricting sEH into the cytosol results in a loss of protection. We conclude that sEH contributes to stroke injury only if it is localized in the cytoplasm, while peroxisomal

sEH may be protective. Strategies targeting the enhancement of peroxisomal localization of sEH may represent a novel therapeutic approach for treating stroke.

Introduction

Soluble epoxide hydrolase (sEH), which metabolizes and inactivates vasodilatory and neuroprotective arachidonic acid derived epoxyeicosatrienoic acids (EETs), has been implicated in multiple cardiovascular diseases, including stroke (54). Both gene deletion of sEH, or pharmacological inhibition have shown to improve the outcome of mice after experimental models of stroke, identifying sEH as a novel and exciting target for new stroke therapeutics (13,46). Further linking sEH to stroke are multiple genetic studies which have identified associations with single nucleotide polymorphisms (SNPs) in the gene that encodes for sEH and the incidence of stroke (75,83,84). While these studies suggest that the effect that different SNPs have may be specific to various populations, the SNP with the strongest evidence for a role in stroke results in a glutamine to arginine substitution at amino acid position 287 (R287Q) (14). In addition to this SNP being associated with a decreased incidence in stroke, it also was shown to improve neuronal survival after *in vitro* ischemia (15).

sEH is a complex protein and the precise mechanisms by which it contributes to stroke injury remain poorly understood. Current therapeutic efforts have focused on the pharmacological inhibition of the hydrolase domain of sEH thus elevating endogenous levels of EETs (54). However, this therapeutic strategy has failed to be translated into

successful human clinical trials, suggesting that there are additional factors contributing to the deleterious effect of sEH (137).

Originally, sEH was thought to be localized exclusively to the cytosol, however, recent work has demonstrated that it distributes between the cytosol and peroxisomes (40). This localization pattern may be the result of a weak C-terminal peroxisome targeting sequence (PTS) (122). However, despite this impaired PTS, sEH protein harboring the R287Q human SNP is localized almost exclusively in the peroxisomes (41). While the R287Q SNP has been shown to affect other aspects of sEH protein function, its influence on the subcellular distribution of sEH in combination with its ability to confer ischemic protection suggests that the subcellular localization of sEH plays a role in ischemic outcome (77). Additionally, there is evidence that cytoplasmic sEH in the brain drops rapidly after stroke (48), suggesting that sEH might translocate to the peroxisomes, possibly as part of an endogenous protective pathway reducing cytoplasmic epoxide hydrolase activity. However, the relevance of peroxisomal translocation and subcellular localization of sEH for stroke injury has not yet been studied.

We hypothesized that translocation of cytoplasmic sEH to the peroxisomes is beneficial after ischemic stroke. To test this hypothesis, we used a unique model of TAT-protein transduction to introduce human sEH variants with intact or defective peroxisomal targeting sequence into sEH-null mice. Mice transduced with the sEH variants were then exposed to experimental stroke, and infarct size was measured.

Experimental Procedure

Expression and purification of TAT-fusion protein

Plasmids for TAT-human sEH fusion proteins were generated by subcloning WT (TAT-sEH-WT) and mutant R287Q sEH (TAT-sEH-287) cDNAs into the pTAT2.1 vector, as previously described (15). PCR mediated deletion was used to remove the C-terminal peroxisomal targeting sequence (PTS) of TAT-sEH-WT to create translocation deficient TAT-sEH-ΔPTS. Appropriate deletion of the PTS was verified by sequencing. Recombinant proteins were expressed in E. coli and purified as previously described (15). Concentrations of purified fusion proteins were measured with a Bradford protein assay (Biorad) using a BSA standard curve. Protein purity and specificity was confirmed by Western blot using anti-sEH antibody (Cayman Chemical).

Western blot and hydrolase assay

Western Blot was performed as previously described (47) with 1:250 rabbit anti-sEH antibody (Cayman Chemical) primary antibody and 1:2000 anti-rabbit Cy5 (GE Healthcare) secondary antibody on a Typhoon imager (GE Healthcare). Densitometry analysis was performed using ImageQuant software (GE Healthcare). Purity of the different TAT-sEH fusion proteins was similar (see Figure 1C), with TAT-sEH-WT purity slightly higher than TAT-sEH-287 and TAT-sEH-ΔPTS. Protein concentrations of TAT-sEH-287 and TAT-sEH-ΔPTS were adjusted based on densitometry data to ensure that equivalent amounts of sEH protein were used for downstream applications (hydrolase

activity assay and in-vivo experiments). Soluble epoxide hydrolase enzyme activity was quantified with an EP7 assay (Cayman Chemical) as previously described (131).

Animals and treatment groups

All experiments and postsurgical care were carried out in compliance with the National Institutes of Health (NIH) Guide for the Care and Use of Laboratory Animals and according to the Institutional Animal Care and Use Committee (IACUC)-approved protocols. Male soluble epoxide hydrolase knockout (sEHKO) mice (20-26 g) on a C57BL/6 background were obtained from our in-house colony (46). Mice (7-8 per group) were randomly assigned to treatment with different TAT-sEH variants, TAT-GFP, or vehicle (phosphate-buffered saline (PBS) containing 2mM $MgCl_2$ and 50mM HEPES). Investigators were blinded to treatment allocation.

TAT-sEH injection and middle cerebral artery occlusion

Mice were anesthetized with isoflurane (1.5 to 2% in O_2 enriched air by face mask). A PE-10 catheter was inserted into the right internal jugular vein and 0.5 nmol of TAT-sEH or TAT-GFP fusion protein in 500 µl vehicle, or vehicle alone, were slowly injected. Rectal temperature was monitored and normothermia was maintained throughout the experiment using a heating lamp.

Ischemic stroke was induced two hours after TAT-sEH injection using the intraluminal filament model of transient middle cerebral artery (MCA) occlusion (13). A silicone-coated 6-0 nylon monofilament was inserted into the right internal carotid artery via the external carotid artery and advanced until the MCA was occluded. Ischemia was

confirmed by laser-Doppler monitoring of cerebral blood flow. After 60 minutes of middle cerebral artery occlusion, the occluding filament was withdrawn and reperfusion verified by laser-Doppler monitoring. At this point, anesthesia was terminated and mice were allowed to recover and observed for 1 day. No animals died during the observation period. One mouse (TAT-sEH-WT) was excluded from the experiment because MCA occlusion could not be achieved.

A separate cohort of mice (n=5 per treatment; TAT-GFP, TAT-sEH-WT, TAT-sEH-ΔPTS) was instrumented with a PE-10 catheter in the right femoral artery before induction of MCA occlusion to allow continuous monitoring of arterial blood pressure throughout the experiment. Blood samples were taken 30 minutes after reperfusion to measure arterial blood gases, pH, and glucose levels.

Infarct size analysis

Infarct size was measured 24h after MCA occlusion in 2 mm thick coronal brain sections (three total) using 2,3,5- triphenyltetrazolium chloride (TTC) staining and digital image analysis, as previously described (Zhang 2007). Sections were incubated in 1.2% TTC in saline for 15 mins at 37°C and fixed in formalin for 24 h. Slices were photographed, and infarcted (unstained) and uninfarcted (red color) areas were measured with MCID software (InterFocus Imaging) and integrated across all slices. Infarct volume was expressed as a percentage of contralateral hemisphere after correction for cerebral edema.

Immunohistochemistry

In order to confirm brain penetration of systemically provided TAT-sEH fusion proteins, sEHKO mice were transcardially perfused with 0.9% saline followed by 4% paraformaldehyde eight hours after injection with TAT-sEH-WT protein. Brains were embedded in paraffin and 6 μm coronal sections were cut. Sections were deparaffinized and stained overnight with sEH antibody (1:200; H-215, Santa Cruz Biotechnology), followed by incubation with a biotin-labeled goat-anti-rat secondary antibody (1:150) and Cy-3 linked streptavidin (1:700, both GE Healthcare).

Statistics

All values are presented as mean ± s.e.m. Statistical analysis was done using SigmaStat (Systat Software Inc.) software. Groups were compared using one-way analysis of variance (ANOVA) followed by Holm-Sidak post-hoc test.

Results

Characterization of translocation deficient human soluble epoxide hydrolase

To examine the effect of the peroxisome localization of sEH, we transduced male sEHKO mice with TAT-fusion proteins containing either wildtype human sEH (TAT-sEH-WT), a human variant sEH containing the R287Q SNP (TAT-sEH-287), which possesses reduced hydrolase activity (15,34), but also enhanced peroxisomal translocation due to conformational changes (41), or a synthetic variant of human sEH engineered to lack the ability to translocate to the peroxisomes (TAT-sEH-ΔPTS). TAT fused to green fluorescent protein (TAT-GFP) was used to control for unspecific effects of TAT. Human sEH-ΔPTS

was produced by removing the C-terminal peroxisome targeting signal (PTS) from sEH-WT (Figure 16A). Specifically, we removed the final three amino acids, serine (S), lysine (K), and methionine (M) from TAT-sEH-WT to construct TAT-sEH-ΔPTS (Figure 16B). Next, we expressed, purified, and sterilized recombinant TAT-sEH-WT, TAT-sEH-287, TAT-sEH-ΔPTS, and TAT-GFP. We used immunoblotting for sEH to confirm concentration of purified sEH fusion proteins (Figure 16C). Next, we confirmed that recombinant sEH proteins were catalytically active by performing a hydrolase activity assay. We found that removal of sEH PTS had no effect on hydrolase enzyme activity, while TAT-sEH-287 had 60% of TAT-sEH-WT activity (Figure 16D) similar to what has previously been reported (15,77). Finally, we confirmed that the TAT-protein transduction domain effectively transported sEH-fusion proteins across the blood-brain-barrier after systemic administration. We easily detected TAT-sEH-WT in parenchymal brain cells, presumably neurons (Figure 16E), which is consistent with previous reports using TAT-mediated protein transduction to introduce neuroprotective proteins into the CNS (138–140).

Translocation deficient human soluble epoxide hydrolase increases infarct damage after stroke

Having characterized our recombinant proteins, we were ready to test the hypothesis that peroxisomal translocation of sEH is protective against ischemic injury. We injected mice IV through the jugular vein, with TAT-GFP, TAT-sEH-WT, TAT-sEH-287 and TAT-sEH-ΔPTS 2 hours prior to subjecting them to 1 hour of transient MCA occlusion. After 24 hours of reperfusion, we quantified the infarct volume by 2,3,5-Triphenyltetrazolium chloride (*TTC*) staining (Figure 17A).

Figure 16. Characterization of TAT recombinant protein.

(A) Schematic of recombinant sEH protein containing TAT-protein transduction domain. N-terminal 6xHis tag facilitates purification without affecting protein function. Wildtype sEH contains phosphatase and hydrolase catalytic domains followed by a C-terminal peroxisome targeting signal (PTS). The R287Q polymorphism (black arrow) which affects hydrolase activity is localized within the hydrolase catalytic domain. (B) Plasmid sequences were verified. Representative Electropheragram DNA sequence and translated protein sequence (above) of TAT-sEH-WT and TAT-sEH-ΔPTS plasmids are shown, the C-terminal PTS of sEH is colored in light gray. (C) Western blot of purified recombinant proteins. sEH content was similar in all fusion proteins (densitometry quantification below blot). Calculation of equimolar amounts of fusion protein for downstream experiments was based on sEH content. (D) Hydrolase activity of recombinant proteins. Hydrolase activity of TAT-sEH-287 was lower than TAT-sEH-WT and TAT-sEH- ΔPTS protein. N=3 experiments. (E) Immunostaining for sEH in brain of a sEHKO mouse treated with TAT-sEH-WT protein. White arrow indicates brain cells that contain sEH.

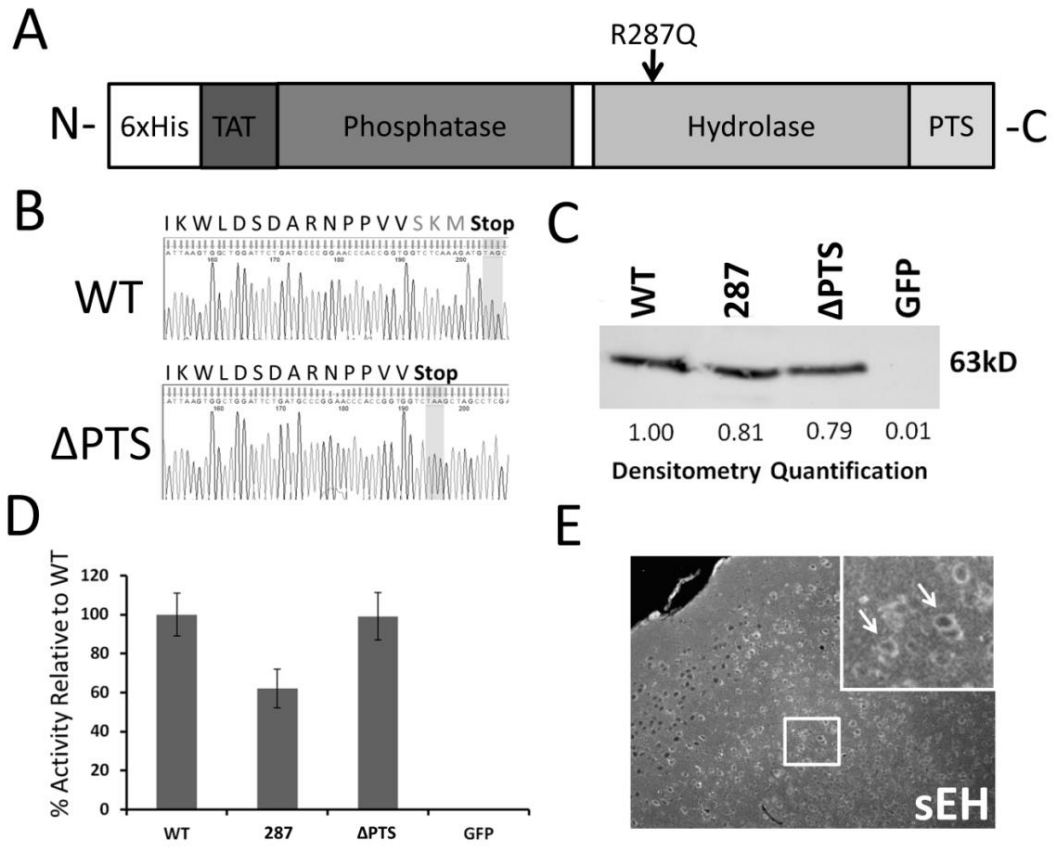
A
R287Q
N-
6xHis
TAT
Phosphatase
Hydrolase
PTS
-C
B
I K W L D S D A R N P P V V S K M Stop
WT
I K W L D S D A R N P P V V Stop
ΔPTS
C
WT
287
ΔPTS
GFP
63kD
1.00
0.81
0.79
0.01
Densitometry Quantification
D
% Activity Relative to WT
120
100
80
60
40
20
0
WT
287
ΔPTS
GFP
E
sEH

We found that, sEHKO mice receiving wildtype human sEH (TAT-sEH-WT) had significantly smaller hemispheric strokes than had mice injected with control TAT-GFP (17 +/- 7% sEH-WT vs 39 +/- 7% GFP, Figure 17). This was a protective effect of TAT-sEH, rather than a sign of TAT-GFP toxicity, as sEHKO mice injected with vehicle only sustained similar infarcts as the TAT-GFP treated animals (data not shown). We used TAT-EH-287 and TAT-sEH-ΔPTS to assess whether the protection was related to sEH ability to translocate to the peroxisomes. Mice treated with TAT-sEH-287, which localizes preferentially to the peroxisomes, were protected to a similar degree as mice receiving TAT-sEH-WT (23 +/- 8% infarct, Figure 17B). In contrast, mice treated with TAT-sEH-ΔPTS, which cannot translocate to the peroxisomes, had significantly larger infarcts compared to mice treated with TAT-sEH-WT (41 +/- 7%, Figure 17B), similar to sEHKO mice treated with TAT-GFP or vehicle control. The reduction in hemispheric infarct size was mostly caused by a reduction of cortical infarct (Figure 17B, $P<0.05$ for difference between groups) whereas the size of infarct in the striatum was not different. This is in line with the observation that the penumbra, or area at risk that is potentially salvageable after middle cerebral artery occlusion is localized in the cortex. Treatment with the different TAT-fusion proteins did not alter cerebral blood flow during or after middle cerebral artery occlusion (Figure 17C). Similarly, arterial blood pressure and blood gases were not different between groups (data not shown).

Discussion

This study has two main findings. First, introduction of human soluble epoxide hydrolase (sEH) in a mouse that is genetically deficient for sEH reduces infarct size after ischemic

Figure 17. Peroxisomal Localization of sEH Protects Against Ischemic Injury.

(A) Timeline of experimental protocol. (B) Quantification of hemispheric infarct size from mice treated with TAT-GFP, TAT-sEH-WT, TAT-sEH-R287Q, or TAT-sEH-ΔPTS protein. * indicates $p<.05$ compared to WT treatment. Number of animals within each group is labeled in each bar graph. Below each bar is a representative TTC stained brain section from each group. (C) Laser Doppler flow measurements of each group during transient MCA occlusion.

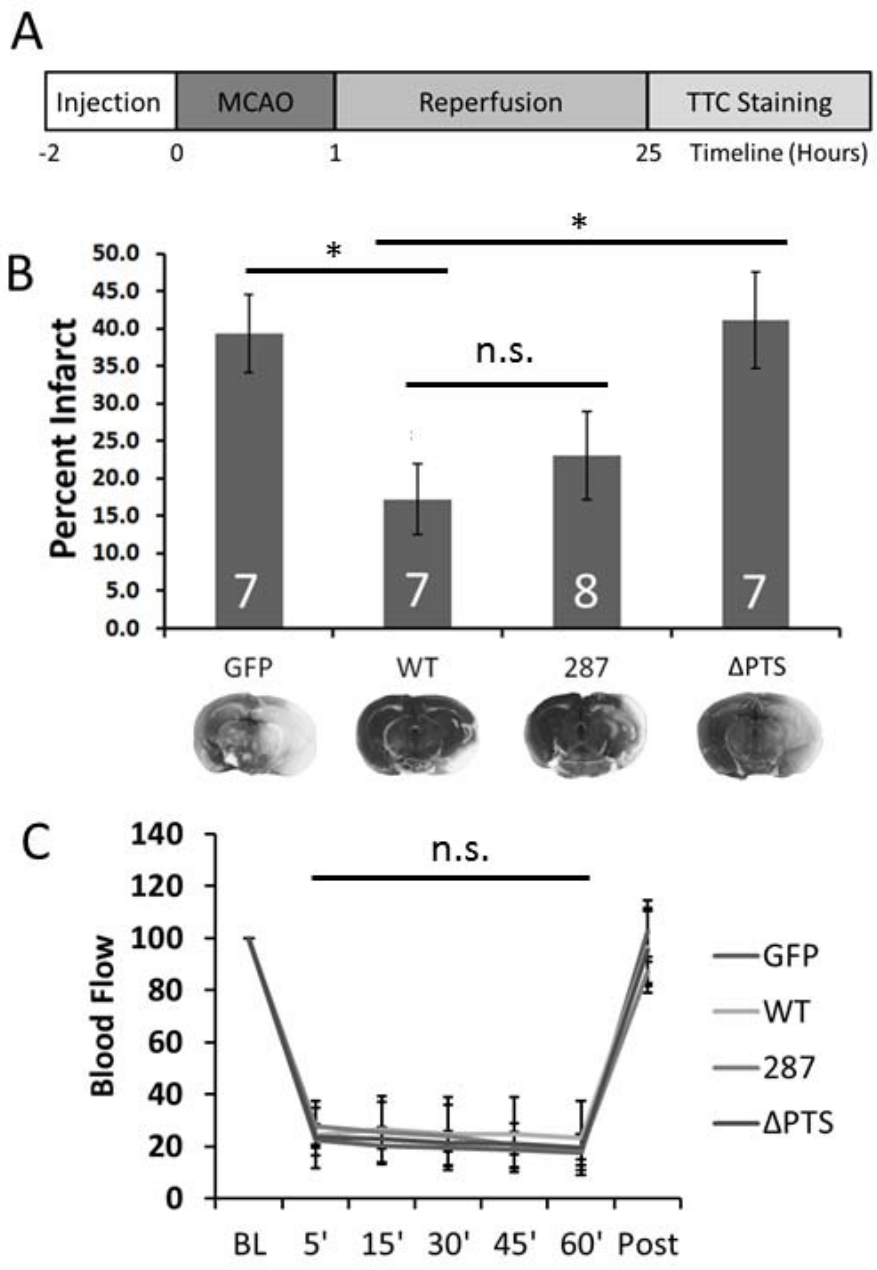
A
Injection
MCAO
Reperfusion
TTC Staining
-2
0
1
25
Timeline (Hours)
B
Percent Infarct
50.0
45.0
40.0
35.0
30.0
25.0
20.0
15.0
10.0
5.0
0.0
*
*
n.s.
7
7
8
7
GFP
WT
287
ΔPTS
C
Blood Flow
140
120
100
80
60
40
20
0
n.s.
BL
5'
15'
30'
45'
60'
Post
GFP
WT
287
ΔPTS

stroke. Second, this protection depends on the ability of sEH to translocate to peroxisomes.

sEH is a therapeutic target for multiple cardiovascular diseases that is localized to both the peroxisomes and the cytosol. We have seen cytosolic levels drop rapidly after stroke, suggesting that ischemia may induce translocation from cytosol to peroxisomes (48). We set out to test the hypothesis that peroxisomal localization of sEH is protective against ischemia by sequestering the enzyme away from the cytosol thus reducing the enzyme capacity for degrading the neuroprotective lipid molecule EETs. For the first time our studies examine the functional significance of sEH localized to peroxisomes peroxisome localization on ischemic injury.

Both of our treatment groups capable of translocating to the peroxisomes (TAT-sEH-WT and TAT-sEH-287) were protective against ischemia, while treatment with a translocation deficient sEH (TAT-sEH-ΔPTS) resulted in a loss of protection. These results suggest that the subcellular localization of sEH has a physiological significance. Specifically, while localized in the peroxisomes, sEH is protective; however, when localized to the cytosol, sEH is harmful.

Previous studies have theorized that the protective effect afforded by the R287Q human polymorphism is due to its decreased hydrolase activity. While that remains a plausible mechanism of protection, our results suggest that another potential mechanism contributing to R287Q-afforded ischemic protection is translocation of the sEH into peroxisomes. Oxidative stress during ischemia/reperfusion may increase production of

highly reactive epoxides from long-chain fatty acid in the peroxisomes (136). Rapid detoxification of these fatty acid epoxides by peroxisomally localized sEH may be necessary to limit injury after ischemia.

In order to study the effect of sEH peroxisome localization in a sEH knockout background, we utilized TAT to facilitate the protein transduction into cells. TAT-mediated protein transduction has been used before *in vivo* to shuttle systemically administered proteins to the brain (138,139,141). We have used TAT-sEH fusion proteins before in cultured neurons and found that compared to sEH-WT, TAT-sEH-287 reduced ischemic neuronal death (15). Our current *in vivo* study does not replicate this difference. The *in vivo* assessment presented here was performed in a because of the sEH-null background which may have compensatory epoxide hydrolase activity in the cytosol (such as epoxide hydrolase 3, ABDH9), but not in the peroxisomes. Providing sEH with peroxisomal targeting sequence would thus enable peroxisomal detoxification and protect from ischemic injury.

This study demonstrates the biological significance of subcellular localization of a protein in the context of disease. Artificially restricting or enriching a protein in specific cellular compartment remains a valuable tool for identifying new roles for proteins under different conditions. Still many questions surround the significance of dual subcellular localization of sEH. Specifically, when and how sEH subcellular localization may be regulated and plays a role in other diseases remains unexplored.

To our knowledge, this is the first study to examining functional significance of sEH peroxisome localization. Furthermore, this is the first study to examine the reintroduction of sEH onto a sEH-null background. Our findings are novel and help understand the complex function of sEH in stroke. Further study is needed to clarify the function of sEH in the peroxisomes. Our model adds a valuable tool for these studies and may lead to novel treatments enhancing peroxisomal detoxification.

In conclusion, our study places new emphasis on a biological role for sEH within the peroxisomes, especially in the context of stroke. Furthermore, our data suggests that sEH plays a protective role in the peroxisomes. Strategies targeting the enhancement of peroxisome localization of sEH may represent a novel therapeutic approach to treating stroke.

Chapter 5

Conclusions and Future Directions

Conclusions

sEH is an exciting therapeutic target for multiple cardiovascular diseases including stroke. In this thesis, I examined the mechanism by which the protective effect of the R287Q human polymorphism of sEH is afforded, and by doing so, elucidated a novel therapeutic strategy for targeting sEH, namely, by disrupting sEH dimerization.

First, in chapter 1, I discuss current therapeutic efforts to target sEH for the treatment of stroke while also proposing that disrupting sEH dimerization may be a novel therapeutic strategy.

In chapter 2, I tested the hypothesis that dimerization is essential for hydrolase enzymatic activity. I developed mutations on the dimerization interface of sEH to control the dimerization of the enzyme. Next, I validated the dimerization state of each of the mutations, with a split-firefly luciferase complementation system, before quantifying their hydrolase activity. I found that mutations that disrupt sEH dimerization significantly decrease hydrolase activity leading to the overall conclusion that dimerization is essential for hydrolase enzymatic activity.

In chapter 3, I tested the hypothesis that dimerization regulates the subcellular localization of sEH. I fused the same mutations used in chapter 2 with green fluorescent protein and transfected them into primary cortical mouse neurons and quantified their

colocalization with a red fluorescent protein targeted to peroxisomes. I found that, as a dimer, sEH distributes between both the cytosol and peroxisomes, while mutations that disrupt sEH dimerization localize sEH to peroxisxomes. From this study, I conclude that disrupting dimerization preferentially translocates sEH into peroxisomes.

Finally, in chapter 4, I tested the hypothesis that the translocation of sEH into peroxisomes is protective against ischemic injury. I fused sEH protein, with or without a peroxisome targeting signal, to the TAT transduction domain. After treatment with the proteins, sEH knockout mice were subjected to an experimental model of stroke. The amount of brain damage was measured 24 hours later. I found that mice treated with sEH deficient for a peroxisome targeting signal had larger brain damage compared to mice treated with sEH containing a peroxisome targeting signal. This suggests that the localization of sEH within the cells has a functional consequence in terms of affording ischemic protection. Specifically, that localization of sEH to peroxisomes is protective.

Taken together, this work suggests that disrupting dimerization represents a novel therapeutic strategy for targeting sEH. Disrupting sEH dimerization should have two effects. First, it should decrease hydrolase activity leading to increased EETs level inside the cell, which is protective, and second, it should translocate the enzyme to peroxisomes, which by itself is also protective. This makes disrupting of sEH dimerization an exciting target for a pharmacological intervention. Therefore, I suggest to explore the the possibility of screening for a pharmacological inhibitor of sEH dimerization.

Development of sEH Dimerization Inhibitors

Targeting protein dimerization as a therapeutic mechanism is an emerging strategy (142). Disrupting protein dimerization has been developed as a therapeutic strategy for treating cancer (143), HIV (144), and Herpes (145). In fact, the same SFL-PFAC system used in chapter 2 has been utilized to screen for small molecule inhibitors of Epidermal Growth Factor (EGF) dimerization to treat cancer (146). Similar to sEH, EGF is activated upon dimerization, leading to downstream signaling that promotes uncontrolled cell growth. Inhibiting this activity, through interfering with EGF dimerization, either with an antibody or small molecule, has been explored as a cancer therapeutic (146).

One of the challenges of converting the SFL-PFAC system used in chapter 2 is scaling it into a high-throughput screen (HTS), in terms of both volume and time. In order to be an effective HTS, the assay needs to be scaled to fit a 384 or 1536 well volume. Additionally, the time of detection for each well needs to be short enough that it is possible to read each well of a plate in a timely manner.

To help overcome these challenges, I worked with the Oregon Translation Research and Development Institute (OTRADI) to test the feasibility of developing the sEH SFL-PFAC system into a HTS. Excitingly, using a 384 well instrument with a detection time of 1 second per well, we were able to detect signal of sEH dimerization (Figure 18). Additionally, we were able to detect inhibition of sEH dimerization using two different doses of a protein inhibitor of sEH-Luc dimerization, similar to experiments performed in

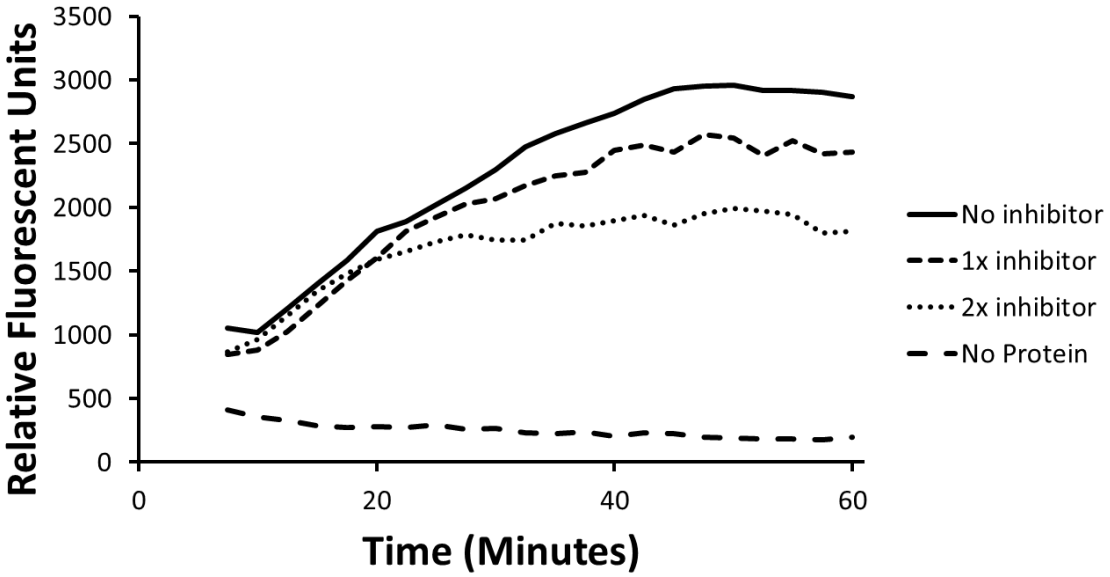

Figure 18. sEH Dimerization High Throughput Screen Development.

Similar to the experiment in Figure 9C, this data is from a 384 well plate examining the signal window and sensitivity high-throughput instrument to measure sEH dimerization. The inhibitor used in this study is a protein inhibitor of sEH-luciferase interactions used in Figure 9C.

Figure 9C. However, there remain a number of issues that need to be addressed to before this assay is ready for an actual HTS.

First, currently, the assay relies on a transient transfection system for synthesizing sEH-luciferase protein. This opens the door for increased variability from assay to assay depending on the efficiency of transfection for that particular set of cells. One potential solution is to develop two cell lines which stably express sEH-nLuc and sEH-cLuc (146). However, one potential problem with this strategy is that stable expression systems can expressing less protein than a transient expression system, thus requiring a larger assay volume for the same amount of dimerization signal. Moving forward, the variability of sEH dimerization signal between transfections should be explored. Should there be substantial variability; a stable cell line expressing sEH-luc may possibly lead to an improved assay.

Second, while it is currently possible to discriminate between sEH dimerization with and without inhibitors, the variability in the assay is too great for an effective HTS. One measure that needs to be optimized for the assay is called Z', which is a measure of the standard deviation of an assay compared to the differences between high and low signals. A workable Z' for a HTS should be greater than or equal to 0.5.

Despite both of these concerns, this work suggests that screening for sEH dimerization inhibitors using a SFL-PFAC system is a plausible strategy that could result in the discovery of a novel compound targeting sEH. Furthermore, based on the results in chapters 2 and 3, compounds identified as sEH dimerization inhibitors could be put

through additional screens such as detecting hydrolase activity using EP7 as a substrate (123), or peroxisome localization using high-content image screening (115).

Unanswered Questions

Below I highlight some of the important questions that remain to be addressed in the future. Additionally, I speculate on potential answers, and propose potential experiments to address them.

Does disrupting dimerization affect the phosphatase activity of sEH?

Unfortunately, one of the limitations of the study in chapter 2 was the inability to measure the phosphatase activity of sEH in the SFL-PFAC system. This limitation arose from the fact that current techniques for measuring sEH phosphatase activity depends on purified protein and not protein in complex lysates derived from transfected cells.

Currently, the only effective strategy for measuring the phosphatase activity of the different sEH mutants would be to express and purify all of the protein variants characterized in chapter 2 and then perform phosphatase assay with either p-NPP (35) or AttoPhos (147) as substrates. However, a major challenge associated with this strategy revolves around optimize expression levels and carefully controlling for protein purity between the different sEH constructs.

Exciting work is currently being done to develop a HTS to identify sEH phosphatase inhibitors (148). This work potentially could lead to the development of sEH-specific phosphatase substrates that could be used to determine the effect of dimerization on phosphatase activity in the SFL-PFAC system.

Is sEH dimerization regulated within the cell?

Unfortunately, another limitation of the study in chapter 2 was that sEH dimerization was not directly measured in living cells. Instead, the measurements were all done using cell lysates. Nevertheless, this is an extremely interesting question given previous observations in our lab that sEH translocation is a dynamic event potentially mediated through ischemia (48). In addition to quantifying the luciferase activity in living cells, another technique for measuring to study the dynamics of sEH dimerization within cells is Förster resonance energy transfer (FRET).

FRET involves tagging proteins with two different fluorescent proteins such as yellow fluorescent protein (YFP) and cyan fluorescent protein (CFP) (149). Laser light is used to excite one of the fluorophores (CFP) which transfers its energy to a neighboring fluorophor. In the case of CFP and YFP, CFP is excited, while YFP signal is detected. FRET is highly sensitive to the distance between fluorophores and is thought to only occur if the interaction is within 10nm (150). However, similar to crosslinking, FRET is not a straight-forward technique and many experimental conditions and controls need to be optimized. Furthermore, one of the major limitations of FRET is the dynamic range in which FRET is able to quantify an interaction.

Does sEH form as a dimer within the peroxisomes?

Based on the data in chapter 3, sEH is translocated to peroxisomes as a monomer. However, it is not clear whether once localized to the peroxisomes sEH reforms as a dimer. Cell fractionation studies which quantified epoxide hydrolase activity from the

peroxisome fraction of mouse liver cells provide indirect evidence that sEH does reform as a dimer in peroxisome (135). This study is limited by the fact that activity assay were performed in cell lysates, and not in living cells, allowing for the possibility sEH may have formed dimers outside of the peroxisomes once the cell was fractionated. Similar to the previous question, a technique to visualize dimerization in living cells, like FRET or luciferase complimentation, would provide more convincing evidence to answer this question. However, one challenge to answer this question will be attaching the FRET or luciferase fragments to sEH in such a way that it does not mask its PTS.

Which domain is responsible for the protecting neurons from ischemia?

The experiments in chapter 4 demonstrate that peroxisomal localization of sEH is protective, but they do not address which activity of sEH is protective. Multiple studies with inhibition of sEH hydrolase activity would suggest that the hydrolase activity of sEH is not protective but rather harmful (13,99). However, it is not clear if the drugs that target sEH hydrolase inhibition are able to penetrate peroxisomes to inhibit sEH that has previously translocated there. Another confounder is that the phosphatase activity of sEH is conferring protection from ischemia. Lack of research tools, such as a sEH-specific phosphatase inhibitor, make these currently difficult questions to address.

One approach that could be taken would be to express each sEH catalytic domains independent from one another in cells and test their effect on neuronal survival after ischemic injury. Similarly, you could make specific mutations such as D9A to knockout

phosphatase activity, or D335S to knockout hydrolase activity of sEH and perform the previously described experiments (38).

Is it sequestration of the sEH out of the cytosol that is protective from ischemia, or metabolism of a factor in the peroxisomes?

It remains plausible that both sequestration of the hydrolase domain and metabolism of a factor in peroxisomes by the hydrolase domain is protective. Sequestration may be protective by reducing the metabolism of EETs in the cytosol, thus boosting the levels of this protective epoxide, while the hydrolase activity in the peroxisomes may detoxify fatty acid epoxides. The lack of knowledge about what role sEH plays as a lipid phosphatase makes it difficult to speculate whether sequestration or localization more directly regulates the function of the phosphatase domain.

One approach to answer this question experimentally would be to express each domain and have it either be restricted from or enriched for peroxisome localization. This could be done by altering the peroxisome targeting signal of sEH domains similar to the experiments altering the localization of GFP-sEH in chapter 3.

Concluding Remarks

sEH is a complex protein with multi-dimensional effects on multiple levels. It has both epoxide hydrolase and lipid phosphatase enzymatic activity (36). It is expressed in multiple cell types in the body (44). It can localize to both the cytosol and peroxisomes. Inhibition of sEH is protective through multiple mechanisms including neuronal and vascular pathways (61). Adding another layer of complexity is the fact that none of

these sEH dichotomies is isolated from another. Different activities of sEH may play an important role in different cell types and in different subcellular compartments. This makes the study of sEH exceptionally challenging.

The work presented in this thesis adds another level of complexity to sEH. Specifically to appreciate does sEH exist primarily as a monomer or a dimer? This is not only relevant to individuals who harbor the R87Q human polymorphism of sEH, but also to researchers who are interested in developing a new class of sEH inhibitors targeting sEH dimerization.

A better understanding of the complexities of sEH will lead not only to better therapeutic approaches, but could potentially suggest how to specifically target sEH differently for intervention in various disease states. Clearly, the field of sEH is alive and well, full of questions that remain to be answered.

References

1. Roger VL, Go AS, Lloyd-Jones DM, Benjamin EJ, Berry JD, Borden WB, et al. Heart disease and stroke statistics--2012 update: a report from the American Heart Association. Circulation. 2012 Jan 3;125(1):e2–e220.

2. Madden JA. Role of the vascular endothelium and plaque in acute ischemic stroke. Neurology. 2012 Sep 25;79(13 Suppl 1):S58–62.

3. Durukan A, Tatlisumak T. Acute ischemic stroke: overview of major experimental rodent models, pathophysiology, and therapy of focal cerebral ischemia. Pharmacology, Biochemistry, and Behavior. 2007 May;87(1):179–97.

4. Phan TG, Wright PM, Markus R, Howells DW, Davis SM, Donnan GA. Salvaging the ischaemic penumbra: more than just reperfusion? Clinical and Experimental Pharmacology & Physiology. 29(1-2):1–10.

5. Kamel H, Iadecola C. Brain-Immune Interactions and Ischemic Stroke. Archives of Neurology. 2013;69(5):576–81.

6. O'Donnell MJ, Xavier D, Liu L, Zhang H, Chin SL, Rao-Melacini P, et al. Risk factors for ischaemic and intracerebral haemorrhagic stroke in 22 countries (the INTERSTROKE study): a case-control study. Lancet. 2010 Jul 10;376(9735):112–23.

7. Cheng YD, Al-Khoury L, Zivin JA. Neuroprotection for ischemic stroke: two decades of success and failure. NeuroRx. 2004 Jan;1(1):36–45.

8. Lemarchant S, Docagne F, Emery E, Vivien D, Ali C, Rubio M. tPA in the injured central nervous system: different scenarios starring the same actor? Neuropharmacology. 2012 Feb;62(2):749–56.

9. Wang X, Tsuji K, Lee S-R, Ning M, Furie KL, Buchan AM, et al. Mechanisms of hemorrhagic transformation after tissue plasminogen activator reperfusion therapy for ischemic stroke. Stroke. 2004 Nov;35(11 Suppl 1):2726–30.

10. Hatcher M a, Starr J a. Role of tissue plasminogen activator in acute ischemic stroke. The Annals of Pharmacotherapy. 2011 Mar;45(3):364–71.

11. Development RD. Recommendations for standards regarding preclinical neuroprotective and restorative drug development. Stroke. 1999 Dec;30(12):2752–8.

12. Sutherland B, Minnerup J, Balami JS, Arba F, Buchan AM, Kleinschnitz C. Neuroprotection for ischaemic stroke: translation from the bench to the bedside. International Journal of Stroke. 2012 Jul;7(5):407–18.

13. Zhang W, Koerner IP, Noppens R, Grafe M, Tsai H-J, Morisseau C, et al. Soluble epoxide hydrolase: a novel therapeutic target in stroke. Journal of Cerebral Blood Flow and Metabolism. 2007 Dec;27(12):1931–40.

14. Zhang L, Ding H, Yan J, Hui R, Wang W, Kissling GE, et al. Genetic variation in cytochrome P450 2J2 and soluble epoxide hydrolase and risk of ischemic stroke in a Chinese population. Pharmacogenetics and Genomics. 2008 Jan;18(1):45–51.

15. Koerner IP, Jacks R, DeBarber AE, Koop D, Mao P, Grant DF, et al. Polymorphisms in the human soluble epoxide hydrolase gene EPHX2 linked to neuronal survival after ischemic injury. The Journal of Neuroscience. 2007 Apr 25;27(17):4642–9.

16. Holmquist M. Alpha/Beta-hydrolase fold enzymes: structures, functions and mechanisms. Current Protein & Peptide Science. 2000 Sep;1(2):209–35.

17. Fleming I. Epoxyeicosatrienoic acids, cell signaling and angiogenesis. Prostaglandins & Other Lipid Mediators. 2007 Jan;82(1-4):60–7.

18. Newman JW, Morisseau C, Hammock BD. Epoxide hydrolases: their roles and interactions with lipid metabolism. Progress in Lipid Research. 2005 Jan;44(1):1–51.

19. Oesch F. Purification and specificity of a human microsomal epoxide hydratase. The Biochemical Journal. 1974 Apr;139(1):77–88.

20. Friedberg T, Löllmann B, Becker R, Holler R, Oesch F. The microsomal epoxide hydrolase has a single membrane signal anchor sequence which is dispensable for the catalytic activity of this protein. The Biochemical Journal. 1994 Nov 1;303 (Pt 3:967–72.

21. Lu AY, Miwa GT. Molecular properties and biological functions of microsomal epoxide hydrase. Annual Review of Pharmacology and Toxicology. 1980 Jan;20:513–31.

22. De Medina P, Paillasse MR, Segala G, Poirot M, Silvente-Poirot S. Identification and pharmacological characterization of cholesterol-5,6-epoxide hydrolase as a target for tamoxifen and AEBS ligands. Proceedings of the National Academy of Sciences of the United States of America. 2010 Jul 27;107(30):13520–5.

23. Cronin A, Decker M, Arand M. Mammalian soluble epoxide hydrolase is identical to liver hepoxilin hydrolase. Journal of Lipid Research. 2011 Apr;52(4):712–9.

24. Orning L, Gierse JK, Fitzpatrick FA. The bifunctional enzyme leukotriene-A4 hydrolase is an arginine aminopeptidase of high efficiency and specificity. The Journal of Biological Chemistry. 1994 Apr 15;269(15):11269–73.

25. Rudberg PC, Tholander F, Andberg M, Thunnissen MMGM, Haeggström JZ. Leukotriene A4 hydrolase: identification of a common carboxylate recognition site for the epoxide hydrolase and aminopeptidase substrates. The Journal of Biological Chemistry. 2004 Jun 25;279(26):27376–82.

26. Knehr M, Thomas H, Arand M, Gebel T, Zeller HD, Oesch F. Isolation and characterization of a cDNA encoding rat liver cytosolic epoxide hydrolase and its functional expression in Escherichia coli. The Journal of Biological Chemistry. 1993 Aug 15;268(23):17623–7.

27. Newman JW, Morisseau C, Harris TR, Hammock BD. The soluble epoxide hydrolase encoded by EPXH2 is a bifunctional enzyme with novel lipid phosphate phosphatase activity. Proceedings of the National Academy of Sciences of the United States of America. 2003 Feb 18;100(4):1558–63.

28. Beetham JK, Grant D, Arand M, Garbarino J, Kiyosue T, Pinot F, et al. Gene evolution of epoxide hydrolases and recommended nomenclature. DNA and Cell Biology. 1995 Jan;14(1):61–71.

29. Harris TR, Aronov P a, Hammock BD. Soluble epoxide hydrolase homologs in Strongylocentrotus purpuratus suggest a gene duplication event and subsequent divergence. DNA and Cell Biology. 2008 Sep;27(9):467–77.

30. Harris TR, Morisseau C, Walzem RL, Ma SJ, Hammock BD. The cloning and characterization of a soluble epoxide hydrolase in chicken. Poultry Science. 2006 Feb;85(2):278–87.

31. Argiriadi M a, Morisseau C, Hammock BD, Christianson DW. Detoxification of environmental mutagens and carcinogens: structure, mechanism, and evolution of liver epoxide hydrolase. Proceedings of the National Academy of Sciences of the United States of America. 1999 Sep 14;96(19):10637–42.

32. Gomez G a, Morisseau C, Hammock BD, Christianson DW. Structure of human epoxide hydrolase reveals mechanistic inferences on bifunctional catalysis in

epoxide and phosphate ester hydrolysis. Biochemistry. 2004 Apr 27;43(16):4716–23.

33. Tran KL, Aronov PA, Tanaka H, Newman JW, Hammock BD, Morisseau C. Lipid sulfates and sulfonates are allosteric competitive inhibitors of the N-terminal phosphatase activity of the mammalian soluble epoxide hydrolase. Biochemistry. 2005 Sep 13;44(36):12179–87.

34. Przybyla-Zawislak BD, Srivastava PK, Vazquez-Matias J, Mohrenweiser HW, Maxwell JE, Hammock BD, et al. Polymorphisms in human soluble epoxide hydrolase. Molecular Pharmacology. 2003 Aug;64(2):482–90.

35. Enayetallah AE, Grant DF. Effects of human soluble epoxide hydrolase polymorphisms on isoprenoid phosphate hydrolysis. Biochemical and Biophysical Research Communications. 2006 Mar 3;341(1):254–60.

36. Cronin A, Mowbray S, Dürk H, Homburg S, Fleming I, Fisslthaler B, et al. The N-terminal domain of mammalian soluble epoxide hydrolase is a phosphatase. Proceedings of the National Academy of Sciences of the United States of America. 2003 Feb 18;100(4):1552–7.

37. Cronin A, Homburg S, Dürk H, Richter I, Adamska M, Frère F, et al. Insights into the catalytic mechanism of human sEH phosphatase by site-directed mutagenesis and LC-MS/MS analysis. Journal of Molecular Biology. 2008 Nov 14;383(3):627–40.

38. EnayetAllah AE, Luria A, Luo B, Tsai H-J, Sura P, Hammock BD, et al. Opposite regulation of cholesterol levels by the phosphatase and hydrolase domains of soluble epoxide hydrolase. The Journal of Biological Chemistry. 2008 Dec 26;283(52):36592–8.

39. Arand M, Cronin A, Oesch F, Mowbray SL, Jones TA. The telltale structures of epoxide hydrolases. Drug Metabolism Reviews. 2003 Dec;35(4):365–83.

40. Enayetallah AE, French R, Barber M, Grant DF. Cell-specific subcellular localization of soluble epoxide hydrolase in human tissues. The Journal of Histochemistry and Cytochemistry. 2006 Mar;54(3):329–35.

41. Luo B, Norris C, Bolstad ESD, Knecht D a, Grant DF. Protein quaternary structure and expression levels contribute to peroxisomal-targeting-sequence-1-mediated peroxisomal import of human soluble epoxide hydrolase. Journal of Molecular Biology. 2008 Jun 27;380(1):31–41.

42. Lundgren B, DePierre JW. Proliferation of peroxisomes and induction of cytosolic and microsomal epoxide hydrolases in different strains of mice and rats after dietary treatment with clofibrate. Xenobiotica. 1989 Aug;19(8):867–81.

43. Enayetallah A. Distribution of soluble epoxide hydrolase and of cytochrome P450 2C8, 2C9, and 2J2 in human tissues. The Journal of Histochemistry & Cytochemistry. 2004;52(4):447–54.

44. Sura P, Sura R, Enayetallah AE, Grant DF. Distribution and expression of soluble epoxide hydrolase in human brain. The Journal of Histochemistry and Cytochemistry. 2008 Jun;56(6):551–9.

45. Shin J-H, Engidawork E, Delabar J-M, Lubec G. Identification and characterisation of soluble epoxide hydrolase in mouse brain by a robust protein biochemical method. Amino Acids. 2005 Feb;28(1):63–9.

46. Zhang W, Otsuka T, Sugo N, Ardeshiri A, Alhadid YK, Iliff JJ, et al. Soluble epoxide hydrolase gene deletion is protective against experimental cerebral ischemia. Stroke. 2008 Jul;39(7):2073–8.

47. Zhang W, Iliff JJ, Campbell CJ, Wang RK, Hurn PD, Alkayed NJ. Role of soluble epoxide hydrolase in the sex-specific vascular response to cerebral ischemia. Journal of Cerebral Blood Flow and Metabolism. 2009 Aug;29(8):1475–81.

48. Koerner I, Zhang W, Cheng J. Soluble epoxide hydrolase: regulation by estrogen and role in the inflammatory response to cerebral ischemia. Frontiers Biosciences. 2008;(6):2833–41.

49. Sinal CJ, Miyata M, Tohkin M, Nagata K, Bend JR, Gonzalez FJ. Targeted disruption of soluble epoxide hydrolase reveals a role in blood pressure regulation. The Journal of Biological Chemistry. 2000 Dec 22;275(51):40504–10.

50. Bianco RA, Agassandian K, Cassell MD, Spector AA, Sigmund CD. Characterization of transgenic mice with neuron-specific expression of soluble epoxide hydrolase. Brain Research. 2009 Sep 29;1291:60–72.

51. Iliff JJ, Close LN, Selden NR, Alkayed NJ. A novel role for P450 eicosanoids in the neurogenic control of cerebral blood flow in the rat. Experimental Physiology. 2007 Jul;92(4):653–8.

52. Marowsky A, Burgener J, Falck JR, Fritschy J-M, Arand M. Distribution of soluble and microsomal epoxide hydrolase in the mouse brain and its contribution to cerebral epoxyeicosatrienoic acid metabolism. Neuroscience. 2009 Oct 6;163(2):646–61.

53. Rawal S, Morisseau C, Hammock BD, Shivachar AC. Differential subcellular distribution and colocalization of the microsomal and soluble epoxide hydrolases in cultured neonatal rat brain cortical astrocytes. Journal of Neuroscience Research. 2009 Jan;87(1):218–27.

54. Imig JD, Hammock BD. Soluble epoxide hydrolase as a therapeutic target for cardiovascular diseases. Nature reviews: Drug discovery. 2009 Oct;8(10):794–805.

55. Capdevila JH, Falck JR, Harris RC. Cytochrome P450 and arachidonic acid bioactivation. Molecular and functional properties of the arachidonate monooxygenase. Journal of Lipid Research. 2000 Feb;41(2):163–81.

56. Spector A, Norris AW. Action of epoxyeicosatrienoic acids on cellular function. American Journal of Physiology. 2007 Mar;292(3):C996–1012.

57. Daikh BE, Lasker JM, Raucy JL, Koop DR. Regio- and stereoselective epoxidation of arachidonic acid by human cytochromes P450 2C8 and 2C9. The Journal of Pharmacology and Experimental Therapeutics. 1994 Dec;271(3):1427–33.

58. Gross GJ, Hsu A, Falck JR, Nithipatikom K. Mechanisms by which epoxyeicosatrienoic acids (EETs) elicit cardioprotection in rat hearts. Journal of Molecular and Cellular Cardiology. 2007 Mar;42(3):687–91.

59. Campbell WB, Fleming I. Epoxyeicosatrienoic acids and endothelium-dependent responses. Pflügers Archiv : European Journal of Physiology. 2010 May;459(6):881–95.

60. Cipolla MJ, Smith J, Kohlmeyer MM, Godfrey JA. SKCa and IKCa Channels, myogenic tone, and vasodilator responses in middle cerebral arteries and parenchymal arterioles: effect of ischemia and reperfusion. Stroke. 2009 Apr;40(4):1451–7.

61. Simpkins AN, Rudic RD, Schreihofer D, Roy S, Manhiani M, Tsai H-J, et al. Soluble epoxide inhibition is protective against cerebral ischemia via vascular and neural protection. The American Journal of Pathology. 2009 Jun;174(6):2086–95.

62. Iliff J, Alkayed N. Soluble epoxide hydrolase inhibition: targeting multiple mechanisms of ischemic brain injury with a single agent. Future Neurology. 2009;4(2):179–99.

63. Larsen BT, Miura H, Hatoum OA, Campbell WB, Hammock BD, Zeldin DC, et al. Epoxyeicosatrienoic and dihydroxyeicosatrienoic acids dilate human coronary arterioles via BK(Ca) channels: implications for soluble epoxide hydrolase inhibition. American Journal of Physiology. 2006 Feb;290(2):H491–9.

64. Watanabe H, Vriens J, Prenen J, Droogmans G, Voets T, Nilius B. Anandamide and arachidonic acid use epoxyeicosatrienoic acids to activate TRPV4 channels. Nature. 2003 Jul 24;424(6947):434–8.

65. Behm DJ, Ogbonna A, Wu C, Burns-Kurtis CL, Douglas SA. Epoxyeicosatrienoic acids function as selective, endogenous antagonists of native thromboxane receptors: identification of a novel mechanism of vasodilation. The Journal of Pharmacology and Experimental Therapeutics. 2009 Jan;328(1):231–9.

66. Yang C, Kwan Y-W, Au AL-S, Poon CC-W, Zhang Q, Chan S-W, et al. 14,15-Epoxyeicosatrienoic acid induces vasorelaxation through the prostaglandin EP(2) receptors in rat mesenteric artery. Prostaglandins & Other Lipid Mediators. 2010 Sep;93(1-2):44–51.

67. Cowart LA, Wei S, Hsu M-H, Johnson EF, Krishna MU, Falck JR, et al. The CYP4A isoforms hydroxylate epoxyeicosatrienoic acids to form high affinity peroxisome

proliferator-activated receptor ligands. The Journal of Biological Chemistry. 2002 Sep 20;277(38):35105–12.

68. Fang X, Hu S, Xu B, Snyder GD, Harmon S, Yao J, et al. 14,15-Dihydroxyeicosatrienoic acid activates peroxisome proliferator-activated receptor-alpha. American Journal of Physiology. 2006 Jan;290(1):H55–63.

69. Liu Y, Zhang Y, Schmelzer K, Lee T-S, Fang X, Zhu Y, et al. The antiinflammatory effect of laminar flow: the role of PPARgamma, epoxyeicosatrienoic acids, and soluble epoxide hydrolase. Proceedings of the National Academy of Sciences of the United States of America. 2005 Nov 15;102(46):16747–52.

70. Ricote M, Li AC, Willson TM, Kelly CJ, Glass CK. The peroxisome proliferator-activated receptor-gamma is a negative regulator of macrophage activation. Nature. 1998 Jan 1;391(6662):79–82.

71. Wray J, Bishop-Bailey D. Epoxygenases and peroxisome proliferator-activated receptors in mammalian vascular biology. Experimental Physiology. 2008 Jan;93(1):148–54.

72. Yu Z, Xu F, Huse LM, Morisseau C, Draper AJ, Newman JW, et al. Soluble epoxide hydrolase regulates hydrolysis of vasoactive epoxyeicosatrienoic acids. Circulation Research. 2000 Nov 24;87(11):992–8.

73. Seubert JM, Sinal CJ, Graves J, DeGraff LM, Bradbury JA, Lee CR, et al. Role of soluble epoxide hydrolase in postischemic recovery of heart contractile function. Circulation Research. 2006 Aug 18;99(4):442–50.

74. Sandberg M, Meijer J. Structural characterization of the human soluble epoxide hydrolase gene (EPHX2). Biochemical and Biophysical Research Communications. 1996 Apr 16;221(2):333–9.

75. Gschwendtner A, Ripke S, Freilinger T, Lichtner P, Müller-Myhsok B, Wichmann H-E, et al. Genetic variation in soluble epoxide hydrolase (EPHX2) is associated with an increased risk of ischemic stroke in white Europeans. Stroke. 2008 May;39(5):1593–6.

76. Srivastava PK, Sharma VK, Kalonia DS, Grant DF. Polymorphisms in human soluble epoxide hydrolase: effects on enzyme activity, enzyme stability, and quaternary structure. Archives of Biochemistry and Biophysics. 2004 Jul 15;427(2):164–9.

77. Przybyla-Zawislak BD, Srivastava PK, Vazquez-Matias J, Mohrenweiser HW, Maxwell JE, Hammock BD, et al. Polymorphisms in human soluble epoxide hydrolase. Molecular Pharmacology. 2003 Aug;64(2):482–90.

78. Sato K, Emi M, Ezura Y, Fujita Y, Takada D, Ishigami T, et al. Soluble epoxide hydrolase variant (Glu287Arg) modifies plasma total cholesterol and triglyceride phenotype in familial hypercholesterolemia: intrafamilial association study in an

eight-generation hyperlipidemic kindred. Journal of Human Genetics. 2004 Jan;49(1):29–34.

79. Wei Q, Doris P a, Pollizotto M V, Boerwinkle E, Jacobs DR, Siscovick DS, et al. Sequence variation in the soluble epoxide hydrolase gene and subclinical coronary atherosclerosis: interaction with cigarette smoking. Atherosclerosis. 2007 Jan;190(1):26–34.

80. Lee CR, North KE, Bray MS, Fornage M, Seubert JM, Newman JW, et al. Genetic variation in soluble epoxide hydrolase (EPHX2) and risk of coronary heart disease: The Atherosclerosis Risk in Communities (ARIC) study. Human Molecular Genetics. 2006 May 15;15(10):1640–9.

81. Burdon KP, Lehtinen AB, Langefeld CD, Carr JJ, Rich SS, Freedman BI, et al. Genetic analysis of the soluble epoxide hydrolase gene, EPHX2, in subclinical cardiovascular disease in the Diabetes Heart Study. Diabetes & Vascular Disease Research. 2008 Jun;5(2):128–34.

82. Lee CR, Pretorius M, Schuck RN, Burch LH, Bartlett J, Williams SM, et al. Genetic variation in soluble epoxide hydrolase (EPHX2) is associated with forearm vasodilator responses in humans. Hypertension. 2011 Jan;57(1):116–22.

83. Fornage M, Lee CR, Doris P a, Bray MS, Heiss G, Zeldin DC, et al. The soluble epoxide hydrolase gene harbors sequence variation associated with susceptibility

to and protection from incident ischemic stroke. Human Molecular Genetics. 2005 Oct 1;14(19):2829–37.

84. Fava C, Montagnana M, Danese E, Almgren P, Hedblad B, Engström G, et al. Homozygosity for the EPHX2 K55R polymorphism increases the long-term risk of ischemic stroke in men: a study in Swedes. Pharmacogenetics and Genomics. 2010 Feb;20(2):94–103.

85. Lee J, Dahl M, Grande P, Tybjaerg-Hansen A, Nordestgaard BG. Genetically reduced soluble epoxide hydrolase activity and risk of stroke and other cardiovascular disease. Stroke. 2010 Jan;41(1):27–33.

86. Fornage M, Hinojos CA, Nurowska BW, Boerwinkle E, Hammock BD, Morisseau CHP, et al. Polymorphism in soluble epoxide hydrolase and blood pressure in spontaneously hypertensive rats. Hypertension. 2002 Oct;40(4):485–90.

87. Monti J, Fischer J, Paskas S, Heinig M, Schulz H, Gösele C, et al. Soluble epoxide hydrolase is a susceptibility factor for heart failure in a rat model of human disease. Nature Genetics. 2008 May;40(5):529–37.

88. Corenblum MJ, Wise VE, Georgi K, Hammock BD, Doris P a, Fornage M. Altered soluble epoxide hydrolase gene expression and function and vascular disease risk in the stroke-prone spontaneously hypertensive rat. Hypertension. 2008 Feb;51(2):567–73.

89. Hutchens MP, Nakano T, Dunlap J, Traystman RJ, Hurn PD, Alkayed NJ. Soluble epoxide hydrolase gene deletion reduces survival after cardiac arrest and cardiopulmonary resuscitation. Resuscitation. 2008 Jan;76(1):89–94.

90. Manhiani M, Quigley JE, Knight SF, Tasoobshirazi S, Moore T, Brands MW, et al. Soluble epoxide hydrolase gene deletion attenuates renal injury and inflammation with DOCA-salt hypertension. American Journal of Physiology. 2009 Sep;297(3):F740–8.

91. Zhang L-N, Vincelette J, Cheng Y, Mehra U, Chen D, Anandan S-K, et al. Inhibition of soluble epoxide hydrolase attenuated atherosclerosis, abdominal aortic aneurysm formation, and dyslipidemia. Arteriosclerosis, Thrombosis, and Vascular Biology. 2009 Sep;29(9):1265–70.

92. Simpkins AN, Rudic RD, Roy S, Tsai HJ, Hammock BD, Imig JD. Soluble epoxide hydrolase inhibition modulates vascular remodeling. American Journal of Physiology. 2010 Mar;298(3):H795–806.

93. Revermann M, Schloss M, Barbosa-Sicard E, Mieth A, Liebner S, Morisseau C, et al. Soluble epoxide hydrolase deficiency attenuates neointima formation in the femoral cuff model of hyperlipidemic mice. Arteriosclerosis, Thrombosis, and Vascular Biology. 2010 May;30(5):909–14.

94. Luo P, Chang H, Zhou Y, Zhang S. Inhibition or deletion of soluble epoxide hydrolase prevents hyperglycemia, promotes insulin secretion, and reduces islet

apoptosis. The Journal of Pharmacology and Experimental Therapeutics. 2010;334(2):430–8.

95. Luria A, Weldon SM, Kabcenell AK, Ingraham RH, Matera D, Jiang H, et al. Compensatory mechanism for homeostatic blood pressure regulation in Ephx2 gene-disrupted mice. The Journal of Biological Chemistry. 2007 Feb 2;282(5):2891–8.

96. Shen HC. Soluble epoxide hydrolase inhibitors: a patent review. Expert Opinion on Therapeutic Patents. 2010 Jul;20(7):941–56.

97. Revermann M. Pharmacological inhibition of the soluble epoxide hydrolase-from mouse to man. Current Opinion in Pharmacology. 2010 Apr;10(2):173–8.

98. Fang X, Hu S, Watanabe T, Weintraub NL, Snyder GD, Yao J, et al. Activation of peroxisome proliferator-activated receptor alpha by substituted urea-derived soluble epoxide hydrolase inhibitors. The Journal of Pharmacology and Experimental Therapeutics. 2005 Jul;314(1):260–70.

99. Dorrance AM, Rupp N, Pollock DM, Newman JW, Hammock BD, Imig JD. An epoxide hydrolase inhibitor, 12-(3-adamantan-1-yl-ureido)dodecanoic acid (AUDA), reduces ischemic cerebral infarct size in stroke-prone spontaneously hypertensive rats. Journal of Cardiovascular Pharmacology. 2005 Dec;46(6):842–8.

100. Fisher M, Feuerstein G, Howells DW, Hurn PD, Kent TA, Savitz SI, et al. Update of the stroke therapy academic industry roundtable preclinical recommendations. Stroke. 2009 Jun;40(6):2244–50.

101. O'Collins VE, Macleod MR, Donnan GA, Horky LL, Van der Worp BH, Howells DW. 1,026 experimental treatments in acute stroke. Annals of Neurology. 2006 Mar;59(3):467–77.

102. Nelson JW, Subrahmanyan RM, Summers S a, Xiao X, Alkayed NJ. Soluble Epoxide Hydrolase Dimerization is Required For Hydrolase Activity. The Journal of Biological Chemistry. 2013 Jan 28;288(11):7697–703.

103. Kumar S, Nussinov R. Relationship between ion pair geometries and electrostatic strengths in proteins. Biophysical Journal. 2002 Sep;83(3):1595–612.

104. Marianayagam NJ, Sunde M, Matthews JM. The power of two: protein dimerization in biology. Trends in Biochemical Sciences. 2004 Nov;29(11):618–25.

105. Matthews J, Sunde M. Dimers, Oligomers, Everywhere. Advances in Experimental Medicine and Biology. 2012;1–18.

106. MacKenzie SH, Clark AC. Death by caspase dimerization. Advances in Experimental Medicine and Biology. 2012 Jan;747:55–73.

107. Jiang G, Den Hertog J, Hunter T. Receptor-like protein tyrosine phosphatase alpha homodimerizes on the cell surface. Molecular and Cellular Biology. 2000 Aug;20(16):5917–29.

108. Xu D, Tsai CJ, Nussinov R. Mechanism and evolution of protein dimerization. Protein Science. 1998 Mar;7(3):533–44.

109. Bennett M, Schlunegger M, Eisenberg D. 3D domain swapping: a mechanism for oligomer assembly. Protein Science. 2008;2455–68.

110. Bennett MJ, Choe S, Eisenberg D. Domain swapping: entangling alliances between proteins. Proceedings of the National Academy of Sciences of the United States of America. 1994 Apr 12;91(8):3127–31.

111. Rutkowska A, Schultz C. Protein tango: the toolbox to capture interacting partners. Angewandte Chemie (International ed. in English). 2012 Aug 13;51(33):8166–76.

112. Kerppola TK. Bimolecular fluorescence complementation (BiFC) analysis as a probe of protein interactions in living cells. Annual Review of Biophysics. 2008 Jan;37:465–87.

113. Geerlof A, Brown J, Coutard B, Egloff MP, Enguita FJ, Fogg MJ, et al. The impact of protein characterization in structural proteomics. Acta Crystallographica. 2006 Oct;62(Pt 10):1125–36.

114. Diekmann Y, Pereira-Leal JB. Evolution of intracellular compartmentalization. The Biochemical Journal. 2013 Jan 15;449(2):319–31.

115. Hung M-C, Link W. Protein localization in disease and therapy. Journal of Cell Science. 2011 Oct 15;124(Pt 20):3381–92.

116. Ebberink MS, Mooyer PAW, Koster J, Dekker CJM, Eyskens FJM, Dionisi-Vici C, et al. Genotype-phenotype correlation in PEX5-deficient peroxisome biogenesis defective cell lines. Human Mutation. 2009 Jan;30(1):93–8.

117. Wanders RJ a, Waterham HR. Peroxisomal disorders I: biochemistry and genetics of peroxisome biogenesis disorders. Clinical Genetics. 2005 Feb;67(2):107–33.

118. Wiedenmann J, Oswald F, Nienhaus GU. Fluorescent proteins for live cell imaging: opportunities, limitations, and challenges. IUBMB life. 2009 Nov;61(11):1029–42.

119. Van der Zand A, Braakman I, Geuze HJ, Tabak HF. The return of the peroxisome. Journal of Cell Science. 2006 Mar 15;119(Pt 6):989–94.

120. Mannaerts GP, Van Veldhoven PP. Metabolic pathways in mammalian peroxisomes. Biochimie. 1993 Jan;75(3-4):147–58.

121. Platta HW, Erdmann R. The peroxisomal protein import machinery. FEBS letters. 2007 Jun 19;581(15):2811–9.

122. Maynard EL, Gatto GJ, Berg JM. Pex5p binding affinities for canonical and noncanonical PTS1 peptides. Proteins. 2004 Jun 1;55(4):856–61.

123. Jones PD, Wolf NM, Morisseau C, Whetstone P, Hock B, Hammock BD. Fluorescent substrates for soluble epoxide hydrolase and application to inhibition studies. Analytical Biochemistry. 2005 Aug 1;343(1):66–75.

124. Jiang Y, Bernard D, Yu Y, Xie Y, Zhang T, Li Y, et al. Split Renilla luciferase protein fragment-assisted complementation (SRL-PFAC) to characterize Hsp90-Cdc37 complex and identify critical residues in protein/protein interactions. The Journal of Biological Chemistry. 2010 Jul 2;285(27):21023–36.

125. Luker KE, Smith MCP, Luker GD, Gammon ST, Piwnica-Worms H, Piwnica-Worms D. Kinetics of regulated protein-protein interactions revealed with firefly luciferase complementation imaging in cells and living animals. Proceedings of the National Academy of Sciences of the United States of America. 2004 Aug 17;101(33):12288–93.

126. Ohtoshi K, Kaneto H, Node K, Nakamura Y, Shiraiwa T, Matsuhisa M, et al. Association of soluble epoxide hydrolase gene polymorphism with insulin resistance in type 2 diabetic patients. Biochemical and Biophysical Research Communications. 2005 May 27;331(1):347–50.

127. Hu C-D, Chinenov Y, Kerppola TK. Visualization of interactions among bZIP and Rel family proteins in living cells using bimolecular fluorescence complementation. Molecular Cell. 2002 Apr;9(4):789–98.

128. Jester B, Cox K, Gaj A. A coiled-coil enabled split-luciferase three-hybrid system: applied toward profiling inhibitors of protein kinases. Journal of the American Chemical Society. 2010;132(33):11727–35.

129. Costantini S, Colonna G, Facchiano AM. Bioinformation ESBRI : A web server for evaluating salt bridges in proteins Bioinformation. 2008;

130. Manders EMM, Verbeek FJ, Aten JA. Measurement of co-localization of objects in dual-colour confocal images. Journal of Microscopy. 1993;169(3):375–82.

131. Fairbanks SL, Young JM, Nelson JW, Davis CM, Koerner IP, Alkayed NJ. Mechanism of the sex difference in neuronal ischemic cell death. Neuroscience. 2012 Sep 6;219:183–91.

132. Monosov EZ, Wenzel TJ, Luers GH, Heyman J a., Subramani S. Labeling of peroxisomes with green fluorescent protein in living P. pastoris cells. Journal of Histochemistry & Cytochemistry. 1996 Jun 1;44(6):581–9.

133. Koch J, Pranjic K, Huber A, Ellinger A, Hartig A, Kragler F, et al. PEX11 family members are membrane elongation factors that coordinate peroxisome

proliferation and maintenance. Journal of Cell Science. 2010 Oct 1;123(Pt 19):3389–400.

134. Wiemer E a, Wenzel T, Deerinck TJ, Ellisman MH, Subramani S. Visualization of the peroxisomal compartment in living mammalian cells: dynamic behavior and association with microtubules. The Journal of Cell Biology. 1997 Jan 13;136(1):71–80.

135. Chang C, Gill SS. Purification and characterization of an epoxide hydrolase from the peroxisomal fraction of mouse liver. Archives of Biochemistry and Biophysics. 1991 Mar;285(2):276–84.

136. Pahan K, Smith BT, Singh I. Epoxide hydrolase in human and rat peroxisomes: implication for disorders of peroxisomal biogenesis. Journal of Lipid Research. 1996 Jan;37(1):159–67.

137. Chen D, Whitcomb R, MacIntyre E, Tran V, Do ZN, Sabry J, et al. Pharmacokinetics and pharmacodynamics of AR9281, an inhibitor of soluble epoxide hydrolase, in single- and multiple-dose studies in healthy human subjects. Journal of Clinical Pharmacology. 2012 Mar;52(3):319–28.

138. Schwarze SR. In Vivo Protein Transduction: Delivery of a Biologically Active Protein into the Mouse. Science. 1999 Sep 3;285(5433):1569–72.

139. Kilic E, Dietz GPH, Hermann DM, Bähr M. Intravenous TAT-Bcl-Xl is protective after middle cerebral artery occlusion in mice. Annals of Neurology. 2002 Nov;52(5):617–22.

140. Kilic U, Kilic E, Dietz GPH, Bähr M. Intravenous TAT-GDNF is protective after focal cerebral ischemia in mice. Stroke. 2003 May;34(5):1304–10.

141. Doeppner TR, Nagel F, Dietz GP, Weise J, Tönges L, Schwarting S, et al. TAT-Hsp70-mediated neuroprotection and increased survival of neuronal precursor cells after focal cerebral ischemia in mice. Journal of Cerebral Blood Flow and Metabolism. 2009 Jun;29(6):1187–96.

142. Cardinale D, Salo-Ahen OMH, Ferrari S, Ponterini G, Cruciani G, Carosati E, et al. Homodimeric enzymes as drug targets. Current Medicinal Chemistry. 2010 Jan;17(9):826–46.

143. Drucker AM, Wu S, Dang CT, Lacouture ME. Risk of rash with the anti-HER2 dimerization antibody pertuzumab: a meta-analysis. Breast Cancer Research and Treatment. 2012 Sep;135(2):347–54.

144. Bannwarth L, Rose T, Dufau L, Vanderesse R, Dumond J, Jamart-Grégoire B, et al. Dimer disruption and monomer sequestration by alkyl tripeptides are successful strategies for inhibiting wild-type and multidrug-resistant mutated HIV-1 proteases. Biochemistry. 2009 Jan 20;48(2):379–87.

145. Shimba N, Nomura A, Marnett A, Craik C. Herpesvirus protease inhibition by dimer disruption. Journal of Virology. 2004;78(12):6657–65.

146. Yang RYC, Yang KS, Pike LJ, Marshall GR. Targeting the dimerization of epidermal growth factor receptors with small-molecule inhibitors. Chemical Biology & Drug Design. 2010 Jul;76(1):1–9.

147. Morisseau C, Schebb NH, Dong H, Ulu A, Aronov P a, Hammock BD. Role of soluble epoxide hydrolase phosphatase activity in the metabolism of lysophosphatidic acids. Biochemical and Biophysical Research Communications. 2012 Mar 23;419(4):796–800.

148. Morisseau C, Sahdeo S, Cortopassi G, Hammock BD. Development of an HTS assay for EPHX2 phosphatase activity and screening of nontargeted libraries. Analytical Biochemistry. 2013 Mar 1;434(1):105–11.

149. Shimozono S, Miyawaki A. Engineering FRET constructs using CFP and YFP. Methods in Cell Biology. 2008 Jan;85(08):381–93.

150. Miyawaki A. Visualization of the spatial and temporal dynamics of intracellular signaling. Developmental Cell. 2003 Mar;4(3):295–305.

151. Decker M, Adamska M, Cronin A, Di Giallonardo F, Burgener J, Marowsky A, et al. EH3 (ABHD9): the first member of a new epoxide hydrolase family with high

activity for fatty acid epoxides. Journal of Lipid Research. 2012 Oct;53(10):2038–45.

152. Oguro A, Imaoka S. Lysophosphatidic acids are new substrates for the phosphatase domain of soluble epoxide hydrolase. Journal of Lipid Research. 2012 Mar;53(3):505–12.